Decay properties of 1*p*-shell hypernuclei: II. Baryon decays

L. Majling
Joint Institute for Nuclear Research, Dubna, and Institute of Nuclear Physics, Academy of Sciences, Řež, Czech Republic

V. N. Fetisov
Lebedev Institute of Physics, Russian Academy of Sciences, Moscow

R. A. Eramzhyan
Institute for Nuclear Research, Russian Academy of Sciences, Moscow

Fiz. Élem. Chastits At. Yadra **28**, 253–332 (March–April 1997)

The baryonic decays of hypernuclear resonances built on $s_\Lambda p^{-1}$, $p_\Lambda p^{-1}$, and $s_\Lambda s^{-1}$ configurations are analyzed within the framework of the translationally invariant shell model. Weak mesonless decays are also studied. Special attention is paid to the effect of the nuclear structure on the population probabilities of excited states of daughter systems. © *1997 American Institute of Physics.* [S1063-7796(97)00102-2]

INTRODUCTION

Hypernuclei are primarily of interest because study of their properties, such as the Λ-hyperon binding energies, the spectra of bound and resonance states, strong and weak decays, electromagnetic transitions, and so on, provides information on the hyperon–nucleon (YN) and hyperon–nucleus (YA) interactions.[1–3] Such studies are especially important because direct experiments on hyperon scattering by nucleons or nuclei are not feasible owing to the unavailability of low-energy hyperon beams. The available data on secondary binary reactions $YN \to Y'N$ are very limited,[4] and, in contrast to NN scattering, they do not give a complete idea of the basic features of the YN interaction. Another important aspect of the physics of hypernuclei is that the hyperon, since it is not identical to the nucleon, can serve as a test body for studying the nature of the nuclear medium.[5] Here we primarily have in mind the response of the shell, cluster, or collective structure of the nuclear core to the presence of a hyperon. It has also been suggested that study of the properties of hypernuclei will shed light on the problem of quark deconfinement in nuclear systems.[6]

The spectroscopy of hypernuclei in (K^-,π^-) and (π^+,K^+) reactions developed rapidly at the CERN, BNL (USA), and KEK (Japan) accelerators in the early 1970s. As a result, the information about the Λ-hyperon binding energies (B_Λ) and individual modes of weak decays of light hypernuclei which had already been obtained using nuclear photoemulsions and bubble chambers was supplemented by extensive data on excited states of hypernuclei, in particular, on the one-particle spectra of the Λ hyperon. Great efforts were made to study hypernuclear γ transitions and weak decays of 1p-shell hypernuclei experimentally. The results of these studies have been discussed in detail in many reviews (see, for example, Refs. 2, 3, 7, and 8).

At the present time the experimental data on the spectra of hypernuclei are analyzed using models which have been developed for ordinary nuclei. The most commonly used models are the shell model,[9–11] the cluster model,[12] and approaches based on the Hartree–Fock method[13] and the mean-field method, explicitly including meson degrees of freedom and relativistic effects.[14] The ΛN interaction is usually chosen in one of the following ways:

- Purely phenomenologically: the available experimental data (binding energies, hypernuclear spectra) are used to determine the parameters of the ΛN and ΛNN potentials[12,13] or the shell matrix elements of the ΛN interaction directly.[9,10,15]
- Derived using the Brueckner G matrix from YN potentials based on the meson theory.[16,17]

Owing to the diversity of the problems which these models are designed to solve, it is difficult to prefer any one of these approaches, especially because they are constantly being improved. We think that the most useful tool for the precision analysis of the low-lying spectra of light hypernuclei for extracting detailed information about the ΛN interaction is the approach[9,10,15] first developed by Gal, Soper, and Dalitz and similar to the approach of Cohen and Kurath in the spectroscopy of ordinary light nuclei.[18] Here the parameters are the two-particle matrix elements of the ΛN interaction, the number of which is five for the lowest hypernuclear configuration $s_\Lambda \otimes s^4 p^k$. They correspond to the spin-independent ($\bar{V}$), spin–spin (Δ), two spin–orbital (S_Λ and S_N), and tensor (T) interactions of the hyperon and the nucleon. In Ref. 15 the potential parameters were corrected using the levels of ${}^{7}_{\Lambda}$Li, ${}^{9}_{\Lambda}$Be, ${}^{10}_{\Lambda}$B, ${}^{12}_{\Lambda}$B, and ${}^{16}_{\Lambda}$O, and the spectra of many light hypernuclei were predicted. The new parametrization was viewed as the simplest explanation of the absence of hypernuclear γ quanta in ${}^{10}_{\Lambda}$B (Ref. 19). In Table I we give the changes in the effective ΛN interaction parameters resulting from the increased amount of experimental data: the binding energies are supplemented by the spectrum of excited states and doublet splitting. In spite of the gradual stabilization in the values of the empirical parameters, the rather wide spread in the values of the matrix elements calculated using ΛN potentials based on the meson theory[17] suggests that the work on determining the ΛN interaction should continue. Moreover, the proposed universality of the parameters of all 1p-shell hypernuclei, the neglect of the three-particle interaction, and the coupling of the Λ and Σ channels all need to be checked further.[20]

In the five years that have elapsed since the first part of

 1063-7796/97/020101-33$10.00

TABLE I. Evolution of the phenomenological parameters of the spin-dependent ΛN interaction determined from the spectra of $1p$-shell hypernuclei. The corresponding matrix elements on the right-hand side of the table were calculated using "realistic" ΛN potentials (Ref. 17).

Year	1978	1985	1991					
V_{eff}	[9]	[10]	[15]	JA	JB	ND	NF	NS
$-\bar{V}$	1.23	1.49	1.49	1.355	1.319	1.492	1.383	1.485
Δ	0.15	0.50	0.30	0.634	2.249	0.187	−0.163	−1.213
S_Λ	0.57	−0.04	−0.02	0.000	0.000	0.345	0.363	0.351
S_N	−0.21	−0.08	0.10	0.000	0.000	0.232	0.267	0.351
T	0.00	0.04	0.02	0.000	0.000	0.000	0.000	0.000

this review[21] was written, the rate of development of purely spectroscopic hypernuclear studies has somewhat slowed. This is because at the BNL and KEK accelerators the emphasis has been on the production of polarized hypernuclei in (π^+,K^+) reactions,[22] weak mesonic decays of the lightest hypernuclei,[23] searches for Σ (Ref. 24) and $\Lambda\Lambda$ hypernuclei[25] and for strange dibaryons in (K^-,K^+) and (K^-,π^+) reactions,[26,27] and other problems. Of these new results, those of Ref. 28 should be singled out. Those investigators used a high-resolution superconducting K^+ spectrometer (at KEK) and succeeded in finding additional levels in the (π^+,K^+) reaction on ^{12}C in the region below the $p_\Lambda p^-$ resonance. These levels are associated with excitation of the nuclear core (see Sec. 1.1 4 below). They also reported preliminary results of measuring the γ quanta from the $E1$ transition $p_\Lambda \to s_\Lambda$ in the reaction $^{13}\mathrm{C}(\pi^-,K^-)^{13}_\Lambda\mathrm{C}$ (Ref. 29).

In Ref. 21 we discussed the properties of bound states of $1p$-shell hypernuclei: the sectra of hypernuclear levels built on known low-lyir.g nuclear states with the s^4p^k configuration, the probabilities of exciting these states in reactions with and without spin flip, and also possible γ transitions of primary hypernuclei. In the present review, which is a continuation of the earlier one, we continue our study of the decay properties of hypernuclear states, focusing on the baryonic decays of excited states of normal and anomalous parity with the hyperon in the s_Λ or p_Λ shell. Even though the spectroscopy of hypernuclei using the (K^-,π^-) reaction has solved the problem of identifying the primary hypernucleus, the hopes of a large gain of spectroscopic data have not been realized. The reaction is dominated by transitions without spin flip, and the γ cascades predicted in Ref. 30 are absent owing to the small splittings of the $|s_\Lambda \otimes s^4p^kJ_N:J=J_N\pm\frac{1}{2}\rangle$ doublets.[1)] It seems that the possibilities offered by the (K^-,π^-) reaction using existing kaon beams of moderate intensity, low purity $(K/\pi\sim 0.1)$, and low charged-pion energy resolution $(\sim 2-3$ MeV) have already been exhausted.

Hypernuclear spectroscopy is developing in two directions:

- The use of *new reactions*, which allows improvement of the energy resolution of the excitation spectrum $[(K^-,\pi^0)]$ or population of more interesting states $[(\gamma,K^+)]$;
- The development of methods for *identifying secondary hypernuclei*. The cross sections of all the reactions used convincingly show that primary hypernuclei are formed in highly excited states. The first stage is associated with nucleon or cluster emission. The baryonic decay channels of hypernuclear resonances have scarcely been studied, although such analysis could significantly aid in the identification of hyperfragments and γ quanta.[31]

In this study we shall give special attention to estimating the probabilities of baryonic decays of hypernuclear resonances with the population of low-lying levels of the daughter nuclei (hypernuclei). Such an analysis can help in designing new experiments to identify new levels and γ lines in daughter hypernuclei. Carrying out the corresponding experiments will broaden the possibilities of hypernuclear spectroscopy, and will allow verification of isospin symmetry in hypernuclei (about which little is yet known) and also of certain configurations following from the shell theory which are forbidden for baryonic decays.

Since the variety of beams available for hypernuclear studies is expected to grow, it is useful to briefly discuss the features of the various hypernucleus production reactions. In addition to the theoretical shell-model description of the decay of states possessing the simple configurations $s_\Lambda p^{-1}$, $p_\Lambda p^{-1}$ and $s_\Lambda s^{-1}$, we thought it appropriate to include weak (also baryonic) mesonless decay in our discussion. This decay channel is realized for the ground and isomeric states of the primary or daughter hypernucleus. The observation of such decays offers the unique possibility of studying the weak process $\Lambda N \to NN$,[32] of verifying the well known $\Delta T=\frac{1}{2}$ rule in nonleptonic interactions,[33] and also of understanding the role of the three-particle reaction $\Lambda NN \to NNN$ in weak decay.[34]

1. FEATURES OF HYPERNUCLEUS PRODUCTION AND SOME INFORMATION ABOUT STRONG BARYONIC DECAYS

Hypernuclei are formed in any reaction of an elementary particle with the nucleons of a nucleus accompanied by hyperon production. As is well known, they were discovered by the Polish physicists Danysh and Pniewski as a result of analysis of cosmic-ray tracks in emulsion. Although hyperfragments have also been found in emulsions exposed to π-meson, proton, and even antiproton beams,[35] it is unarguably easiest to systematically seek them using K^--meson beams, as these already carry the strange quark necessary for hyperon production.[2)] However, in photoemulsions it was possible not only to verify the fact of hypernucleus production (partial breakup of the nucleus, due to the large momentum of the Λ hyperon, ~ 250 MeV/c), but also to identify only light hyperfragments from the π-meson decay of the bound hyperon.[3)]

Further progress was made thanks to the brilliant suggestion of Podgoretskiĭ:[37] instead of hunting down decays of random hyperfragments, it is more useful to study hypernuclear *production*. If the incident kaon momentum is 530 MeV/c, the Λ hyperon is at rest in the lab frame; i.e., it sticks to the nucleus, replacing the nucleon on which the reaction occurred. Therefore, in the two-particle *strangeness-exchange* reaction

$$K^- + {}^A\mathrm{Z} \to {}^A_\Lambda\mathrm{Z} + \pi^- \qquad (1)$$

it is easy to identify the primary hypernuclei, and the π^- momenta can be used to determine the spectra of their excited states. Use of the counter technique allows concentration of the cross section for the reaction (1) at small pion emission angles.

The sensational achievements of the hypernuclear spectroscopy using the in-flight (K^-,π^-) reaction (Ref. 38) stimulated the study of two-particle *associative production* reactions

$$a+N\rightarrow\Lambda+K^+, \tag{2}$$

because the intensities available for beams of ordinary particles (pions, protons, electrons) compensate for the fact that the cross section of reaction (2) is several orders of magnitude smaller than that of the reaction (1).[39,40]

The constantly expanding set of hypernuclear production reactions and the nearly unlimited choice of targets allow the following goals to be set for new experiments:

- The *excitation* of specific modes in various reactions:

$$a+A\rightarrow H+b \tag{3}$$

where A is a nucleus and H is a hypernucleus;

- Study of the features of *baryonic decays* (production of the needed hyperfragments);
- Search for γ quanta in selected hypernuclei;
- Study of the characteristics of hyperon *weak decay* in a nucleon medium.

1.1. Hypernuclear production reactions

When studying excited states, special attention is focused on processes occurring on a single nucleon of the target nucleus. They can be described using the impulse approximation with distorted waves. The most important characteristics of the reactions are:

(i) The momentum q transferred to the hyperon (hypernucleus), which determines the transferred orbital angular momentum ΔL and, via the transition form factor, the probability that the hyperon sticks to the nucleus;

(ii) The spin dependence of the one-nucleon reaction amplitude, which specifies the ratio of nucleus→hypernucleus transitions with and without spin flip;

(iii) The energy and angular dependence of the cross sections for the elementary process, which are important for choosing the optimal kinematical conditions and obtaining the maximum yield.

Factors *(i)* and *(ii)* play a key role in the selectivity of different types of hypernuclear excitation.

The stage of hypernucleus formation in the reaction (3) induced by mesons is described by the cross section

$$\frac{d\sigma^{\rm lab}}{d\Omega_b}=\frac{(2\pi)^4 p_b^2\overline{|T_{if}^{\rm lab}|^2}E_aE_bE_H}{p_a(p_b(E_H+E_b)-p_ap_b\cos\theta_b)}, \tag{4}$$

where

$$T_{if}^{\rm lab}=\langle H,f|\int d\mathbf{r}\chi_{p_b}^{(-)*}(\mathbf{r})\chi_{p_a}^{(+)}(\mathbf{r})\sum_{j=1}^{A}u_j(N\rightarrow\Lambda)\times\delta(\mathbf{r}-\mathbf{r}_j)\Lambda[f+ig(\bar{\sigma}\cdot\bar{\mathbf{n}})]_j|A,i\rangle. \tag{5}$$

Here $\chi_{p_b}^{(-)*}(\mathbf{r})$ and $\chi_{p_a}^{(+)}(\mathbf{r})$ are the meson wave functions, u_j is the operator transforming a nucleon into a hyperon, λ is a kinematical coefficient taking into account the relation between the two-body amplitudes in the c.m. and laboratory frames, p and E are the particle momenta and energies, θ_b is the meson emission angle, and $\mathbf{n}=[\hat{\mathbf{p}}_b\times\hat{\mathbf{p}}_a]$.

The spin-flip part of the amplitude g in the (K^-,π^-) reaction at angles $\theta_\pi<20°$ gives a small contribution to the cross section for $p_K\leqslant 800$ MeV/c, but it becomes large at $p_K\sim 1200$ MeV/c. In the (π^+,K^+) reaction the contribution from g reaches $\sim 50\%$ already at $\theta_K\sim 20°$ and $p_\pi\sim 1200$–1300 MeV/c (Ref. 41). Here the hyperon (hypernucleus) acquires a large polarization.[4)]

The analysis of the features of the hypernuclear excitation spectra becomes simpler if the elementary amplitude $t(aN\rightarrow\Lambda b)$ is extracted from the matrix element (5) at some nucleon momentum, the elementary cross section is averaged over the Fermi motion of the nucleons in the target nucleus, and the spin-flip part of the amplitude is neglected. The meson wave functions are expanded in multipoles:

$$\chi_{p_b}^{(-)*}\chi_{p_a}^{(+)}=\sum_{\Delta L}i^{\Delta L}\sqrt{4\pi(2\Delta L+1)}\,\tilde{j}_{\Delta L}(p_a,p_b,\theta_b,r)Y_{\Delta L,0}(\hat{r}), \tag{6}$$

and the states of the nucleus $|A,i\rangle\equiv|{}^AZ(i)\rangle$ $(i\equiv J_iT_iE_i)$ and of the hypernucleus $|H,f\rangle\equiv|{}^A_\Lambda Z'(f)\rangle$ $(f\equiv J_fT_fE_f)$ are expanded in shell-model wave functions:

$$|{}^AZ(i)\rangle=\sum_{l_Nj_N}\sum_c G_c^i(l_Nj_N)[|l_Nj_N\tau_N\rangle\otimes|{}^{A-1}Z'(c)\rangle]^{J_iT_i},\quad (N=n,p) \tag{7}$$

$$|{}^A_\Lambda Z'(f)\rangle=\sum_{l_\Lambda j_\Lambda}\sum_c a_c^f(l_\Lambda j_\Lambda)[|l_\Lambda j_\Lambda\rangle\otimes|{}^{A-1}Z'(c)\rangle]^{J_f}\quad (c\equiv J_cT_cE_c). \tag{8}$$

Then the cross section for (3) is written in factorized form:

$$\frac{d\sigma^{\rm lab}}{d\Omega_b}=\sum_{\Delta L l_\Lambda l_N}\sigma^{\Delta L}(\theta_b,E)N_{\rm eff}^N(\Delta L,l_\Lambda,l_N). \tag{9}$$

where the first factor,

$$\sigma^{\Delta L}(\theta_b,E)\sim\left|\int\tilde{j}_{\Delta L}(qr)u\Psi_{n_\Lambda l_\Lambda}(r)\Psi_{n_Nl_N}(r)r^2dr\right|^2\equiv\langle n_\Lambda l_\Lambda||\tilde{j}_{\Delta L}Y_{\Delta L}u||n_Nl_N\rangle^2, \tag{10}$$

contains information about the reaction used, and via the radial integrals determines the absolute values of the cross section for a given momentum transfer (and angle). The second factor, the effective number of nucleons,

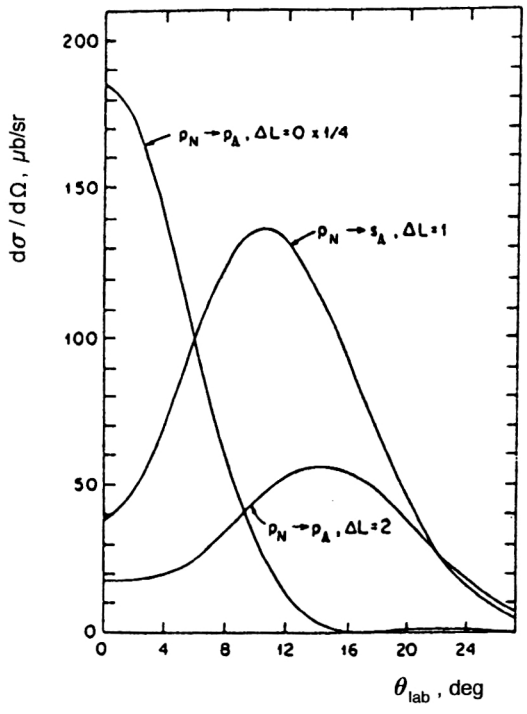

FIG. 1. Dependence of the matrix elements $\langle n_\Lambda l_\Lambda \| \tilde{j}_{\Delta L} Y_{\Delta L} u \| n_N l_N \rangle$ on θ_π.

$$N^N_{ef}(\Delta L, l_\Lambda, l_N) = \begin{pmatrix} l_\Lambda & \Delta L & l_N \\ 0 & 0 & 0 \end{pmatrix} \left(T_i \tau_i \frac{1}{2} \tau_N | T_f \tau_f \right)^2 \times (G^i_c(l_N j_N))^2 (a^f_c(l_\Lambda j_\Lambda))^2, \quad (11)$$

contains all the *structural* information: the possible values of $l_\Lambda = l_N + \Delta L$, the excitations of the nuclear core, and the deviations from the approximation of weak coupling between the hyperon and the nuclear core. In favorable circumstances (certain reactions with suitable targets) the hypernuclear excitation spectrum turns out to be a superposition of a small number of easily identified particle–hole excitation bands:

$$|[j_\Lambda j_N^{-1}]^{\Delta L} J_i : J_f, \quad T_f = T_c, \quad E_f \approx E_c + \varepsilon(l_\Lambda j_\Lambda)\rangle.$$

The (K^-, π^-) substitution reaction

The maximum value of the cross section (10) is obviously reached for complete overlap of the radial wave functions of the hyperon and the nucleon, when $q=0$, and, accordingly, $\Delta L=0$. As noted by Podgoretskiĭ,[37] these conditions are possible in the "in-flight" (K^-, π^-) reaction, for $p_K \sim 530$ MeV/c and $\theta_\pi \sim 0°$. "Substitution states" $(n_\Lambda l_\Lambda = n_N l_N)$ are predominantly populated in this kinematical region. As q (i.e., the angle θ_π) increases, the cross section for transitions with $\Delta L=0$ falls sharply, and the off-diagonal elements governing transitions with $\Delta L=1$ and $\Delta L=2$ become more important. In Fig. 1 we show the θ_π dependence of the cross section Eq. (4) for $p_\Lambda p^{-1}$ $(\Delta L=0)$, $s_\Lambda p^{-1}(\Delta L=1)$, and $p_\Lambda p^{-1}$ $(\Delta L=2)$ transitions calculated in Ref. 43 for the (K^-, π^-) reaction on $^{13}_\Lambda$C $(p_K = 800$ MeV/$c)$.

Nuclei of the $1p$ shell offer favorable conditions for the extraction of spectroscopic information. The number of possible one-particle transitions $(\sigma^{\Delta L}(\theta_\pi, E))$ is small, and moreover they correspond to different parities and excitation energies:

$\Delta L=0(0^+)$	$\Delta L=1(1^-)$	$\Delta L=2(2^+)$	$\Delta L=3(3^-)$
$p_\Lambda p^{-1}(1\hbar\omega_\Lambda)$	$s_\Lambda p^{-1}(0\hbar\omega)$	$p_\Lambda p^{-1}(1\hbar\omega_\Lambda)$	$d_\Lambda p^{-1}(2\hbar\omega_\Lambda)$
$s_\Lambda s^{-1}(1\hbar\omega_N)$	$d_\Lambda p^{-1}(2\hbar\omega_\Lambda)$.		

The spectra of all $1p$-shell hypernuclei (not only $^{16}_\Lambda$O and $^{12}_\Lambda$C) for small θ_π display only isolated resonances with $\Delta L=0$ corresponding to "hole excitations" of the target. As the angle θ_π increases "satellites" appear:[44] the $s_\Lambda p^{-1}$ $(\Delta L=1)$ ground-state band accompanied by $p_\Lambda p^{-1}$ $(\Delta L=2)$ multiplets. The strong θ_π dependence of the cross sections for individual transitions ΔL, shown in Fig. 1, reveals a unique possibility of determining the quantum numbers of excited states. In fact, the results on this reaction have been used to assign the quantum numbers $(2^+_1, 0^+_1, 2^+_2)$ and structure $(p_\Lambda p^{-1})$ to the narrow resonances of the hypernucleus $^{12}_\Lambda$C $(E \sim 11$ MeV) found from proton decay in emulsion,[45] and also the quantum numbers of the individual bands $|j_\Lambda j_N^{-1}; J_f\rangle$ in the (π^+, K^+) spectra.

Careful analysis of the spectra of p-shell hypernuclei has proved the advantages of the multiparticle shell model not only for the systematics of the binding energies B_Λ, but also to a large degree for the systematics of the excitation spectra. The approximation of weak coupling between the hyperon and the nuclear core has proved to be especially effective. The nucleon states are described by the wave functions obtained by Cohen and Kurath,[18] (or Boyarkina and Barker[46]) in the diagonalization of the residual NN interaction. It is assumed that all deviations from the weak-coupling approximation $(a^{f\,2}_c(l_\Lambda j_\Lambda))^2 \neq 1$; splitting of the multiplets $[|l_\Lambda j_\Lambda\rangle \otimes |^{A-1} Z' J_c T_c E_c\rangle]^{J_f}$; difference of the level population intensity from that predetermined by the spectroscopic factors $G^i_c(l_N j_N)]$ are due to the ΛN interaction. Although the appearance of new data was accompanied by the unavoidable correction of the ΛN-interaction parameters, the evolution of the parameters (see Table I) does seem to be converging.

In heavier hypernuclei, substitution resonances correspond to excitations which are too high ($2\hbar\omega, 3\hbar\omega, \ldots$). The spectroscopic information is extracted from the (π^+, K^+) reaction, which possesses selectivity of a different type.

The (K^-, π^0) reaction

The possibilities offered by the (K^-, π^-) reaction are limited owing to both the need to use thick targets (to obtain a reasonable yield of hypernuclei) and the poor resolution ($\sim 2-3$ MeV) of the charged-pion detectors. New hopes are pinned on the (K^-, π^0) reaction. It turns out that the neutral-meson spectrometer constructed at Los Alamos can provide an energy resolution of $\sim 200-300$ keV (Ref. 47). It has recently been suggested that it be used for hypernuclear studies at BNL.[48]

The (K^-, π^0) reaction has some special features. Λ-hyperon production occurs on the protons of the target, and so other hypernuclei ${}^{A}_{\Lambda}(Z-1, N)$ are produced in (K^-, π^0) reactions. Whereas in (K^-, π^-) reactions on nuclei with isospin $T_i \neq 0$ both isospin states are accessible ($T_c = T_< \equiv T_i - \frac{1}{2}$ and $T_c = T_> \equiv T_i + \frac{1}{2}$), the (K^-, π^0) reaction acts as an isospin filter, populating only states with $T_>$. For targets with $N=Z$ ($T_i=0$) the spectra $N_{\text{eff}}^{n(p)}$ in (K^-, π^-) and (K^-, π^0) reactions should be identical (up to small effects from isospin symmetry breaking). However, the decay properties of the levels differ owing to the difference between the energy thresholds of the decay channels.[30,49] In $1p$-shell hypernuclei ${}^{A}_{\Lambda}(Z-1, N)$ the neutron thresholds often turn out to be low (see Table IV), and so the resonance structure can be studied using the neutron spectra.[50]

The $(K^-_{\text{stop}}, \pi^-)$ reaction

Reactions involving stopped kaons, $(K^-_{\text{stop}}, \pi^-)$, have been and continue to be studied at KEK.[51] In the excitation spectra that have been obtained, it has been possible to clearly distinguish only $s_\Lambda p^{-1}$ and $p_\Lambda p^{-1}$ transitions in the hypernucleus ${}^{12}_{\Lambda}\text{C}$. The loss of selectivity can be attributed to the increase of q (~ 250 MeV/c) and the replacement of $\chi^{(+)}_{p_a}(r)$ in the matrix element (4) by the peripheral wave function of the K^- meson bound in the $4d$ mesonic atom orbit.

The high efficiency of hypernucleus production in the reaction $(K^-_{\text{stop}}, \pi^-)$ mentioned above has made it possible to uncover a surprisingly high yield of the easily detected hyperfragment ${}^{4}_{\Lambda}\text{H}$ from Li, Be, C, and O targets.[52] This advantage of the $(K^-_{\text{stop}}, \pi^-)$ reaction will also be used at a special setup, the ϕ factory DAΦNE at Frascati.[53] The expected yield of hypernuclei obtained in the capture of slow kaons from the decay $\phi \to K^- K^+$ (80 events/hour) exceeds the number of hypernuclei produced in reactions on secondary kaon beams or in (π^+, K^+) associative production reactions (5 events/hour), and the guaranteed purity of the "kaon beam" makes it possible to perform large-scale hypernuclear studies.[54] In particular, it will be possible to study the (K^-, π^+) reaction, which is realized successively on two protons of the target nucleus.[55] The reaction cross sections are close to those of (π^+, K^+) reactions, amounting to several μb/sr at $p_K \sim 800$ MeV/c (Ref. 27). Owing to the low intensity of the kaon beams relative to pion beams ($I_K/I_\pi \sim 10^{-2}$), hypernuclear levels have not yet been observed in this reaction. There are no estimates of the reaction rate for stopped K^- mesons, although its possible role for light nuclei has been discussed[56] in connection with the cluster (${}^{4}_{\Lambda}H$) decay of hypernuclei.

It has been suggested[57] that the (K^-, π^+) reaction be used to study hypernuclei with a neutron excess ${}^{6}_{\Lambda}\text{H}$, ${}^{7}_{\Lambda}\text{H}$, and so on, many of which should be stable, or at the edge of stability to neutron decay. Some of these hypernuclei contain weakly coupled neutrons (a neutron halo), and they are interesting to study because this clear feature of nuclear structure is now being widely discussed and studied in other nuclear reactions.[58]

The (π^+, K^+) reaction

In reactions of associative hyperon production, $(a + N \to \Lambda + K^+)$, two heavy quarks s and $\bar{s}$ are produced, so that the momentum transfer is unavoidably large. Consequently, the probability for hyperon emission from the nucleus is also large. However, as mentioned above, an acceptable hypernuclear yield is ensured by the high intensity of the pion beam. In 1980 Thiessen[39] suggested the study of hypernucleus production in the (π^+, K^+) reaction, and Dover[40] showed that for the large momentum transfers ($q \sim 350$ MeV/c) characteristic of this reaction, the matrix elements (10) $\langle n_\Lambda l_\Lambda \| j_{\Delta L} \| n_N l_N \rangle$ attain a maximum if the transferred orbital angular momentum ΔL takes the maximum value: $\Delta L = l_N + l_\Lambda$. The (π^+, K^+) reaction selectively populates particle–hole states of a completely determined type, those with maximum possible orbital angular momentum: the *stretched states* $|j_\Lambda j_n^{-1} : J_H = l_\Lambda + l_n\rangle$. The inclusion of distortion of the meson waves enhances the suppression of transitions with small ΔL and transitions between states with radial nodes. Since the Λ hyperon, being not identical with a nucleon, sits in the deepest shell of the hyperon–nucleus potential, a series of *one-particle hyperon states* is excited in the (π^+, K^+) reaction.[5)]

Use of the (π^+, K^+) reaction for hypernuclear spectroscopy has begun at BNL. At first, the feasibility of the project was demonstrated by comparing the cross sections for the (K^-, π^-) and (π^+, K^+) reactions on a ${}^{12}\text{C}$ target.[60] The A dependence of the Λ hyperon binding energy in the s_Λ, p_Λ, d_Λ, and f_Λ shells was obtained in subsequent measurements on ${}^{9}\text{Be}$, ${}^{12}\text{C}$, ${}^{13}\text{C}$, ${}^{16}\text{O}$, ${}^{28}\text{Si}$, ${}^{40}\text{Ca}$, ${}^{51}\text{V}$, and ${}^{89}\text{Y}$ targets,[61] and became one of the sterling results of hypernuclear spectroscopy.[62] A recently completed series of experiments at KEK used ${}^{10}\text{B}$, ${}^{139}\text{La}$, and ${}^{208}\text{Pb}$ targets in addition to ${}^{12}\text{C}$, ${}^{28}\text{Si}$, and ${}^{89}\text{Y}$ targets.[28]

It is interesting that in heavy hypernuclei, despite the low threshold for neutron emission (~ 8 MeV), the rearrangement of the baryon orbitals (the nuclear Auger effect) makes the one-particle states of the hyperon quite narrow and accessible to observation.[63] Population of the lowest s_Λ, p_Λ, and possibly d_Λ orbitals can lead to emission of hypernuclear γ quanta.

Owing to the experimental resolution (~ 3 MeV), in some hypernuclei in which neutron holes are strongly fragmented (for example, ${}^{40}_{\Lambda}\text{Ca}$), individual resonances overlap,

and the structural features of the cross section disappear. The impressive picture of the "one-particle hyperon spectrum" in ${}^{89}_{\Lambda}$Y is due to the high concentration of the $1g_{9/2}^{-1}$ hole (the f^{-1} and p^{-1} holes produce only an overall background).

Using the new superconducting kaon spectrometer (SKS), the authors of Ref. 28 managed to isolate two weak resonances in the ${}^{12}_{\Lambda}$C spectrum corresponding to core excitation ($E=2.58\pm0.17$ MeV and $E=6.89\pm0.42$ MeV). Unfortunately, their quantum numbers were not determined. (The dependence on the angle θ_K for *all* transitions without spin flip has a maximum at 0°.) On the basis of analysis of the spectrum of levels populated in the (K^-,π^-) reaction, the authors assign the values $J^\pi=1^-$ to both new resonances. However, in the standard shell-model calculations there is no place for a 1^- state near 7 MeV. We think that in this case the large momentum transfer brings more complicated hole states of the core into play: to the already known states of the $0\hbar\omega$ band, p^{-1}: $\frac{3}{2}^-$, $\frac{1}{2}^-$, are added states of the $1\hbar\omega$ band, $p^{-2}(2s-d)$: $\frac{5}{2}^+,\frac{3}{2}^+,\frac{1}{2}^+$. Mixing of the strong doorway state $|p_\Lambda p^{-1}:2^+,E\sim11$ MeV$\rangle$ with the weak intruder state $|s_\Lambda\otimes[p^{-2}(2s-d):\frac{5}{2}]:2^+,E\sim7$ MeV$\rangle$ induced by the ΛN interaction easily explains the experimental data.

The improvement of the energy resolution and study of heavy nuclei (^{139}La and ^{208}Pb) again raises the question of the magnitude of the spin–orbital splitting $j_\Lambda=l_\Lambda\pm\frac{1}{2}$ of the hyperon orbitals. It has been suggested that a resolution to 200 keV can be reached at the PILAC setup in Los Alamos, which would allow determination of even the effects of the quark structure of the hyperon in the splitting $\varepsilon(p_\Lambda)-\varepsilon(s_\Lambda)$.

Ejiri has drawn attention to the unique ability of the (π^+,K^+) reaction to generate *polarized hypernuclei*.[64] Hypernucleus polarization is manifested as asymmetry of the angular distribution

$$W(\theta)=1+A\cos\theta$$

of protons from the mesonless weak decay $(\Lambda+p\to n+p)$. The coefficient A is proportional to the product of the polarization of the decaying hypernucleus and the asymmetry of the weak decay, itself due to interference of the parity-conserving $({}^3S_1\to{}^3S_1+{}^3D_1)$ and parity-nonconserving $({}^3S_1\to{}^3P_1)$ amplitudes:

$$A\sim\mathrm{Re}[{}^3P_1({}^3S_1+{}^3D_1)^*].$$

The possibility of hypernuclear studies of this type was first demonstrated in the experiment of Ref. 22. The asymmetry attributed to the decay of the ${}^{11}_{\Lambda}$B hypernucleus obtained in the reaction

$${}^{12}\mathrm{C}(\pi^+,K^+){}^{12}_{\Lambda}\mathrm{C}^*(2^+;\sim11\ \mathrm{Mev});\quad {}^{12}_{\Lambda}\mathrm{C}^*(2^+)\to p+{}^{11}_{\Lambda}B$$

turned out to be large: $A=-0.2\pm0.1$.

The preliminary results of a new experiment were recently reported.[42] The asymmetry of protons from the ${}^{5}_{\Lambda}$He hypernucleus,

$${}^6\mathrm{Li}(\pi^+,K^+){}^6_{\Lambda}\mathrm{Li};\quad {}^6\mathrm{Li}\to p+{}^{5}_{\Lambda}\mathrm{He}$$

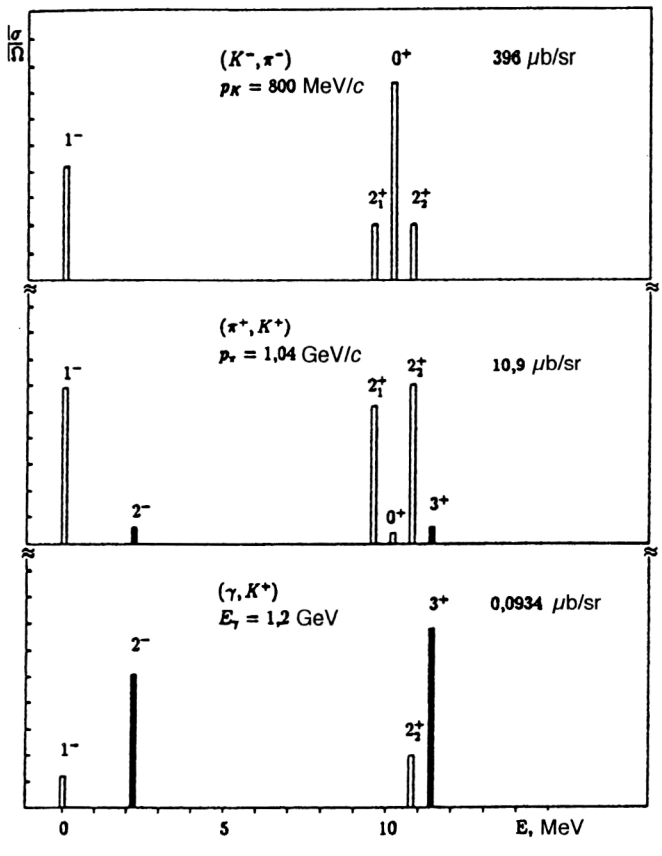

FIG. 2. Cross sections and excitation spectra of ${}^{12}_{\Lambda}$C(${}^{12}_{\Lambda}$B) calculated for three different rections: (K^-,π^-) ($p_K=800$ MeV/c), (π^+,K^+) ($p_\pi=1.04$ GeV/c), and (γ,K^+) ($E_\gamma=1.2$ GeV). The states excited in spin flip are shaded. The cross sections of the dominant resonances are given.[2]

was studied. A simpler interpretation of the data for light hypernuclei will significantly supplement the information about the partial amplitudes of weak decay.

The study of the properties of polarized hypernuclei forms an independent subfield of hypernuclear spectroscopy.

The (γ,K^+) reaction

The theoretical possibilities of studying hypernuclei in the electromagnetic processes (γ,K^+) and $(e,e'K^+)$ were discussed long ago[65,66] and again recently in connection with the CEBAF accelerator.[67] These reactions occur on intranuclear protons in Λ-hypernucleus production. Like (π^+,K^+) reactions, they are characterized by large q, but the spin dependence of the elementary amplitude is stronger even at small kaon emission angles. This dependence leads to strong spin-flip transitions and significant hypernucleus polarization,[68] which is important for studying doublets of hypernuclear levels and weak decays. Since the nuclear interaction of the K^+ mesons is weak, the contribution from protons in deep shells is enhanced in these reactions. Owing to the large values of q, in both these processes and (π^+,K^+) reactions states with high spin should be excited, and it becomes possible to study the one-particle Λ-hyperon spectrum built on proton hole states of the nucleus.

Figure 2 demonstrates the consistency and complementarity of the spectra of excited states of the ${}^{12}_{\Lambda}$C hypernucleus

formed in three different reactions. The substitution state $|p_\Lambda p^{-1}:0^+\rangle$ dominates in the (K^-,π^-) reaction ($p_K=800$ MeV/c, $\theta_\pi=10°$), but transitions without spin flip, $|s_\Lambda p^{-1}:1^-\rangle$ and $|p_\Lambda p^{-1}:2^+\rangle$, can also be seen. Stretched states without spin flip, $|s_\Lambda p^{-1}:1^-\rangle$ and $|p_\Lambda p^{-1}:2^+\rangle$, dominate in the (π^+,K^+) reaction ($p_\pi=1.04$ GeV/c, $\theta_K=10°$), and satellites of these states also appear: stretched states with spin flip, $|s_\Lambda p^{-1}:2^-\rangle$ and $|p_\Lambda p^{-1}:3^+\rangle$. It is predicted that the contribution of stretched states with spin flip dominates for the (γ,K^+) reaction ($E_\gamma=1.2$ GeV, $\theta_K=10°$). The absolute values of the cross sections at the corresponding maxima should be noted.

The spectroscopy of hypernuclei in electromagnetic processes will undoubtedly add important information to that obtained in reactions induced by K^- and π^+ mesons. The cross sections for the photo- and electroexcitation of individual hypernuclear levels are expressed in terms of combinations of amplitudes different from those determining the reaction on a free nucleon, so that study of the partial transitions can be used to check the proposed variants of the amplitudes describing the elementary reaction.[66]

The (p,K^+) reaction

Owing to the large value of q, the $(p,p'K^+)$ and (p,K^+) reactions can lead to high-spin states of the hypernucleus. In contrast to (π^+,K^+) reactions, in (p,K^+) processes $NN\to\Lambda NK^+$ collisions can lead to the excitation of more complex configurations, when the baryon pair, a Λ hyperon and a nucleon, end up in different shells. For example, in the (p,K^+) reaction on ^{4}He it is possible to study the structure of the $^5_\Lambda$He hypernucleus and its excited states in the continuum, which is difficult to do in other reactions owing to the absence of a nuclear target with $A=5$. Here the large momentum transfer makes it possible to study short-lived baryon–baryon correlations and possible quark effects.[69,70]

As a result of the realization of the brilliant proposal of Podgoretskiĭ[37] to study hypernucleus production, a simple particle–hole structure $|j_\Lambda j_N^{-1}:J_H\rangle$ of the excitations of primary hypernuclei was found, and the parameters of the *hyperon–nuclear* potential were determined (its depth, radius, smearing, and spin–orbital splitting).

The *hyperon–nucleon* interaction parameters (spin dependence, role of three-particle ΛNN forces) are extracted from the splitting of hypernuclear bound-state multiplets. For studying the characteristics of weak hyperon decay in a nucleon medium it is also necessary to identify secondary hypernuclei, and, even better, to control the processes leading to their production.

1.2. Experimental data on baryon decays

The difficulty of this problem is clear from the fact that the entire chain of events (formation of the primary hypernucleus→baryon decay→hyperfragment weak decay) can be traced only in a single case, that of $^{12}_\Lambda$C*($E\sim11$ MeV)$\to p+^{11}_\Lambda$B (Ref. 45). Proton decay and narrow widths of excited states of the hypernucleus $^{12}_\Lambda$C*($E\sim11$ MeV) have been discovered in emulsion;[71] their quantum numbers (2^+_1, 0^+_1, 2^+_2) were determined from the data on the (K^-,π^-) reaction.[44]

States found in emulsions

Unfortunately, the final summary of the results of the European Hypernucleus Collaboration[72] contains no data on the decays $^{14}_\Lambda$N*$\to p+^{13}_\Lambda$C and $^{16}_\Lambda$O*$\to p+^{15}_\Lambda$N, which were discussed at conferences. This is presumably because of the large widths of the resonances in these primary hypernuclei.

Identification of hyperfragments in (K^-,π^-) and (π^+,K^+) reactions

Experiments performed by the counter technique use thick targets, and so the protons from hypernucleus decay are not detected.

The authors of Refs. 22, 42 and 73 produced $^5_\Lambda$He and $^{11}_\Lambda$B hyperfragments in the ground state in order to study their weak decay modes in detail using the difference between these modes found in emulsions: mesonic decay of a free Λ hyperon and light hypernuclei, and mesonless decay (fast nucleons) of hypernuclei with A≥5:

$$
\begin{aligned}
{}^6\mathrm{Li}\,{}^{(K^-,\pi^-)}_{(\pi^+,K^+)}\ & {}^6_\Lambda\mathrm{Li}(0;\ \sim20\ \mathrm{MeV})\\
& {}^6_\Lambda\mathrm{Li}(0;\ \sim20\ \mathrm{MeV})\to p+{}^5_\Lambda\mathrm{He}\\
& {}^5_\Lambda\mathrm{He(w.d.)}\to p(T\sim80\ \mathrm{MeV})+\cdots\ ; \qquad (12)
\end{aligned}
$$

$$
\begin{aligned}
{}^{12}\mathrm{C}\,{}^{(K^-,\pi^-)}_{(\pi^+,K^+)}\ & {}^{12}_\Lambda\mathrm{C}^*(\sim11\ \mathrm{MeV})\\
& {}^{12}_\Lambda\mathrm{C}^*(\sim11\ \mathrm{MeV})\to p+{}^{11}_\Lambda\mathrm{B}\\
& {}^{11}_\Lambda\mathrm{B(w.d.)}\to p(T\sim80\ \mathrm{MeV})+\cdots\ . \qquad (13)
\end{aligned}
$$

In analyzing the polarization of protons from hyperfragment weak decay, the Japanese group[22] discovered something unexpected: even at high excitations ($30<E<60$ MeV) of the $^{12}_\Lambda$C hypernucleus, up to 10% of the Λ particles decay in the hyperfragment.

The products of baryonic decay can be identified only indirectly:

1. The γ quanta of the ^{6}Li daughter nucleus can be used to determine the decay of $^7_\Lambda$Li* with Λ-hyperon emission:[74,75]

$$
\begin{aligned}
{}^7\mathrm{Li}(K^-,\pi^-)\ & {}^7_\Lambda\mathrm{Li}^*(\sim13\ \mathrm{MeV};\ 1^+1)\\
& {}^7_\Lambda\mathrm{Li}^*(\sim13\ \mathrm{MeV};\ 1^+1)\to\Lambda+{}^6\mathrm{Li}^*(0^+1)\\
& {}^6\mathrm{Li}^*(0^+1)\to{}^6\mathrm{Li}+\gamma. \qquad (14)
\end{aligned}
$$

2. The hypernuclear γ quanta from $^4_\Lambda$H*(~1.04 MeV) and $^4_\Lambda$He*(~1.15 MeV) found in (K^-,π) reactions on ^{6,7}Li targets suggest cluster decays of excited states of these hypernuclei.[74,76,77]

3. The experiments of Ref. 73 probably observed the cluster decay of $^{12}_\Lambda$C (Ref. 78):

TABLE II. Yield Y (in % of the number of captured kaons) of the hyperfragment ${}^{4}_{\Lambda}H$ in the reaction $(K^-_{\text{stop}},\pi^-)$ on certain nuclei [52] and in emulsion.[72]

${}^{A}Z$	^{7}Li	^{9}Be	^{12}C	^{16}O	^{40}Ca	CNO
Y	3.3	1.6	1.0	0.5	<0.3	0.7

$$
\begin{aligned}
{}^{12}\mathrm{C}(K^-,\pi^-)\quad & {}^{12}_{\Lambda}\mathrm{C}^*(\sim 18\ \mathrm{MeV}) \\
& \overset{?}{\rightarrow} \\
& {}^{12}_{\Lambda}\mathrm{C}^*(\sim 18\ \mathrm{MeV}) \rightarrow {}^{3}\mathrm{He}+{}^{9}_{\Lambda}\mathrm{Be} \\
& {}^{9}_{\Lambda}\mathrm{Be}(\mathrm{w.d.}) \rightarrow p(T\sim 80\ \mathrm{MeV})+\cdots . \qquad (15)
\end{aligned}
$$

4. The absence of reliable identification of the hyperfragments appearing in the decay of highly excited states is strongly felt in the analysis of the experiment of Ref. 79. Instead of the expected γ quanta ($E_\gamma = 170$ keV) from the first excited state of the ${}^{10}_{\Lambda}$B hypernucleus formed in the reaction ${}^{10}\mathrm{B}(K^-,\pi^-){}^{10}_{\Lambda}\mathrm{B}$, the γ quanta ($E_\gamma = 440$ keV) of an *unknown* hyperfragment were detected. We think[80] (see Sec. 5) that they correspond to the decay ${}^{10}_{\Lambda}\mathrm{B}^*(\sim 25\ \mathrm{MeV}) \rightarrow {}^{3}\mathrm{He}+{}^{7}_{\Lambda}\mathrm{Li}^*$, although the authors attribute them to the hypernucleus ${}^{8}_{\Lambda}$Li or ${}^{8}_{\Lambda}$Be.

Identification of hyperfragments in the $(K^-_{\text{stop}},\pi^-)$ reaction

So far, in "counter" experiments it has been possible to correctly identify only ${}^{4}_{\Lambda}$H hyperfragments from the momenta of the pions from the two-particle weak decay

$$
{}^{4}_{\Lambda}\mathrm{H} \rightarrow {}^{4}\mathrm{He}+\pi^-(p_\pi \sim 133\ \mathrm{MeV}/c). \qquad (16)
$$

Tamura noticed[52] this characteristic peak in the spectra of the $(K^-_{\text{stop}},\pi^-)$ reaction on ^{7}Li, ^{9}Be, ^{12}C, ^{16}O, and ^{40}Ca nuclei and determined the A dependence of the yield of the ${}^{4}_{\Lambda}$H hyperfragment. We see from Table II that the results of Tamura give the details of the emulsion data[72] (C, N, and O nuclei) averaged over A.

There is no satisfactory interpretation of the results.[41,56] The decision to continue the very interesting simultaneous study[81] of the yield of ${}^{5}_{\Lambda}$He and hypernuclear γ quanta [${}^{4}_{\Lambda}$He (1.15 MeV) and ${}^{4}_{\Lambda}$He (1.04 MeV)] is a good one. It has been suggested that the effect of structural and statistical factors on the hyperfragment production process be determined. Curiously, according to the preliminary data,[82] the ${}^{5}_{\Lambda}$He yield grows with increasing A, in contrast to the ${}^{4}_{\Lambda}$H yield.

A definitive determination of the role of structural factors in hyperfragment production may be obtained in an experiment which combines the advantages of the counter technique (determination of the excitation spectrum of the primary hypernucleus) and the emulsion technique (identification of the hyperfragment from pion decay). This is possible in principle at the FINUDA setup at the DAΦNE ϕ factory.[53] Thin targets will be used already in the first stage of the experiments, but measurements of pions from weak decay will be postponed until a later time.

2. THEORETICAL DESCRIPTION OF BARYONIC DECAY CHANNELS OF HYPERNUCLEAR RESONANCES

In the preceding section we showed that the need to identify secondary hypernuclei implies that a reliable model of baryon decay channels is necessary.

All the available data on the hypernuclear excitation spectra obtained in in-flight (K^-,π^-) reactions and (π^+,K^+) reactions suggest a simple particle–hole structure $j_\Lambda j_N^{-1}$ of the hypernuclear resonances. In what follows we shall focus on the detailed study of $1p$-shell hypernuclei. We shall take into account "*deep*" holes (s^{-1}) and estimate the partial decay *widths*.

The set of problems to be solved is shown in Fig. 3, where we schematically give:

- The spectrum of hypernuclear resonances (depending on the production reaction);
- The proposed gross structure ($s_\Lambda p^{-1}$, $p_\Lambda p^{-1}$, $s_\Lambda s^{-1}$) of these resonances;
- The thresholds of the main decay channels;
- The products of strong, electromagnetic, and weak decays.

In our discussion of production reactions (Sec. 1.1), we noted that all the information about the structure of a nuclear system is concentrated in the fractional parentage coefficient (7) $G^i_c(l_N,j_N)$. When studying the *decay* properties of hypernuclear resonances corresponding to high excitation energies, it is useful to use the techniques of the translationally invariant shell model (TISM), which automatically eliminates oscillations of the center of mass of the system. In the first part of this review[21] we gave a detailed discussion of the construction of hypernuclear wave functions in the TISM when the translationally invariant nuclear-core function is known. We recall that for states of normal parity ("a hole in a valence shell," $1p^{-1}$), the relation between the TISM wave functions and those of the standard shell model (SSM) is very simple:

$$
\Psi_0(R_c)\Phi^{A-1}_{k-1}(JTE) \equiv |s^4p^{k-1}{:}JTE\rangle . \qquad (17)
$$

(It is sufficient to indicate the number of oscillator quanta, $k-1$, and to recall that the function Φ^{A-1}_{k-1} depends on $A-2$ Jacobi coordinates). These states have been studied carefully by many authors and are satisfactorily described in the SSM with intermediate coupling:[18,46]

$$
\begin{aligned}
|s^4p^k{:}JTE\rangle &= \sum_{fLS} a^e_\alpha |s^4p^k[f]\ LST\rangle, \quad (e\equiv JTE, \\
& \alpha \equiv [f]LS). \qquad (18)
\end{aligned}
$$

The Young tableau $[f]$ is perhaps the clearest structural characteristic of excited states of $1p$-shell nuclei. It enters into the set of additional quantum numbers of the LS-coupling basis, where the orbital and spin–isospin components of the wave function of a system of A particles are symmetrized separately.

The quantum numbers $[f]$ and $(\lambda\mu)$ are a natural characteristic of fragmented hole states s^{-1} (Ref. 83). They can

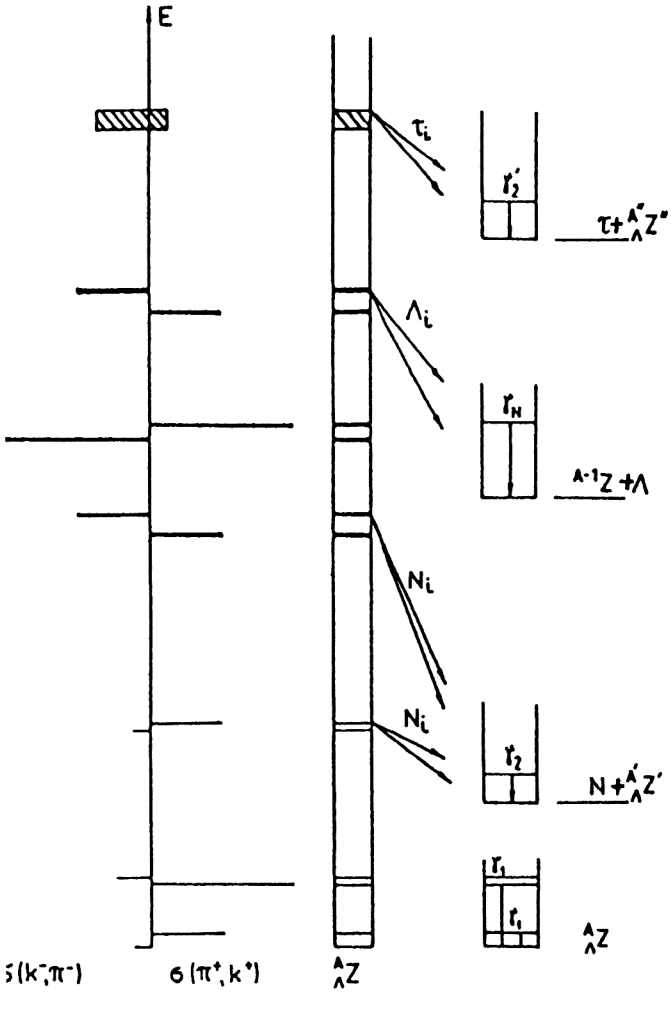

FIG. 3. Schematic picture of the production and decay of hypernuclear resonances. On the left is the excitation function for two production reactions, substitution and associative production. The shell structure of the lowest resonances is given in the center: thin lines—$s_\Lambda p^{-1}$, thick lines—$p_\Lambda p^{-1}$, shaded band—$s_\Lambda s^{-1}$. On the right are the products of successive decays: the ground and excited states of the daughter (hyper)nuclei after *baryon* (Λ, nucleon, cluster) emission, and their electromagnetic transitions: the primary (γ_1), secondary (γ_2), and nuclear (γ_N) quanta. In the last column we give the source of the final *weak* decay: a free Λ or hyperfragment.

be used to find "false" excitations of the nuclear core: $[\Psi_1(R_c)\Phi^{A-1}_{k-1}[f](\lambda_0\mu_0)]^{(\lambda\mu)}$. The preliminary set of suitable pairs of SSM functions

$$|s^{-1}:[f](\lambda\mu)\rangle \equiv |s^3[3],p^k[f_2](\lambda_2\mu_2):[f](\lambda\mu) = (\lambda_2\mu_2)\rangle,$$

$$|p^{-2}l:[f](\lambda\mu)\rangle \equiv |s^4p^{k-2}[4f_2'](\lambda_2'\mu_2'),l[1](20):[f] \times(\lambda\mu)\rangle, \quad (19)$$

($l=2s,2d$) simplifies the construction of the "pure" combination

$$\Psi_0(R_c)\Phi^{A-1}_k([f](\lambda\mu):LST) = \{\alpha|s^{-1}[f](\lambda\mu)L\rangle \times+\beta|p^{-2}l[f](\lambda\mu)L\rangle\}\cdot|[\tilde{f}]ST\rangle. \quad (20)$$

TABLE III. Examples of hole-state fragmentation dependent on Young tableau.

	l^{-1}	p^{-1}	$[f_c]$		s^{-1}	$[f_c]$	
A	$[f_0]$		[·41]	[·32]		[·41]	[·32]
6	[42]	$\frac{2}{5}$	(1	0)	$\frac{3}{5}$	$(\frac{2}{27}$	$\frac{25}{27})$
10	[442]	$\frac{6}{9}$	$(\frac{4}{9}$	$\frac{5}{9})$	$\frac{3}{9}$	$(\frac{1}{9}$	$\frac{8}{9})$
14	[4442]	$\frac{10}{13}$	$(\frac{1}{3}$	$\frac{2}{3})$	$\frac{3}{13}$	$(\frac{8}{63}$	$\frac{55}{63})$

The interpretation of the results of the calculations in intermediate coupling is clearest in terms of the basis functions. For example, the maximum energy range of the spectrum of p^{-1} holes in the ^{8}Be and ^{12}C nuclei, $\Delta E\sim 15$–18 MeV, is explained by the splitting of the [44] and [431] multiplets (α-particle breakup). Table III shows that the reason for the predominant population of *excited states* of $1p$-shell nuclei with $J_0\neq 0$ and $T_0\neq 0$ is hidden in the strong parentage coupling of the ground-state wave function of the target with the states corresponding to the "broken quaduplet."

All the authors who have analyzed the spectra of excited states of $1p$-shell hypernuclei[44,84] have noticed the surprising accuracy of the weak-coupling approximation: after diagonalization of the ΛN interaction, only a single hole state dominates in the wave functions of the observed resonances.[6)] We decided to take the next step,[11] that is, to use the available wave functions to calculate the reduced decay widths.

The simple particle–hole $j_\Lambda j_N^{-1}$ structure of hypernuclear resonances predetermines the dominant role of the hyperon decay channel. In fact, the stability of light hypernuclei ($A\leqslant 9$) can be attributed to the cluster channel ($^5_\Lambda$He), and that of heavier nuclei to the nucleon channel.

Using the experimental data on the hypernuclear decay thresholds given in Table IV, together with the data on the spectra of p^{-1} hole states and also the theoretical indications of the applicability of weak coupling, it is easy to see the *qualitative* differences in the behavior of the decays of *three groups* of resonances of $1p$-shell hypernuclei.

• In $s_\Lambda p^{-1}$ resonances the hyperon decreases the decay probability of the unstable nuclear core. [In hypernuclei with $A=10,14$ (^{8}Be$+N+\Lambda$, ^{12}C$+$N$+\Lambda$), the nucleon threshold is located between the levels of this band.]

• Hyperon emission should dominate in $p_\Lambda p^{-1}$ resonances. However, in the region $A\approx 12$ the hyperon binding energy B_Λ reaches the value $1\hbar\omega_\Lambda\approx 10$ MeV, and for heavy $1p$-shell hypernuclei the first levels of this band do not decay via the hyperon channel. The detailed study of the decay of $p_\Lambda p^{-1}$ resonances serves as an excellent *test of the weak-coupling approximation*. At the same time, one can follow the strangeness exchange between the emitted Λ hyperon and nuclear fragment and explain the role of $s_\Lambda p^{-2}l$ states.

• In $s_\Lambda s^{-1}$ resonances the combination of the stabilizing role of the s_Λ hyperon with the weak-coupling approximation must be reflected in clear *structural selection rules* which suppress the emission of one baryon in favor of *three-nucleon* clusters (^{3}He, $^4_\Lambda$He). Identification of the secondary

TABLE IV. Energies (in MeV) of thresholds for emission of baryons, clusters, and hyperfragments in $1p$-shell hypernuclei. The thresholds determining the stability of a given hypernucleus are marked.

${}^{A}_{\Lambda}Z$	Λ	p	n	d	t	τ	α	${}^{3}_{\Lambda}$H	${}^{4}_{\Lambda}$H	${}^{4}_{\Lambda}$He	${}^{5}_{\Lambda}$He
${}^{3}_{\Lambda}$H	[0.13]										
${}^{4}_{\Lambda}$H	[2.04]		8.17					8.17			
${}^{4}_{\Lambda}$He	[2.39]	7.75						7.75			
${}^{5}_{\Lambda}$He	[3.12]	20.89	21.31	26.84				26.84	20.89	21.31	
${}^{6}_{\Lambda}$He	4.18		[0.17]	18.84	20.75			20.75	18.84	21.47	[0.17]
${}^{6}_{\Lambda}$Li	4.50	[−0.59]		18.50		20.76		20.76	20.31	18.50	[−0.59]
${}^{7}_{\Lambda}$He	5.23		[2.92]		15.50				15.50		3.08
${}^{7}_{\Lambda}$Li	5.58	5.99	6.74	[3.93]	18.98	19.33	6.92	6.92	19.33	18.98	[3.93]
${}^{8}_{\Lambda}$Be	6.84	6.87	12.36	11.39		5.31	6.04	15.76		6.04	[5.31]
${}^{9}_{\Lambda}$Li	8.50	13.79	[3.73]	13.05	9.71			18.15	11.85		
${}^{9}_{\Lambda}$Be	6.71	17.17	18.77	23.41	23.90	23.91	[3.50]	28.86	26.36	25.70	[3.50]
${}^{10}_{\Lambda}$Be	9.11	17.47	[4.07]	19.01	21.22	25.06	7.40	25.68	24.76	27.90	8.46
${}^{10}_{\Lambda}$B	8.89	[2.00]	19.59	18.54	24.64	19.91	6.05	25.25	27.76	23.10	7.46
${}^{11}_{\Lambda}$B	10.24	[7.71]	9.79	9.56	22.07	21.23	9.12	16.14	26.87	25.64	11.58
${}^{12}_{\Lambda}$B	[11.37]		12.59	18.08	15.88	30.05	13.23	27.06	20.55	36.19	16.91
${}^{12}_{\Lambda}$C	[10.80]	[9.25]	13.68	16.81	30.19	13.31	11.50	25.57	35.98	17.63	15.28
${}^{13}_{\Lambda}$C	[11.69]	16.28	19.65	26.64	30.17	28.86	12.35	36.75	37.02	35.58	15.94
${}^{14}_{\Lambda}$C	12.17		[5.43]	19.48	25.81		13.71	30.72	34.01	34.19	19.70
${}^{14}_{\Lambda}$N	12.17	[2.42]		19.85		23.57	12.78	30.48	35.43	31.42	18.55
${}^{15}_{\Lambda}$N	13.59	[8.97]	11.97	12.17	25.57	22.96	14.96	23.73	34.29	31.94	22.08
${}^{16}_{\Lambda}$O	13	[6.71]		16.46		13.39	12.46	28.50	40.39	22.69	20.10

hypernuclei (from the γ quanta of their products) significantly expands the set of experimental data.

A theory describing the formation of a hypernuclear resonance and its subsequent decay via baryonic channels must somehow take into account the fact that these states lie in the continuum. Balashov[85] has formulated a program for the combined description of the resonance and quasielastic mechanisms of hypernucleus formation within the framework of the shell model which directly takes into account the continuum: the continuous shell model (CSM).[86] In the CSM the wave function of a "particle" is calculated in the mean field of a Woods–Saxon type of baryon–nucleus potential, the thresholds of which are determined from the thresholds of the decay channels. Wünsch has shown[87] that the contribution of the quasielastic process depends not only on the value of the momentum transfer, but also on the YA-potential parameters. The Λ-hyperon potential (in contrast to that of the Σ hyperon) is deep enough for resonance formation. The wave functions of "hole" states coincide with the shell wave functions (18) only for nuclei near closed shells. This significantly limits the applicability of the CSM.[88,89]

As the first step, to present the big picture and explain the most interesting cases, it is best to use a more developed SSM without the direct inclusion of the continuum: the bound shell model (BSM).[43] Below in describing the decay of hypernuclear states we shall use the formalism of the reduced widths calculated in R-matrix theory. The SSM, which describes many aspects of hypernuclear structure, is attractive because it is universal and flexible. However, in some cases it is necessary to go beyond the BSM (see, for example, Refs. 89 and 90), to the direct inclusion of the continuum. These cases will be treated specially.

We have described the formal theory of the decay of hypernuclear states within the TISM using the R-matrix approach in Ref. 21. We shall not repeat that description, but only give the basic relation of R-matrix theory. The width for decay via baryonic channels $b(=\Lambda,p,n)$ is given by the product of several quantities:

$$\Gamma_b(c)=2kP_l^b(k)S_{b,c}\gamma_0^2, \tag{21}$$

where k is the wave number of the relative motion of the emitted baryon and the residual nucleus, $P_l^b(k)$ is the penetration factor, l is the angular momentum of the relative motion, γ_0 is the reduced width, and $S_{b,c}$ is a spectroscopic factor proportional to the square of the TISM fractional parentage coefficient relating the wave functions of the decaying resonance, the daughter nucleus, and the emitted baryon:

$$S_{b,c}=\langle {}^{A}_{\Lambda}Z(JTE)||{}^{A-1}Z'(J_cT_cE_c),\ \varphi_{nl}^b(R_c-r_b)\rangle^2. \tag{22}$$

TABLE V. States of ${}^{10}_{\Lambda}$B with the $s_\Lambda p^{-1}$ configuration, decay channels, populated levels, and γ-transition energies. N_i are the excitation intensities in the (K^-,π^-) reaction, and Γ_p are the total proton widths of the doublets.

Doublet J^π	E_i, MeV	N_i, %	Γ_p	Principal component of the wave function	E_γ, MeV
1^-	0	0			
2^-	0.06	19			
2^-	2.43	5	0.1 keV	$\lvert s_\Lambda \otimes {}^8\text{Be}(0^+;0.00)\rangle$	
3^-	2.52	15	0.01–0.1 eV		2.52*
4^-	7.10	5	400 keV	$\lvert s_\Lambda \otimes {}^8\text{Be}(2^+;3.08)\rangle$	3.08
3^-	7.14	9			
	ΣN_i	53			

*See the discussion in the text.

3. DECAY OF HIGH-LYING STATES OF HYPERNUCLEI WITH $s_\Lambda p^{-1}$ CONFIGURATION AND γ DEEXCITATION OF THE DECAY PRODUCTS

Most of the states described by the $s_\Lambda p^{-1}$ configuration belong to the discrete spectrum. However, a few of them built on high-lying p-hole states turn out to be located above the threshold for breakup in the baryonic channel. Using the decays of such states as an example, we shall show how the R-matrix approach works and find its limits of applicability, and we shall study the role of channel coupling via the continuum.

Since we are mainly interested in baryonic decays which lead to γ emission, we shall restrict ourselves to $1p$-shell hypernuclei, in which such emission can be expected. These are the hypernuclei ${}^{10}_{\Lambda}$B, ${}^{14}_{\Lambda}$N, and ${}^{13}_{\Lambda}$C.

Before discussing these three hypernuclei, we note that the energy locations of the hypernuclear levels are calculated using the hyperon–nucleon interaction parameters proposed in Ref. 15. In the nuclear part of the problem we use the Barker parameters[46] for $A \leqslant 9$ and the Cohen–Kurath parameters[18] for $A \geqslant 10$. In the calculations of the hypernuclear energy spectra, the theoretical values of the locations of the nuclear levels are replaced by the experimental values in all cases where they are available.[91]

3.1. The hypernucleus ${}^{10}_{\Lambda}$B

In Fig. 4 we show the calculated locations of three spin doublets of ${}^{10}_{\Lambda}$B having the $s_\Lambda p^{-1}$ configuration. The various thresholds of ${}^{10}_{\Lambda}$B decay are not given here. In Table V we give the population intensities N_i (in %) of these levels in the (K^-,π^-) reaction, the proton widths Γ_p, and the populated levels of the daughter hypernucleus after proton emission. We also indicate the energies of the γ quanta arising in their deexcitation. The calculated intensity of the excitation of all states corresponding to the $s_\Lambda p^{-1}$ configuration is taken to be 100%.

The states of the nuclear core ^{9}B in the hypernucleus ${}^{10}_{\Lambda}$B make up 53% of the p-hole spectroscopic factor of the ground state of ^{10}B. The rest comes from higher states of ^{9}Be ($E=11.7$ MeV and 14.9 MeV). We shall not study the formation of the ${}^{10}_{\Lambda}$B hypernucleus on these states of ^{9}B. The decay of these states turns out to be complicated and requires special treatment.

TABLE VI. Ratio of the probabilities for decay of the level ${}^9\text{Be}(7^-/2)$;7.10 MeV) to states of ^{8}Be.

J^π	E	l_n	W (%)
0^+	0	3	<2
2^+	3.04	1	41–69

The doublet $J^\pi=3^-$ and 4^-, $E\sim7$ MeV

The wave functions of the doublet levels can be written as

$$\left|{}^{10}_{\Lambda}\text{B}(3^-;7.14)\right\rangle = \sqrt{0.974}\left|s_\Lambda \otimes {}^9\text{B}\left(\frac{7}{2^-};6.97\right)\right\rangle + \alpha\left|s_\Lambda \otimes {}^9\text{B}\left(\frac{5}{2^-};2.36\right)\right\rangle + \cdots , \quad (23)$$

$$\left|{}^{10}_{\Lambda}\text{B}(4^-;7.10)\right\rangle = \sqrt{0.992}\left|s_\Lambda \otimes {}^9\text{B}\left(\frac{7}{2^-};6.97\right)\right\rangle + \cdots , \quad (24)$$

where the dots denote components with configurations constructed on higher states of negative parity of the ^{9}B nucleus.

The population of states of the nuclear core ^{8}Be as a result of proton decay of this doublet is controlled by the fractional parentage coefficients

$$\left\langle {}^9\text{Be}\left(\frac{7}{2^-};6.97\right)\middle|\middle|{}^8\text{Be}(J^\pi;E);p\right\rangle \text{ and}$$

$$\times\left\langle {}^9\text{B}\left(\frac{5}{2^-};2.36\right)\middle|\middle|{}^8\text{Be}(J^\pi;E);p\right\rangle .$$

Owing to conservation of total angular momentum, they are strictly zero for the ground state ${}^8\text{Be}(0^+;0)$, but nonzero for the level $|2^+;3.04\text{ MeV}\rangle$. For this reason, in the R-matrix approach the decay of this doublet to the ground state of ${}^9_{\Lambda}$Be is forbidden, but decay to the doublet of the first excited state of ${}^9_{\Lambda}\text{Be}(E=3.08\text{ MeV})$ is allowed.

Nevertheless, decay to the ground state of ${}^9_{\Lambda}$Be can occur as a result of channel coupling due to the f wave of the emitted proton. This effect is automatically taken into account if the CSM is used, as shown in Ref. 90. The decay width in the f wave is given by

$$\Gamma = 2\pi\left|\left\langle[s_\Lambda \otimes {}^8\text{Be}(0^+;0)],f:J\middle|V_{\Lambda N}\middle|\left[s_\Lambda \otimes {}^9\text{B}\left(\frac{7}{2^-};6.97\right)\right]:J\right\rangle\right|^2 .$$

The relation between the p and f channels in this case can be obtained directly from the experimental data without calculation. The needed information[92] is given in Table VI, which contains data on the neutron decay channel of the $J^\pi=\frac{7}{2}^-$ level in the mirror nucleus ^{9}Be.

We see from Table VI that the f wave contributes no more than a few percent to the decay of the nuclear level. The contribution of this wave in the case of hypernuclear decay can be expected to be about the same. Therefore, if

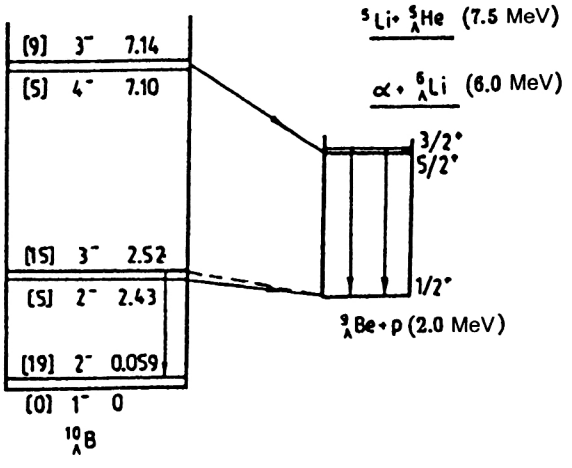

FIG. 4. Decay scheme of low-lying $s_\Lambda p^{-1}$ states of $^{10}_{\Lambda}$B hypernuclei. The population intensities $[N_i]$ (in %), quantum numbers J^π, and excitation energies calculated with the interaction are given.[15] On the right-hand side are the decay thresholds and spectrum of the daughter hypernucleus $^{9}_{\Lambda}$Be.

there is no suppression of the component via which decay occurs in the R-matrix approach, the coupling of the p and f waves realized in the CSM can be neglected.

For low-lying doublets of this and some other hypernuclei, the R-matrix width sometimes turns out to be zero. In this situation the coupling of the two waves is important, as it opens a decay channel. It follows from the data of Table V that the expected width will then be small.

The $|\frac{7}{2}^-;6.97\ \text{MeV}\rangle$ level of ^{9}B has a width of about 2 MeV (Ref. 91). The expected width of this level when ^{9}B is located in a hypernucleus is considerably smaller owing to the decreased energy release; it is estimated[75] to be 400 keV. It should therefore be born in mind that this is the sum of widths of the levels forming a doublet and separated from each other by about 40 keV. The resolution of the neutral-meson spectrometer at BNL[48] should be high enough (300 keV) to determine such a width of a hypernuclear level. This doublet can decay via the channel $\alpha+^{6}_{\Lambda}$Li only via the d component of the relative motion. Owing to the small energy release, we expect an insignificant contribution from this channel.

The decrease of the width of a level of the nuclear core when it is located in a hypernucleus demonstrates the stabilizing role of the hyperon in the s_Λ orbital. The stabilization occurs owing to the raising of the energy of the proton threshold. The stabilizing role of the hyperon in ^{9}B can be traced in all states beginning with the ground state. It is unstable in the absence of the s_Λ hyperon, and turns out to be bound ($B_p=2$ MeV) in its presence. A similar effect also occurs in other hypernuclei ($^{6}_{\Lambda}$He and $^{9}_{\Lambda}$Be).

Here and below we shall not indicate the states of the doublet from and to which a decay occurs. We only note that vector coupling of the angular momenta favors transitions without spin change, i.e., doublet levels with high spin decay primarily into doublet levels of the final hypernucleus which also have high spin.

The doublet $J^\pi=2^-$ and 3^-, $E=2.5$ MeV

The distinguishing feature of this doublet is that it is located just above the threshold (see Fig. 4) for decay via the proton channel. The structure of the wave functions of this doublet can be written schematically as

$$|^{10}_{\Lambda}\text{B}(3^-;2.52)\rangle=\sqrt{0.996}\left|s_\Lambda\otimes{}^9\text{B}\left(\frac{5^-}{2};2.36\right)\right\rangle+\alpha\left|s_\Lambda\otimes{}^9\text{B}\left(\frac{7^-}{2};6.97\right)\right\rangle+\cdots, \quad (25)$$

$$|^{10}_{\Lambda}\text{B}(2^-;2.43)\rangle=\sqrt{0.997}\left|s_\Lambda\otimes{}^9\text{B}\left(\frac{5^-}{2};2.36\right)\right\rangle+\alpha\left|s_\Lambda\otimes{}^9\text{B}\left(\frac{3^-}{2};0.00\right)\right\rangle+\cdots, \quad (26)$$

where the dots again denote components with configurations built on higher states of the ^{9}B nucleus.

Via the principal component of the wave function the level $|2^-;2.43\ \text{MeV}\rangle$ cannot decay through the proton channel to the ground state of $^{9}_{\Lambda}$B, because the fractional parentage coefficient $\langle{}^9\text{B}(\frac{5}{2}^-;2.36)\|{}^8\text{Be}(0^+;0);p\rangle$ is equal to zero. However, owing to deviations from weak coupling [see (26)], the appearance in the wave function of the component $|s_\Lambda\otimes{}^9B(\frac{3}{2}^-;0)\rangle$ makes decay via the proton channel to the $^{9}_{\Lambda}$B ground state possible, because the fractional parentage coefficient $\langle{}^9\text{B}(\frac{3}{2}^-;0)\|\text{Be}(0^+;0);p\rangle$ is nonzero.

Let us now consider the level $|3^-;2.52\ \text{MeV}\rangle$. According to the BSM, it cannot decay to the ground state of $^{9}_{\Lambda}$B. However, proton decay is possible in the CSM. As shown in Ref. 90, in this case strong decay with emission of an f nucleon and width 0.01–0.10 eV is expected. Given this situation, it is necessary to study the alternative possibility of the deexcitation of this state by γ emission. The electromagnetic width of the level can be estimated using the nuclear data on the $J^\pi=\frac{5}{2}^-\to J^\pi=\frac{3}{2}^-$ transition in the mirror nucleus ^{9}Be. According to Ref. 91, the corresponding width due to the M1 transition is only 0.10 eV. The two widths are of the same order, which does not exclude the possibility of hypernuclear deexcitation by the emission of a γ quantum of energy $E_\gamma=2.52$ MeV.

This analysis shows that the decay of $^{10}_{\Lambda}$B levels with configuration $s_\Lambda p^{-1}$ must be accompanied by the emission of a secondary hypernuclear γ quantum of energy $E_\gamma=3.08$ MeV and, possibly, a γ quantum of energy $E_\gamma=2.52$ MeV.

3.2. The hypernucleus $^{14}_{\Lambda}$N

The proton threshold in this hypernucleus is very low ($B_p=2.4$ MeV; see Fig. 5). The levels up to $E=12$ MeV decay only via the proton channel, populating either the ground state or the doublet of the first excited state of $^{13}_{\Lambda}$C. The partial widths Γ_{p0}, Γ_{p1} of proton emission with population of the ground state and the doublet of the first excited state of $^{13}_{\Lambda}$C are given in Table VII.

It follows from the values of the partial widths given in Table VII that the excited-state doublet of $^{13}_{\Lambda}$C($J^\pi=\frac{3}{2}^+$ and $\frac{5}{2}^+$) described by the configuration $|s_\Lambda$

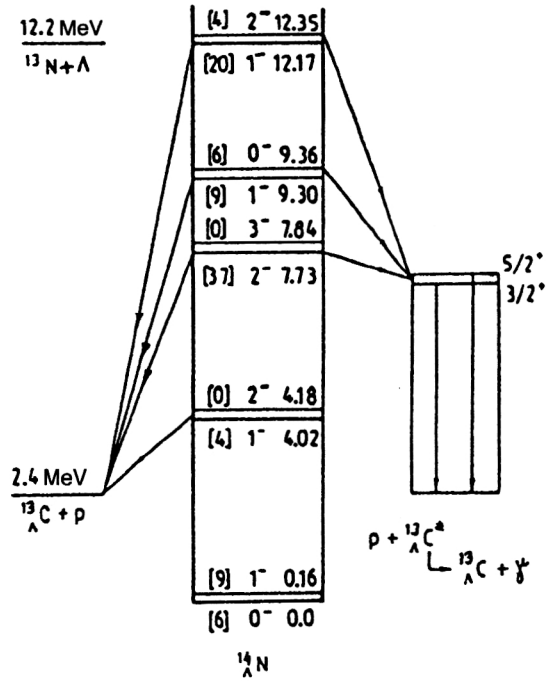

FIG. 5. Decay scheme of low-lying $s_\Lambda p^{-1}$ states of $^{14}_{\Lambda}$N. The population intensities $[N_i]$ (in %), quantum numbers J^π, and excitation energies calculated with the interaction are given.[15]

$\otimes\, ^{12}$C(2$^+$;4.44 MeV)$\rangle$ should be intensely populated. It deexcites with the emission of γ quanta of energies $E_\gamma = 4.68$ and 4.72 MeV.

The picture of the decay of the doublet at $E = 12.3$ MeV in this hypernucleus is unclear. It is located right by the Λ-hyperon emission threshold. Two decay variants are possible depending on where the doublet is actually located:

1. If the doublet lies below the threshold of the Λ channel, decay can only occur via the proton channel and $\Gamma_{p1}/\Gamma_{p0} = 32/13$. In this case it can be expected that a secondary hypernuclear γ quantum of energy $E_\gamma = 4.7$ MeV will appear.

TABLE VII. Partial widths (Γ_{p1} and Γ_{p0}) of the decay of the hypernuclear doublets in $^{14}_{\Lambda}$N via the proton channel with population of the doublet of the excited ($E \approx 4.7$ MeV) and ground states of $^{13}_{\Lambda}$C.

Doublet J^π	E_i, MeV	N_i, %	Principal component of the wave function	Γ_{p1}, keV	Γ_{p0}, keV
0⁻	0.00	6	$\lvert s_\Lambda \otimes ^{13}$N(1/2⁻;0.00)$\rangle$		
1⁻	0.16	9			
1⁻	4.02	4	$\lvert s_\Lambda \otimes ^{13}$N(3/2⁻;3.51)$\rangle$	0	50
2⁻	4.18	0			
2⁻	7.73	37	$\lvert s_\Lambda \otimes ^{13}$N(5/2⁻;7.38)$\rangle$	30	0.3
3⁻	7.84	0			
1⁻	9.30	9	$\lvert s_\Lambda \otimes ^{13}$N(1/2⁻;8.92)$\rangle$	16	17
0⁻	9.36	6			
1⁻	12.17	20	$\lvert s_\Lambda \otimes ^{13}$N(3/2⁻;11.9)$\rangle$	32	13*
2⁻	12.35	4			
	ΣN_i	95			

*See the discussion in the text.

TABLE VIII. Partial widths $\Gamma_{\gamma j}$ (in eV) of the decay into final states $J_j^\pi T_j; E_j$ of the level $J^\pi = 1^+$, $T = 1$; 15.1 MeV of the ^{12}C nucleus and its total γ and α widths (Ref. 91).

$J_j^\pi T_j; E_j$	0⁺0; 0.0	2⁺0; 4.4	0⁺0; 7.6	1⁺0; 12.7	$\Sigma\Gamma_{\gamma j}$	Γ_α	Γ_{tot}
$\Gamma_{\gamma j}$	38.5	0.96	1.09	0.59	41.8	1.8	43.6

2. If the doublet lies above the threshold of the Λ channel, decay can occur also via the Λ channel; however, its width is difficult to calculate reliably. The absolute proton widths remain the same as before.

It should therefore be expected that decay of $^{14}_{\Lambda}$N levels with configuration $s_\Lambda p^{-1}$ must be accompanied by the emission of the secondary γ quanta of the hypernucleus $^{13}_{\Lambda}$C of energy $E_\gamma \approx 4.7$ MeV.

3.3. The hypernucleus $^{13}_{\Lambda}$C

Two groups of states differing by the isospin of the nuclear core ($T = 0$ and $T = 1$) are populated in the reaction of neutron substitution by a Λ hyperon in the hypernucleus $^{13}_{\Lambda}$C. It is well known that in ^{12}C excited states with $T = 1$ are located rather high, $E > 15$ MeV, which is associated with the α-cluster structure of ^{12}C. However, in contrast to the situation in ^{8}Be, the isospin of the $\lvert 1^+1;\ 15.1\ \text{MeV}\rangle$ level in ^{12}C is highly pure: the admixture of the state $\lvert 1^+0;\ 12.7\ \text{MeV}\rangle$ is ~0.6% (Ref. 93). We see from Table VIII that the dominant decay channel is the M1 γ transition to the ground state.

There is no doubt that the $\lvert \frac{1}{2}^+1;\ 15.1\rangle$ resonance in $^{13}_{\Lambda}$C is narrow, because it is located below the threshold for proton emission (16.3 MeV), and strong decays with Λ ($B_\Lambda = 11.7$ MeV) and α-particle ($B_\alpha = 12.4$ MeV) emission are possible only owing to the admixture of states with $T = 0$ (Ref. 94).

Therefore, the intensity of the hypernuclear γ transition $E_\gamma = 15$ MeV can be used to determine the strong-decay width $\Gamma_s = \Gamma_\Lambda + \Gamma_\alpha$ involved in the expression

$$B_\gamma(15) = \frac{\Gamma_\gamma}{\Gamma_\gamma + \Gamma_s}. \tag{27}$$

The phenomenological approach based on the experimental data on the neutron spectroscopic factors found in the reaction ^{13}C$(p,d)^{12}$C allows the cross sections for the production of individual resonances to be set equal:[95]

$$\sigma_{\text{prod}}^{\Delta L=1}\left(\frac{1^+}{2}1;\ 15\ \text{MeV}\right) = 0.5\sigma_{\text{prod}}^{\Delta L=1}\left(\frac{3^+}{2}0;\ 4.6\ \text{MeV}\right) = \sigma_{\text{prod}}^{\Delta L=1}\left(\frac{1^+}{2}0;\ 0\ \text{MeV}\right).$$

The intensity of the corresponding γ quanta $I_\gamma(E_\gamma)$ is simply

$$I_\gamma(4.6\ \text{MeV}) = k\sigma_{\text{prod}}\left(\frac{3^+}{2}0;\ 4.6\ \text{MeV}\right);$$

$$I_\gamma(15\ \text{MeV}) = k\sigma_{\text{prod}}\left(\frac{1^+}{2}11;\ 15\ \text{MeV}\right) \times B_\gamma(15),$$

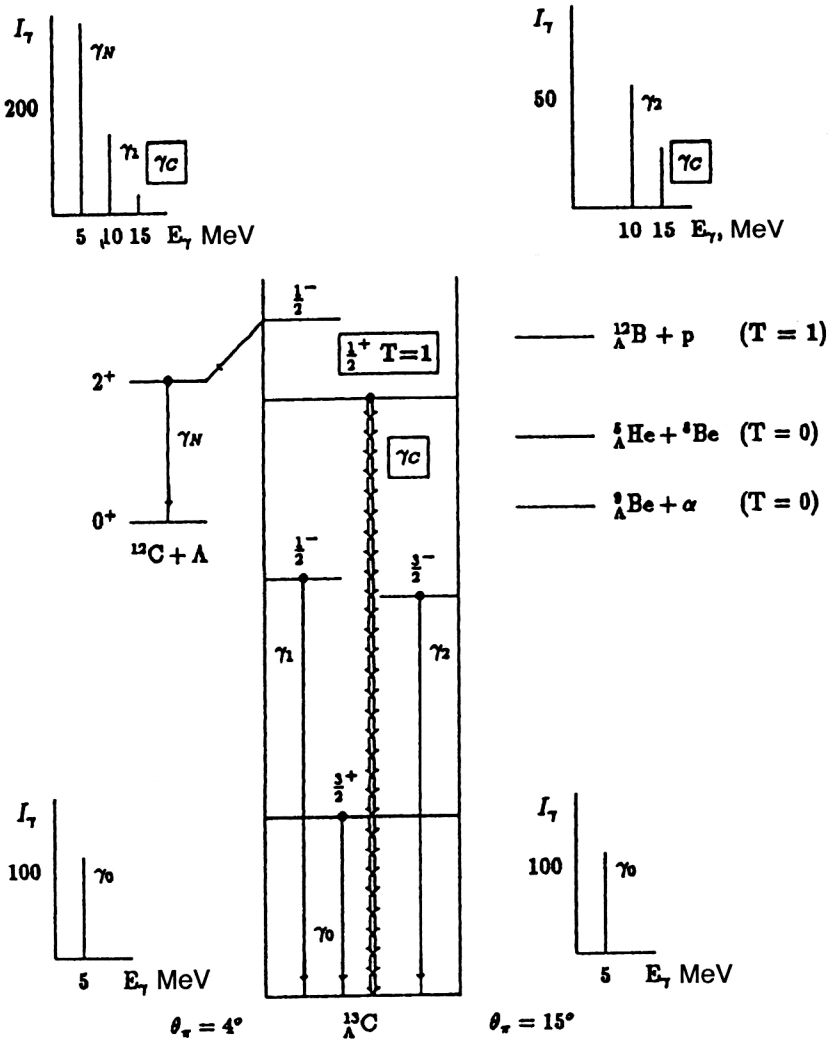

FIG. 6. Spectra of γ quanta in the reaction $^{13}C(K^-,\pi^-\gamma)^{13}_{\Lambda}C^*$ ($p_K=800$ MeV/c) calculated for two scattering angles $\theta_\pi=4°$ (left) and $\theta_\pi=15°$ (right) and two excitation regions $E^*<10$ MeV (bottom) and $E^*>10$ MeV (top). At the center we show the level scheme of $^{13}_{\Lambda}$C and indicate the principle γ transitions.[95]

and for $B_\gamma(15)$ we obtain

$$B_\gamma(15)=2\frac{I_\gamma(15\ \text{MeV})}{I_\gamma(4.6\ \text{MeV})}. \tag{28}$$

However, other levels which can decay by γ emission are also observed in this region of $^{13}_{\Lambda}$C excitation energies. First, these are the $p_\Lambda p^{-1}$ substitution states with $T=0(E\approx 10$ MeV). The results of Ref. 43 (see also Fig. 1), where pion distortion is taken into account, were used to expand the cross section for excitation reactions $\sigma_{\text{prod}}(\theta_\pi,E)$ ($\theta_\pi=4°$, 15°) in multipoles $\sigma^{\Delta L}_{\text{prod}}(J^\pi T;E)$ ($\Delta L=0,1,2$).

The expected spectrum of γ quanta from the reaction $^{13}C(K^-,\pi^-\gamma)^{13}_{\Lambda}C$ at $p_K=800$ MeV/c, $\theta_\pi=4°$, and $\theta_\pi=15°$ (Fig. 6 and Table IX) also include the secondary γ quanta (γ_N) from the reaction

TABLE IX. Intensities of γ transitions (in relative units) expected in the reaction $^{13}C(K^-,\pi^-\gamma)^{13}_{\Lambda}C$.

E_i (MeV)	J^π	$J^\pi_c T$	l_Λ	$\sigma_{\text{prod}}(4°)$, μb/sr	$\sigma_{\text{prod}}(15°)$, μb/sr	γ	$I_\gamma(4°)$	$I\gamma(15°)$
0.0	$\frac{1}{2}^+$	0^+0	s_Λ	41	60			
4.6	$\frac{3}{2}^+$	2^+0	s_Λ	76	111	γ_0	100	100
~10.0	$\frac{3}{2}^-$	0^+0	p_Λ		68	γ_2		61
~10.5	$\frac{1}{2}^-$	0^+0	p_Λ	123		γ_1	162	
15.1	$\frac{1}{2}^+$	0^+1	s_Λ	41	60	γ_C	26	27
~17.0	$\frac{1}{2}^-$	2^+0	p_Λ	850		γ_N	372	

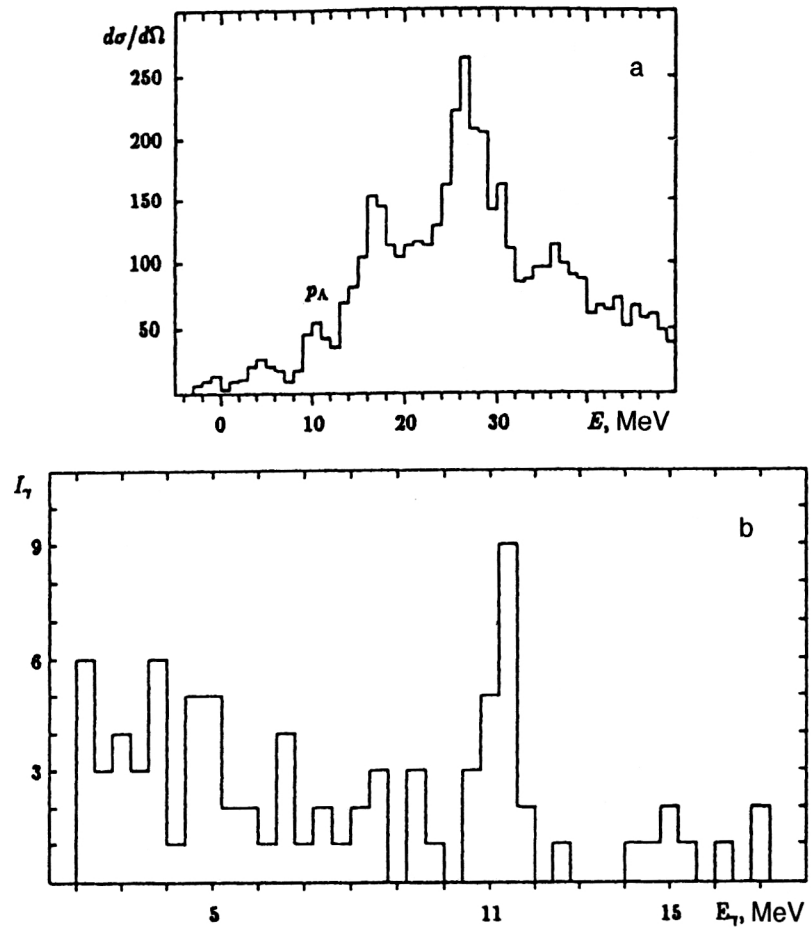

FIG. 7. Preliminary results of the $^{13}C(K^-,\pi^-\gamma)^{13}_{\Lambda}C^*$ experiment.[29] (a) Excitation spectrum; (b) γ spectrum.

$$^{13}C(K^-,\pi^-\gamma)^{13}_{\Lambda}C^*\left(\frac{1}{2^-}0;\ \sim 17\ \text{MeV}\right)$$
$$\rightarrow \Lambda + {}^{12}C^*(2^+0;\ 4.4\ \text{MeV})$$

(see the next section and Tables XI and Tables XII). The γ quanta from cascade transitions to states of $^{13}_{\Lambda}C$ weakly excited in the (K^-,π^-) reaction have not yet been included.

The final analysis of the results of the E781 experiment performed at BNL[29] to determine the one-particle hyperon energies $\varepsilon(p^{\Lambda}_{1/2})$ and $\varepsilon(p^{\Lambda}_{3/2})$ from the γ energies $E_\gamma \sim 10$ MeV (Fig. 7) should also include the unique possibility of estimating Γ_s using Eqs. (27) and (28).

4. DECAY OF HYPERNUCLEAR STATES WITH $p_\Lambda p^{-1}$ CONFIGURATION AND GAMMA DEEXCITATION OF THE DECAY PRODUCTS

States assigned the configuration $p_\Lambda p^{-1}$ are intensely excited in all hypernucleus production reactions:

- In $(K^-_{\text{stop}},\pi^-)$ reactions with stopped kaons;
- In (π^+,K^+) associated production reactions;
- In (K^-,π^-) reactions with strangeness exchange.

Of special interest are reactions with strangeness exchange at small pion emission angles, because they possess high selectivity and small momentum transfer. Of the huge number of possible states with the configuration $p_\Lambda p^{-1}$, only those coresponding to replacement of a neutron by a Λ hyperon ($\Delta L=0$, $\Delta S=0$, $\Delta J=0$) are excited. They practically mimic the spectrum of p-hole levels of the ground state of the target nucleus. As an example, in Fig. 8 we show the experimental hypernuclear excitation spectra obtained in the (K^-,π^-) reaction at angle $\theta_\pi=0°$ (unshaded region). In the same figure we show the region of high excitation energies to which the production of states with configuration $s_\Lambda s^{-1}$ is assigned. We shall discuss them in the following section.

Other levels of multiplets with $J=j_\Lambda+J_N$ are excited under other kinematical conditions. States corresponding to the selection rule $\Delta L=2$ are detected in (K^-,π^-) reactions at large pion emission angle ($\theta_\pi=15°-20°$). The (π^+,K^+) reaction leads primarily to excitation of levels with spin $J=J_N+2$.

In this study we focus our attention on states excited as a result of transitions with the selection rules $\Delta L=0$, $\Delta S=0$, and $\Delta J=0$.

The energy of the ith multiplet of levels with the configuration $p_\Lambda p^{-1}$ is approximately

$$E(p_\Lambda p^{-1};\ i)\approx\varepsilon(p_\Lambda)+E_i(p^{-1}) \tag{29}$$

where $E_i(p^{-1})$ is the excitation energy of the ith state of the nuclear core. Experiments have shown that for $1p$-shell hy-

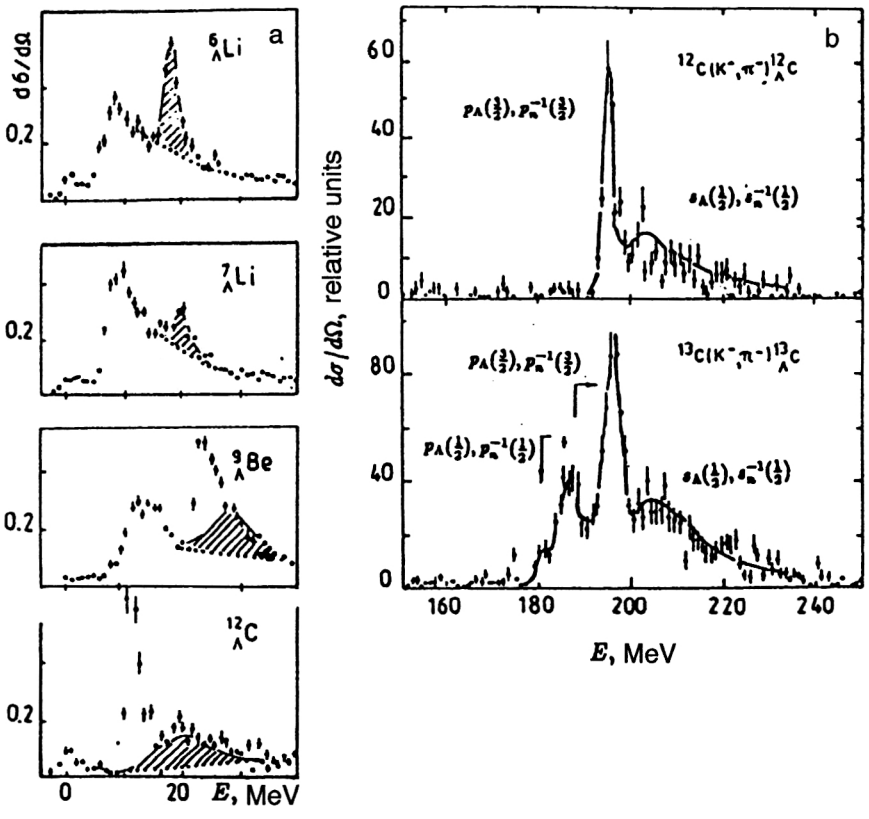

FIG. 8. Excitation cross sections of hypernuclei in the substitution reaction on $1p$-shell nuclei. Resonances with the $s_\Lambda s^{-1}$ configuration are indicated.[99] (a) $p_K = 720$ MeV/c; (b) $p_K = 550$ MeV/c.

pernuclei the energy of the lowest multiplet of states of this type is nearly independent of the number of nucleons A in the nuclear core and is

$$\varepsilon(p_\Lambda) \approx 1\hbar\omega_\Lambda = 10 \pm 1 \text{ MeV}. \tag{30}$$

Practically all levels with the configuration $p_\Lambda p^{-1}$ lie above the baryonic decay threshold. The general regularities of the decay of such states have been analyzed in Ref. 11 using the R-matrix approach based on hypernuclear functions calculated in the TISM on the basis of all states corresponding to the configuration $p_\Lambda p^{-1}$. Let us discuss the main results of that study.

As long as emission into the continuum of the $1p$ hyperon is energetically allowed (here the nucleus remains in the p-hole state) by the principal component of the wave function, this channel will dominate over the nucleon channels or channels for decay with the emission of nuclear clusters or light hyperfragments. The component describing the level in the weak-coupling approximation is the principal one. This situation occurs in hypernuclei at the beginning of the $1p$ shell: ${}^{6}_{\Lambda}$Li, ${}^{7}_{\Lambda}$Li, ${}^{9}_{\Lambda}$Be, ${}^{10}_{\Lambda}$B, and ${}^{11}_{\Lambda}$B. Table X illustrates this for the example of the states of the hypernuclei ${}^{7}_{\Lambda}$Li and ${}^{11}_{\Lambda}$B most intensely populated in the substitution reaction. The calculated sum of the intensities of excitation of all states of a given hypernucleus with the configuration $p_\Lambda p^{-1}$ is taken to be 100%. For example, in ${}^{7}_{\Lambda}$Li there are 17 of them and in ${}^{11}_{\Lambda}$B there are 106.

In odd hypernuclei, for the configuration $p_\Lambda p^{-1}$ there are actually two bands of hypernuclear states corresponding to two values of the isospin of the nuclear core: $T=0$ and $T=1$. This situation also occured for the $s_\Lambda p^{-1}$ configuration of ${}^{13}_{\Lambda}$C. If the isospin of the nuclear core remains a good quantum number, these bands do not mix. In this case hyperon emission must lead to the population of states of the final nucleus with the same isospin as the nuclear core. In particular, after the emission of the Λ hyperon from the hypernuclei ${}^{7}_{\Lambda}$Li and ${}^{11}_{\Lambda}$B the states $J^\pi T = 0^+1$ in ^{6}Li and ^{10}B must be strongly populated, and their deexcitation leads to the emission of a nuclear γ quantum of energy $E_\gamma({}^{6}\text{Li}) = 3.56$ MeV in the first case, and a cascade $E_\gamma({}^{10}\text{B}) = 1.02$ MeV + 0.72 MeV ($J^\pi T = 0^+1 \to 1^+0 \to 3^+0$) in the second. The authors of Ref. 74 reported the detection in the reaction ${}^{7}\text{Li}(K^-,\pi^-){}^{7}_{\Lambda}\text{Li}^*$ of γ emission with $E_\gamma = 3.6$ MeV associated with $E = 10$–16 MeV of the hypernucleus ${}^{7}_{\Lambda}$Li*.

As expected, the calculated widths of Λ-hyperon emission turned out to be large, but a tendency for them to decrease with increasing A can be clearly seen. The decay of the lowest state of hypernuclei of the first half of the $1p$ shell with the configuration $p_\Lambda p^{-1}$ as a result of Λ-hyperon emission populates the ground state of the final nucleus, and the decay of the states above it populates discrete excited states whose deexcitation is associated with γ emission.

The hypernuclei ${}^{9}_{\Lambda}$Be and ${}^{10}_{\Lambda}$B were also studied in Ref. 11. However, since they are not associated with the emission

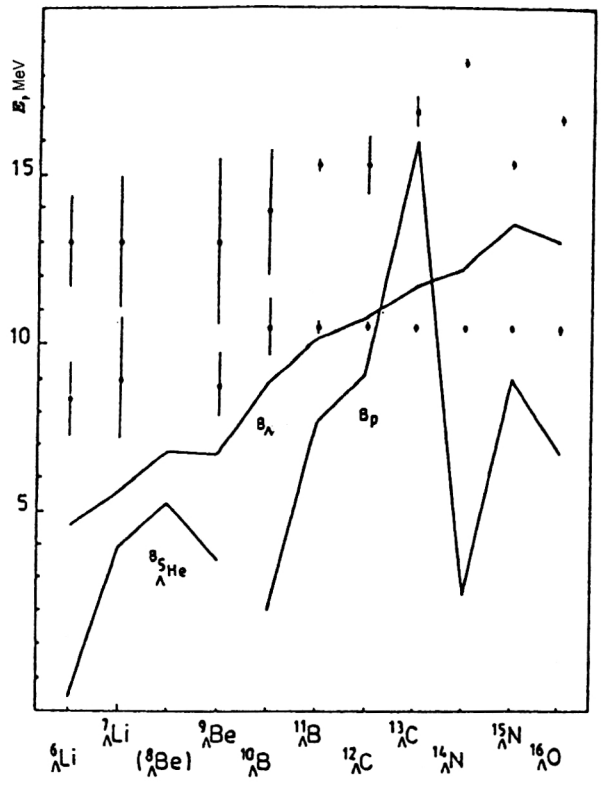

FIG. 9. A dependence of the widths of resonances with the $p_\Lambda p^{-1}$ configuration in $1p$-shell hypernuclei. The solid lines connect the locations of the Λ-hyperon, and also proton and $^5_\Lambda$He, emission thresholds determining the stability of hypernuclei to strong decay.

of a secondary γ quantum because the final nucleus has no bound states, we shall not discuss them here.

As the $1p$ shell is filled and its center is approached, the Λ emission threshold rises; see Fig. 9. The decrease of the energy released in the decay leads to a decrease of the absolute value of the width of hypernuclear states. After the center of the $1p$ shell is passed, the Λ threshold becomes even higher than the lowest state with the configuration $p_\Lambda p^{-1}$. (In $^{13}_\Lambda$C the lowest state of the $p_\Lambda p^{-1}$ configuration is even bound.) This means that the hypernuclear level is located at an energy below the hole level of the nucleus, having formed it in the weak-coupling approximation. From this it follows that Λ decay of the hypernuclear states of the second half of the $1p$ shell described by the configuration $p_\Lambda p^{-1}$ via the principal component of the wave function becomes impossible, because it is forbidden by the configuration. In this case the nucleon channel comes into play and competes with the hyperon channel. Therefore, a second reason for the decrease of the baryonic decay widths is that baryonic decay occurs via the small components in hypernuclei of the second half of the $1p$ shell. For describing the nucleon and even the hyperon channel it is now no longer sufficient to know the gross structure of the wave function of the level.

Admixtures with the dominant component now begin to control the decay. In addition, intruder states which do not participate directly in the hypernuclear production process but, owing to channel coupling, mix with $p_\Lambda p^{-1}$ states, become important. Let us discuss these two points in more detail. The wave function of the ith multiplet of states built on the $p_\Lambda p^{-1}$ configuration of the hypernucleus can be represented as a sum of the wave functions of the weak-coupling basis states. If we restrict ourselves to only the $1\hbar\omega$ excitation band, the full wave function will look like

$$\begin{aligned}|p_\Lambda p^{-1}:J^\pi E\rangle=&|(a_i(\tfrac{1}{2})p_\Lambda(\tfrac{1}{2})+a_i(\tfrac{3}{2})p_\Lambda(\tfrac{3}{2}))\otimes p^{-1};i\rangle\\&+|(a_{i+1}(\tfrac{1}{2})p_\Lambda(\tfrac{1}{2})+a_{i+1}(\tfrac{3}{2})p_\Lambda(\tfrac{3}{2}))\\&\otimes p^{-1};i+1\rangle+|(a_{i-1}(\tfrac{1}{2})p_\Lambda(\tfrac{1}{2})\\&+a_{i-1}(\tfrac{3}{2})p_\Lambda(\tfrac{3}{2}))\otimes p^{-1};i-1\rangle+\cdots\\&+b|s_\Lambda\otimes p^{-2}l\rangle+c|s_\Lambda\otimes s^{-}\rangle.\end{aligned}\tag{31}$$

Here the first component describes the hypernuclear level in the weak-coupling approximation, and i is the order of the p-hole state of the initial target nucleus. The $s_\Lambda p^{-2}l$ configuration is a group of intruder states. These configurations are mixed by the ΛN interaction. These are the so-called "dynamical" correlations in the nucleus. However, the real situation is such that the component forming the level in weak coupling gets a weight greater than 90%: $a_i^2(\frac{1}{2})+a_i^2(\frac{3}{2})>0.9$. We shall not distinguish the $p_\Lambda(\frac{1}{2})$ and $p_\Lambda(\frac{3}{2})$ components, because the spin–orbital splitting of the one-particle levels of the Λ hyperon is small. The other components do not noticeably affect the level location, population intensity, or even decay, if it occurs via the main component.

The role of dynamical correlations associated with the inclusion of intruder states has not yet been analyzed quantitatively. In Ref. 11, where the TISM was used, the wave function (31) automatically included states based on the $s_\Lambda p^{-2}l$ configuration, but only owing to the "kinematical correlations" due to the multiparticle nature of the wave function.

Instead of including intruder states directly in the wave function, the authors of Ref. 96 suggested opening the proton decay channel in a two-stage process: first a particle (hyperon)–hole $p_\Lambda p^{-1}$ state is formed, then, as a result of "inelastic rescattering" due to the ΛN interaction, it becomes a $s_\Lambda p^{-2}l$ state:

$$S(i\to f,l_j)\sim\langle p_\Lambda p^{-1}|V_{\Lambda N}|_\Lambda\varphi;l_j;f\rangle.\tag{32}$$

The dynamical correlations are partially taken into account in this manner. However, we note that neglect of the kinematical correlations in such a schematic treatment can lead to unphysical effects due to the motion of the center of mass of the entire system. Therefore, special care should be taken in the analysis.

It is important to perform a complete diagonalization of the calculation for the example of $^{16}_\Lambda$O, for which there are no great technical obstacles. If complete diagonalization is not used, the effect of kinematical and dynamical correlations can be included using perturbation theory, writing the wave function Ψ_k of the hypernuclear $1\hbar\omega$ excited state schematically as

TABLE X. Levelsofthe ${}^{7}_{\Lambda}$Li and ${}^{11}_{\Lambda}$B hypernuclei strongly populated in the (K^-,π^-) substitution reaction.

${}^{A}_{\Lambda}Z(J^{\pi})$	E_i, MeV	N_i, %	Γ_Λ, MeV	Γ_p, MeV	Principal component of the wave function	E_γ, MeV
${}^{7}_{\Lambda}$Li($\frac{3}{2}^-$)	9.0	72	3.4	0.2	$\lvert p_\Lambda \otimes {}^{6}$Li($1^+0$;0.00)$\rangle$	
	13.0	23	4.0	0.6	$\lvert p_\Lambda \otimes {}^{6}$Li($0^+1$;3.56)$\rangle$	3.56
	ΣN_i	95				
${}^{11}_{\Lambda}$B($\frac{3}{2}^-$)	10.5	44	0.2	0.05	$\lvert p_\Lambda \otimes {}^{10}$B($3^+0$;0.00)$\rangle$	
	12.6	6	1.2	0.06	$\lvert p_\Lambda \otimes {}^{10}$B($1^+0$;0.72)$\rangle$	0.72
	15.3	25	0.4	0.10	$\lvert p_\Lambda \otimes {}^{10}$B($0^+1$;1.74)$\rangle$	0.72+1.02
	ΣN_i	75				

$$\Psi(E;1\hbar\omega)=|p_\Lambda p^{-1}:E\rangle + \Sigma_k \frac{1}{E-E_k}\langle\Psi_k(E)|V_{\Lambda N}|p_\Lambda p^{-1}:E\rangle|\Psi_k\rangle. \quad (33)$$

The summation runs over all states corresponding to $1\hbar\omega$ excitation of the nuclear core. These are nuclear giant dipole resonance states, which have been studied in considerable detail. In this case the interaction with the continuum can be incorporated using R-matrix theory. We shall return to the discussion of rescattering effects at the end of this section.

The dynamics of the variation of the width with increasing A are shown in Fig. 9, where we give the locations of the hypernuclear states with the $p_\Lambda p^{-1}$ configuration in the entire $1p$ shell which are most strongly excited in the (K^-,π^-) substitution reaction. We again note that only kinematical correlations have been taken into account in the calculation. The column height reflects the width of a state. In Fig. 9 we also give the locations of the proton (B_p) and hyperon (B_Λ) thresholds, together with the threshold for emission of the ${}^{5}_{\Lambda}$He hyperfragment, which is the lowest for hypernuclei at the beginning of the $1p$ shell. In this figure we clearly see the tendency for the width to decrease with increasing A. The width of hypernuclear states remains small even in those cases where they are located high in the continuum.

TABLE XI. Levels of the ${}^{13}_{\Lambda}$C, ${}^{14}_{\Lambda}$N, and ${}^{15}_{\Lambda}$N hypernuclei strongly populated in the (K^-,π^-) substitution reaction.

${}^{A}_{\Lambda}Z(J^{\pi})$	E_i, MeV	N_i, %	Γ_Λ, keV	Γ_p, keV	Principal component of the wave function
${}^{13}_{\Lambda}$C($\frac{1}{2}^-$)	10.5	5	0	0	$\lvert p_\Lambda \otimes {}^{12}$C($0^+0$;0.00)$\rangle$
	16.6	29	1000	0	$\lvert p_\Lambda \otimes {}^{12}$C($2^+0$;4.44)$\rangle$
	24.4	7	10	50	$\lvert p_\Lambda \otimes {}^{12}$C($1^+0$;12.71)$\rangle$
	26.2	24	0	60	$\lvert p_\Lambda \otimes {}^{12}$C($1^+1$;15.11)$\rangle$
	27.0	8	60	50	$\lvert p_\Lambda \otimes {}^{12}$C($2^+1$;16.11)$\rangle$
	27.1	7	320	60	$\lvert p_\Lambda \otimes {}^{12}$C($2^+0$;15.44)$\rangle$
	ΣN_i	80			
${}^{14}_{\Lambda}$N(1^+)	10.5	8	0	30	$\lvert p_\Lambda \otimes {}^{13}$N($\frac{1}{2}^-$;0.00)$\rangle$
	18.4	50	140	30	$\lvert p_\Lambda \otimes {}^{13}$N($\frac{3}{2}^-$;7.38)$\rangle$
	21.6	17	20	30	$\lvert p_\Lambda \otimes {}^{13}$N($\frac{1}{2}^-$;11.9)$\rangle$
	ΣN_i	75			
${}^{15}_{\Lambda}$N($\frac{1}{2}^-$)	10.5	13	0	2	$\lvert p_\Lambda \otimes {}^{14}$N($1^+0$;0.00)$\rangle$
	13.0	5	0	12	$\lvert p_\Lambda \otimes {}^{14}$N($0^+1$;2.31)$\rangle$
	13.9	7	8	7	$\lvert p_\Lambda \otimes {}^{14}$N($1^+0$;3.95)$\rangle$
	15.4	11	130	20	$\lvert p_\Lambda \otimes {}^{14}$N($2^+0$;7.03)$\rangle$
	17.9	22	110	30	$\lvert p_\Lambda \otimes {}^{14}$N($2^+1$;9.17)$\rangle$
	20.0	24	65	25	$\lvert p_\Lambda \otimes {}^{14}$N($1^+1$;13.7)$\rangle$
	23.7	8	20	20	$\lvert p_\Lambda \otimes {}^{14}$N($1^+0$;15.2)$\rangle$
	ΣN_i	90			

TABLE XII. Population of levels of daughter nuclei as a result of the decay of $p_\Lambda p^{-1}$ resonances in ${}^{13}_{\Lambda}$C.

Decay channel	$J^\pi_f T_f$	E_f, MeV	I_f, %
$\Lambda+{}^{12}$C	0^+0	0.0	12.5
	2^+0	4.4	19.5
	1^+1	10.3	5.0
	1^+0	12.7	4.0
	1^+1	15.1	5.0
		ΣI_f	46.0
$n+{}^{12}_{\Lambda}$C	1^-	0.00	6
	2^-	0.08	7
	1^-	2.14	2
		ΣI_f	15

The numerical values of the proton and hyperon widths (taking into account only kinematical correlations) for the hypernuclei ${}^{7}_{\Lambda}$Li, ${}^{11}_{\Lambda}$B, ${}^{13}_{\Lambda}$C, ${}^{14}_{\Lambda}$N, and ${}^{15}_{\Lambda}$N are given in Tables X and XI, which also give the population intensities of the corresponding hypernuclear states in the (K^-,π^-) reaction at $\Delta L=0$, the wave function of the level for weak coupling, the populated level of the final system, and the γ quantum expected from deexcitation. The information in Tables XII, XIII, and XIV is arranged differently. There we give the final systems for three hypernuclear decay channels:

- $\Lambda+$ nucleus;

TABLE XIII. Poplation of levels of daughter nuclei as a result of the decay of $p_\Lambda p^{-1}$ resonances in ${}^{14}_{\Lambda}$N.

Decay channel	$J^\pi_f T_f$	E_f, MeV	I_f, %
$\Lambda+{}^{13}$N	$\frac{1}{2}^-\frac{1}{2}^-$	0.0	40.5
	$\frac{3}{2}^-\frac{1}{2}^-$	3.5	13.0
	$\frac{1}{2}^-\frac{1}{2}^-$	8.9	3.0
		ΣI_f	56.5
$p+{}^{13}_{\Lambda}$C	$\frac{1}{2}^+$	0.00	6.5
	$\frac{3}{2}^+$	4.51	3.0
	$\frac{5}{2}^+$	4.51	8.0
	$\frac{1}{2}^+$	10.3	2.0
	$\frac{1}{2}^+$	≈12.7	4.0
	$\frac{3}{2}^+$	≈12.7	4.0
		ΣI_f	27.5

TABLE XIV. Poplation of levels of daughter nuclei as a result of the decay of $p_\Lambda p^{-1}$ resonances in ${}^{15}_{\Lambda}$N.

Decay channel	$J^\pi_f T_f$	E_f, MeV	I_f, %
$\Lambda+{}^{14}$N	1^+0	0.0	26
	0^+1	2.3	18
	1^+1	3.9	6
		ΣI_f	50
$p+{}^{14}_{\Lambda}$C	0^-	0.00	3
	1^-	0.01	17
	1^-	≈4.0	3
	2^-	≈4.0	1
		ΣI_f	24
$n+{}^{14}_{\Lambda}$N	0^-	0.00	2
	1^-	0.01	2
	1^-	3.48	3
		ΣI_f	7

- proton + hypernucleus;
- neutron+hypernucleus.

We also give their populations N_i. The calculated intensity of the population of all states of the primary hypernucleus with the $p_\Lambda p^{-1}$ configuration was taken to be 100%. The population of the states of the decay products is given separately for two energy ranges. These levels account for 82% of the entire intensity in ${}^{13}_{\Lambda}$C, 83% in ${}^{15}_{\Lambda}$N, and 91% in ${}^{14}_{\Lambda}$N. The small difference from 100% is accounted for by the other levels of the produced system.

The neutron channel is manifested significantly in only one hypernucleus, ${}^{13}_{\Lambda}$C, at a level of 15%. It is already half as intense in ${}^{15}_{\Lambda}$N, and even weaker in ${}^{14}_{\Lambda}$N. The proton channel is manifested at a level of 21% in ${}^{13}_{\Lambda}$C, 27% in ${}^{14}_{\Lambda}$N, and 24% in ${}^{15}_{\Lambda}$N.

The results given in Tables XII, XIII, and XIV serve as a rough guide as to what γ radiation can be expected in the population of levels corresponding to the $p_\Lambda p^{-1}$ configuration which are excited in (K^-,π^-) substitution reactions.

4.1. Baryonic decay of ${}^{12}_{\Lambda}$C

The proton decay of low-lying levels of ${}^{12}_{\Lambda}$C has recently been analyzed in detail.[45] However, it is appropriate to re-evaluate the results in light of the new calculations of the locations of the low-lying levels of the final hypernucleus ${}^{11}_{\Lambda}$B into which it decays.

The Λ-decay channel is energetically forbidden for levels of ${}^{12}_{\Lambda}$C lying in the range of excitation energies 9.25–10.1 MeV. This allowed the authors of Ref. 45 to use the negative-pion spectrum to extract information about the relatively small proton widths of three closely spaced resonances with widths $\Gamma(1)=120$ keV, $\Gamma(2)=570$ keV, and $\Gamma(3)=420$ keV. The first two of these proved to be very close in energy ($\Delta E<0.05$ keV), and the third is located about 0.8 MeV lower. The question is, what are the structure and quantum numbers of these levels? What can we learn from further study of the proton decays of these resonances in (K^-,π^-) or (π^+,K^+) reactions?

The authors of Ref. 45 made the natural assumption that the three resonances observed in ${}^{12}_{\Lambda}$C correspond to a single $J^\pi=0^+$ state with configuration $|p_\Lambda(\frac{3}{2})p^{-1}(\frac{3}{2}):0^+\rangle$ and two states with $J^\pi=2^+$ described by a superposition of configurations:

$$\alpha|p_\Lambda\left(\frac{1}{2}\right)p^{-1}\left(\frac{3}{2}\right):2^+\rangle+\beta|p_\Lambda\left(\frac{3}{2}\right)p^{-1}\left(\frac{3}{2}\right):2^+\rangle.$$

In discussing the decay it is necessary to know the scheme of the low-lying levels of ${}^{11}_{\Lambda}$B. The authors[45] used the standard set of hyperon–nucleon interaction parameters.[10] The expected spectrum of ${}^{12}_{\Lambda}$C and its proton decay modes, together with the orbital angular momentum l of the emitted proton and level of ${}^{11}_{\Lambda}$B, shown in Fig. 10, are taken from Ref. 45.

As noted in Ref. 45, it is difficult to explain the proton widths of all three levels. Our views on this question are the following. The Coulomb-barrier penetration factor $P^p_l(E)$ ensures that angular momentum $l=0$ dominates in the decay, while the other partial waves $l=2$ and 4 are suppressed. Since for $l=0$ the $J^\pi=0^+$ level decays into a $\frac{1}{2}^+$ state of the

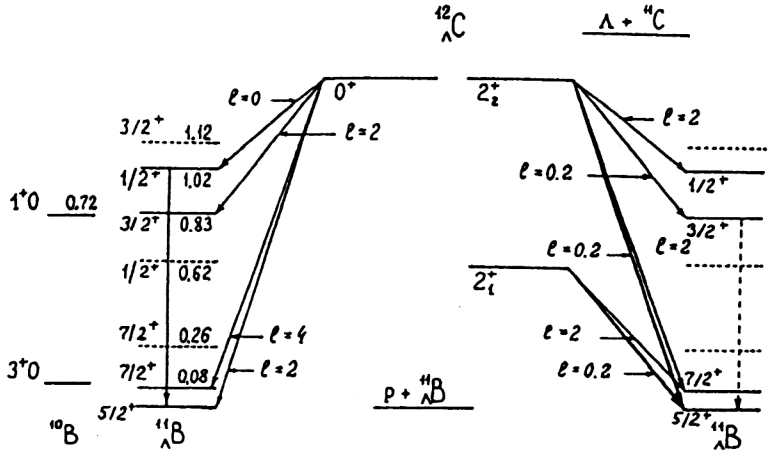

FIG. 10. Part of the excitation spectra of the hypernuclei ${}^{12}_{\Lambda}$C and ${}^{11}_{\Lambda}$B. The location of the ${}^{11}_{\Lambda}$B levels is calculated using two different sets of ΛN interaction parameters, from Ref. 15 (solid lines) and Ref. 10 (dashed lines).

TABLE XV. Partial widths (in keV), calculated in the TIMO (Ref. 11), of baryonic decays of $|p_\Lambda p^{-1}: J_i^\pi\rangle$ resonances of the ${}^{16}_{\Lambda}$O hypernucleus and relative probabilities (in %) of populating excited states of the daughter nuclei. The threshold energies and expected ranges of the energy levels are given in the first column.

	E_i, MeV	10.5		16.7		10.2		15.9		16.9	
	J_i^π	0^+		0^+		2^+		2^+		2^+	
E_f, MeV	J_f^π	Γ_f	I_f	Γ_f	I_f	Γ_f	I_f	Γ_f	I_f	Γ_f	I_f
$p+{}^{15}_{\Lambda}$N 6.71											
0–0.18	$\frac{1}{2}^+$	1	2	0	0	4	9	0	0	0	0
0–0.18	$\frac{3}{2}^+$	11	20	1	1	9	21	2	2	2	2
2.38–2.58	$\frac{1}{2}^+$	2	3	1	1	2	5	0	0	1	1
3.89–4.42	$\frac{1}{2}^+$			15	21			1	1	3	3
4.24–4.71	$\frac{3}{2}^+$			0	0			9	10	7	6
7.10–7.53	$\frac{3}{2}^+$			3	4			9	10	1	1
7.18–7.71	$\frac{5}{2}^+$							1	1	16	15
	Γ_p	14		20		15		22		30	
	I_p		25		27		35		24		29
$\Lambda+{}^{15}$O 13.0											
0.00	$\frac{1}{2}^-$			34	46			4	4	9	8
$n+{}^{15}_{\Lambda}$O 13.2											
0.00	$\frac{1}{2}^+$			1	2			0	0	0	0
	Γ_{tot}	14		55		15		26		39	
	I_{tot}		25		75		35		28		37

hypernucleus ${}^{11}_{\Lambda}$B with energy release $E=0.6$ MeV (for the standard set of parameters), all the widths $\Gamma(i)$ for states with $J^\pi=0^+$ and 2^+ must be comparable, because each $J^\pi=2^+$ level can also decay via the $l=0$ channel. But then why is one of the observed resonances narrow?

The authors of Ref. 45 note that the $J^\pi=0^+$ level would be narrow if the decay energy were lower, i.e., if the $J^\pi=\frac{1}{2}^+$ level in ${}^{11}_{\Lambda}$B were for some reason significantly shifted upward in energy by about 1 MeV.

In Ref. 15 the ${}^{11}_{\Lambda}$B spectrum was calculated with the new set of interaction parameters. The $J^\pi=\frac{1}{2}^+$ level is actually higher, by $E=1.02$ MeV, and so the problem of the incorrect ratio of widths when only the penetration factor $P_l^p(E)$ is included goes away.

Levels analogous to those seen in ${}^{12}_{\Lambda}$C (corresponding to the $p_\Lambda p^{-1}$ configuration and lying above the proton emission threshold but below the Λ emission threshold) are also present in ${}^{14}_{\Lambda}$N and ${}^{16}_{\Lambda}$O. Therefore, experiment itself has presented the problem of the systematic inclusion of intruder states in the description of the decay of states of the $p_\Lambda p^{-1}$ configuration.

In light of our discussion of the partial widths and decay of the low-lying states of ${}^{12}_{\Lambda}$C, it appears important to measure the excitation function of this special group of levels with high resolution (and also for ${}^{14}_{\Lambda}$N and ${}^{16}_{\Lambda}$O) and to experimentally determine the nature of the deexcitation of the corresponding states of ${}^{11}_{\Lambda}$B in coincidence with ${}^{12}_{\Lambda}$C production in this energy range.

4.2. Baryonic decay of ${}^{16}_{\Lambda}$O

In Ref. 96 in discussing the decay of the $J^\pi=0^+$ states of ${}^{16}_{\Lambda}$O, it was suggested that the ground state in ${}^{15}_{\Lambda}$N is the state with $J^\pi=\frac{3}{2}^+$. However, not all the sets of hyperon–nucleon interaction parameters lead to this result. This state may turn out to lie above its $\frac{1}{2}^+$ partner in a doublet, as suggested by calculations with the parameter set proposed in Ref. 15. Then, if the decay really follows the scenario proposed in Ref. 96, but the $\frac{3}{2}^+$ level is not the ground state, we should expect an intense yield of γ quanta associated with the $\frac{3}{2}^+\to\frac{1}{2}^+$ transition between the states of the ground-state doublet. According to the parameters given in Ref. 15, the expected separation of the doublet states is $\Delta E=180$ keV.

The baryonic decay scheme of ${}^{16}_{\Lambda}$O obtained using the TISM[11] is given in Table XV for both $\Delta L=0$ and $\Delta L=2$ transitions. The calculation was performed taking into account only kinematical correlations, which open the nucleon decay channel. The proton channel accounts for $I_p=52\%$ of the intensity of $\Delta L=0$ transitions, and the neutron channel for $I_n=2\%$.

The neutron channel is discussed in Ref. 89 within the framework of the CSM. The authors concluded that the coupling between the Λ and nucleon channels works such that the most intense channel for a level with configuration $p_\Lambda p^{-1}$ is the channel ${}^{16}_{\Lambda}\text{O}\to{}^{15}_{\Lambda}\text{O}(1/2^+)+n$. Its contribution to the width of the level with configuration $|p_\Lambda p^{-1}:0^+\rangle$ was 58%, which differs sharply from the predictions of

TABLE XVI. Relative probabilities for emission of a Λ hyperon, a proton, and a correlated Λp pair.

	E_R, MeV	$W(\Lambda)$	$W(p)$	$W(\Lambda p)$
${}^{6}_{\Lambda}$Li	8.5	69	4	27
${}^{14}_{\Lambda}$N	8.7	57	31	12

R-matrix theory. This difference is attributed to rescattering associated with the $2s$ wave. Here we see that the $2s$ wave is important, in contrast to the result in Ref. 11 for the proton channel.

4.3. The two-baryon decay channel of hypernuclear resonances

In the preceding sections we discussed one-baryon and some cluster decays of hypernuclei. Here we want to point out the possibility of decay of a hypernuclear resonance with the simultaneous emission of a two-baryon system ΛN (Ref. 97). Although in the free state the ΛN pair is not bound, inside the hypernucleus it can be sufficiently compact that it can pass as a single object through the barrier to the outside. Without going into the details of the dynamics of formation of a correlated baryon pair in a hypernucleus, which is analogous to the mechanism of decay of an ordinary nucleus with emission of a correlated NN pair (a dineutron or diproton[98]), we can estimate the probability for this type of decay for the example of $p_\Lambda p^{-1}$ substitution resonances using the formalism of the R-matrix theory and the fractional parentage coefficients of the separation of a ΛN pair from the $1p$ shell of the hypernucleus. Here the final nucleus will be produced in low-lying states, and the ΛN pair will be emitted into the s or d states of relative motion.

Two-baryon decay can occur in the hypernuclei ${}^{6}_{\Lambda}$Li, ${}^{10}_{\Lambda}$Be, ${}^{10}_{\Lambda}$B, and ${}^{14}_{\Lambda}$N, in which there are sufficiently strong resonances above the two-baryon threshold. The importance of the two-baryon decay channel is already indicated by the ratio of the spectroscopic amplitudes:

$$SA(\Lambda):SA(N):SA(\Lambda N)=1:(\sqrt{2}/A):(1/\sqrt{2}). \qquad (34)$$

The relative probabilities of emission of Λ, N, and Λp pairs taking into account the barrier penetration factor are given in Table XVI for the strongest substitution resonances in the (K^-,π^-) reaction on ^{6}Li and ^{14}N.

The decay of ${}^{10}_{\Lambda}$B is like that of ${}^{14}_{\Lambda}$N: the Λp pair is emitted in both the s and the d states of relative motion, while for ${}^{10}_{\Lambda}$Be the Λn pair is produced in the s state. We see from Table XVI that there is a sizable probability for two-baryon decay, and an attempt can be made to find it. Study of decays with the emission of a ΛN pair can give information about the structure of the hypernuclear resonance and the ΛN interaction in states with definite orbital angular momentum.

5. DECAY OF HYPERNUCLEAR STATES WITH THE $s_\Lambda s^{-1}$ CONFIGURATION

A region which can be interpreted as excitation of a $1s$ hole in the nuclear core is clearly manifested in the (K^-,π^-) substitution reaction on $1p$-shell nuclei (Fig. 8).[38,99] The corresponding maxima are seen most clearly in the ${}^{6}_{\Lambda}$Li and ${}^{7}_{\Lambda}$Li excitation spectra. As the atomic number A increases the maxima broaden significantly and their intensity falls, which is naturally related to the enhancement of the role played by the outer nucleons in hypernucleus production.

Let us first discuss the situation regarding $1s$-hole states of ordinary $1p$-shell nuclei. They have been studied much less than $1p$-hole states. They are characterized by a large energy spread.[100] In nuclei at the end of the $1p$ shell the energy of $1s$-hole states covers the range 50–60 MeV, which even exceeds the limit of the optical potential usually used in the calculations.

The large width of a $1s$-hole state indicates that it is widely spread over states with complex configurations. Calculations using the BSM[101] show that the inclusion of all configurations only in the $1\hbar\omega$ excitation band is insufficient for explaining the observed width. An important additional source of the spread may be polarization of the valence shell due to the sudden appearance of a deep hole, which leads to the appearance of a large number of soft particle–hole pairs. As a result, part of the nucleons of an outer shell can be disordered, which disrupts the Young tableau of the valence nucleons.[102] All these questions need to be considered together.

Important information on the nature of these states can be obtained from hypernuclei in which a $1s$-nucleon hole is formed in a softer regime. In a hypernucleus there also may be a stabilizing effect from an s_Λ hyperon, as a result of which the degree of concentration of the purely hole component in real states is higher than in ordinary nuclei.

Information on the $1s$-hole state can be obtained by performing coincidence experiments to record the decay products. In ordinary nuclei, there is a sizable probability for the excitation of a $1s$ hole to be accompanied by star decay. This follows from the experimental data on the absorption of photons with energy above the dipole resonance in nuclear emulsions. For example, the photodisintegration of ^{12}C with formation of a $1s$ hole leads to final products like ^{8}Be$+{}^{3}$H$+p$. As shown in Ref. 103, here the ^{8}Be nucleus is produced not only in the ground state but also in an excited state, which should be followed by γ deexcitation. Therefore, the role of direct coincidence measurements can to some degree be played by experiments to detect the γ deexcitation of the products of star decay.

Let us now turn to hypernuclei. The hypernuclear wave function corresponding to a $1s$-hole state of the nuclear core can be written schematically as

$$\begin{aligned}|s_\Lambda s^{-1}:[f](\lambda\mu)J^\pi TE\rangle = c|s_\Lambda\otimes s^3[3],p^k[f_p]:[f](\lambda\mu)J^\pi T\rangle \\ +b|s_\Lambda\otimes s^4[4],p^{k-2}[f''_p],l:[f] \\ \times(\lambda\mu)J^\pi T\rangle + a|p_\Lambda \\ \otimes s^4[4],p^{k-1}[f'_p]:[f](\lambda\mu)J^\pi T\rangle,\end{aligned} \qquad (35)$$

where we have omitted all components above $1\hbar\omega$ in the excitation band, and also the components corresponding to

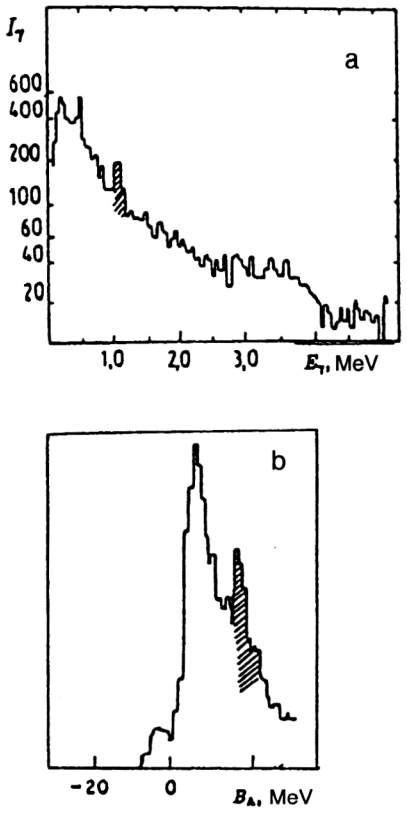

FIG. 11. (a) Cross section of the reaction $^7\mathrm{Li}(K^-,\pi^-\gamma)^7_\Lambda\mathrm{Li}^*$ ($p_K=820$ MeV/c). (b) γ yield from $^4_\Lambda\mathrm{He}^*$ (Ref. 74).

complete Young tableau $[f]$ and quantum numbers $(\lambda\mu)$ differing from the purely $1s$-hole state. The first component determines the decay via cluster channels, the second via the nucleon channel, and the third via the hyperon channel.

If the spread of the hole state is small ($c\approx 1$), a narrow resonance is observed, as occurs in the case of $^6_\Lambda\mathrm{Li}$ and $^7_\Lambda\mathrm{Li}$ (see Fig. 8). A broad maximum should be expected in the limit of very strong coupling of the hole configuration to more complex ones ($c\ll 1$). When the spread is large it is natural to expect that the system breaks up into a large number of composite particles, while in the intermediate case we can expect the formation of $^4_\Lambda\mathrm{He}$ and a residual nucleus containing k nucleons. If the hyperon sticks to the outer nucleons, then ^{3}He and a hyperfragment containing k nucleons can be observed in the final state.

In the (K^-,π^-) reaction on ^{7}Li in the recoilless kinematics, a yield of $^4_\Lambda\mathrm{He}^*$ has been observed[74] from the high-energy excitation region of the $^7_\Lambda$Li hypernucleus ($E=22$–39 MeV) by detection of the γ deexcitation of the produced hyperfragment. In Fig. 11 we show the intensity of hypernucleus production in the high-energy region and the intensity of $^7_\Lambda$Li production accompanied by the γ emission of $^4_\Lambda$He.

A γ-quantum yield has also been observed[79] in the production of $^{10}_\Lambda$B with high excitation energy. As shown in Ref. 80, the decay of the $1s$-hole state of this hypernucleus leads to the formation of a $^7_\Lambda$Li hyperfragment in an excited state. In ^{10}B nearly all the "strength" of the $(8/9)s^{-1}$ hole comes from the configuration with Young tableau $[f]=[432]$ (see Table III). If we assume that the state $|s_\Lambda\otimes s^3p^6[432]^{24}D{:}[442](22)3^+\rangle$ preserves its individuality, the selection rules in the quantum numbers $[f]$ and $(\lambda\mu)$ (Ref. 104) explain the suppression of energetically favorable channels. Decay via the channels $p+^9_\Lambda\mathrm{Be}$ and $^5_\Lambda\mathrm{He}+\alpha+p$ is possible only when the nucleon orbital function possesses the symmetry $[f]=[441]$. Since a pair of nucleons carries off three oscillator quanta, the deuteron cannot be found in the s-wave state of the relative motion. This means that decay with the emission of a three-nucleon cluster ^{3}He with population of the excited state $^7_\Lambda\mathrm{Li}^*$ ($L=2$) is most probable. (This is favored by the total and orbital angular momenta of the target nucleus, $J=3$, $L\geq 2$). The secondary γ quanta serve to label the decay sequence:

$$
\begin{aligned}
&^{10}_\Lambda\mathrm{B}(s_\Lambda s^{-1}{:}3^+)\rightarrow 3\mathrm{He}+^7_\Lambda\mathrm{Li}^*(7/2^+,\ 5/2^+)\\
&\qquad ^7_\Lambda\mathrm{Li}^*(7/2^+,\ 5/2^+)\rightarrow ^7_\Lambda\mathrm{Li}^*(3/2)+\gamma_1\\
&\qquad ^7_\Lambda\mathrm{Li}^*(3/2^+)\rightarrow ^7_\Lambda\mathrm{Li}(1/2^+)+\gamma_2 .
\end{aligned}
\tag{36}
$$

Our interpretation (see Fig. 12) of the data of Ref. 79 is based on this chain of transformations. We attribute the observed γ line with $E_\gamma=440$ keV to the transition $^{14}S_{\frac{3}{2}}\rightarrow{}^{12}S_{\frac{1}{2}}$ in $^7_\Lambda$Li. The detection of the γ quantum of the $5/2^+\rightarrow 1/2^+$ transition already known with $E_\gamma=2.03$ MeV supports our proposed identification of the strong decay channel.

It was noted in Ref. 90 that in the decay of the $1s$-hole states of $^{12}_\Lambda\mathrm{C}$ and $^{16}_\Lambda\mathrm{O}$, the hyperfragments $^9_\Lambda$Be and $^{13}_\Lambda$C can be in an excited state as a result of ^{3}He emission. The fractional parentage coefficients governing the decay determine the ratio of the populations of the excited ($L_c=2$) and ground ($L_c=0$) states. This ratio is 5:4 and 5:1 for the cases

$$^{12}_\Lambda\mathrm{C}((\lambda\mu)=(04))\rightarrow{}^9_\Lambda\mathrm{Be}((\lambda\mu)=(40))+{}^3\mathrm{He}$$

and

$$^{16}_\Lambda\mathrm{O}((\lambda\mu)=(00))\rightarrow{}^{13}_\Lambda\mathrm{C}((\lambda\mu)=(04))+{}^3\mathrm{He},$$

respectively. We should therefore expect hypernuclear γ quanta with energy $E_\gamma=3$ MeV ($^9_\Lambda$Be) and $E_\gamma=4.7$ MeV ($^{13}_\Lambda$C).

Therefore, the structural selection rules in the quantum numbers $[f]$ and $(\lambda\mu)$ based on the assumption of small fragmentation of the $s_\Lambda s^{-1}$ state give a completely natural interpretation of the features observed in the decay of highly excited states of the primary hypernucleus.

The results of Tamura's careful analysis[81] of the yield of $^5_\Lambda$He, $^4_\Lambda$He, $^4_\Lambda$He*, and $^4_\Lambda$H* hyperfragments from $1p$-shell hypernuclei produced in the reaction $(K^-_{\mathrm{stop}},\pi^-)$ should determine the role played by the resonance and statistical mechanisms.[105]

The localization of the characteristic decay channels in a narrow energy range provides convincing proof of the survival of the $s_\Lambda s^{-1}$ resonance in the hypernucleus. This localization will be checked experimentally in the near future, for example, at CEBAF by detecting "tagged" γ quanta from $^4_\Lambda$H* in the reaction $(\gamma,K^+\gamma_{1.1\ \mathrm{MeV}})$. Another method might be identification of hyperfragments, products of the

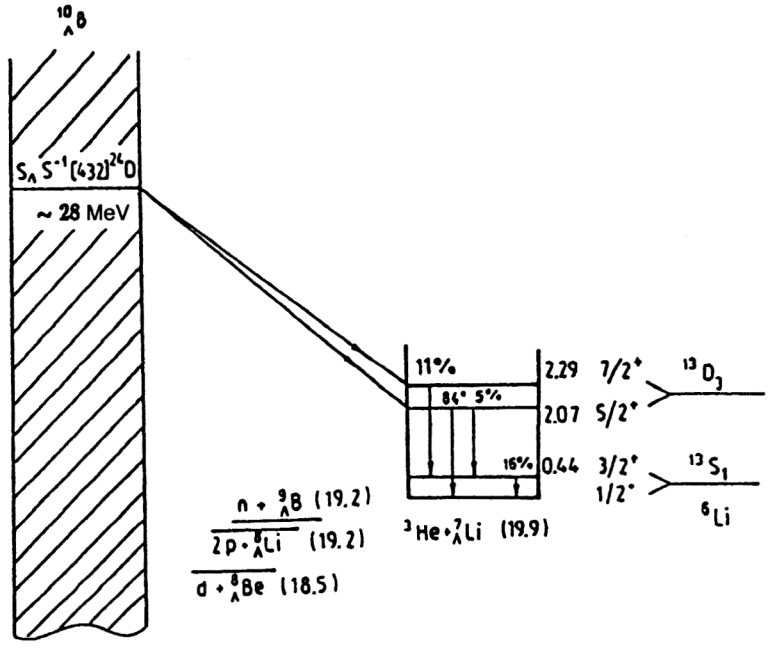

FIG. 12. Predicted γ cascade of ${}^{7}_{\Lambda}\mathrm{Li}^{*}$ accompanying the decay of the $s_{\Lambda}s^{-1}$ resonance in ${}^{10}_{\Lambda}\mathrm{B}$ (Ref. 79).

breakup of the primary hypernucleus, with simultaneous determination of its excitation energy, which has been included in the program of the second stage of hypernuclear studies at FINUDA. This will significantly extend the information obtained by the Tamura technique.[82]

In ending our discussion of the decay of hypernuclear states with the $s_{\Lambda}s^{-1}$ configuration, we recall that deep nucleon holes affect processes of double $\Lambda\Lambda$-hypernucleus production,[106] and also the production of pairs of hypernuclei[107] in the reaction $\Xi^{-}_{\mathrm{stop}}+{}^{12}\mathrm{C}\rightarrow{}^{9}_{\Lambda}\mathrm{Be}+{}^{4}_{\Lambda}\mathrm{He}$.

6. COMPARISON WITH THE RESULTS OF THE SHELL MODEL INCLUDING THE CONTINUUM AND BOUND STATES

Up to now we have studied the decay properties of hypernuclear resonances in the continuum using the multiparticle shell model with bound one-particle states (the BSM). This approach allows us to include a large number of basis states in the calculation of the hypernuclear structure, and to take into account the fragmentation of different types of particle–hole excitations fairly completely. When making a comparison with experiment, the line spectrum of hypernuclear excitations obtained in the BSM by diagonalizing the energy matrices is usually smeared in accordance with the width of each resonance and the detector resolution. However, when this is done the possibility of obtaining a unified description of resonance and quasifree processes inherent in systems with a continuum is lost. Actual calculations show that quasifree processes can significantly change the energy dependence of the excitation function. In R-matrix calculations of the resonance widths one is forced to use parameters which are not very well defined: the channel radii. These features of the BSM make it necessary to justify the use of the BSM in the continuum region. This served as the starting point for the development of the shell model with one-particle potential of finite depth, which takes into account continuum states directly (the CSM).

A unified theory of reactions in the continuum has been developed in greatest detail in Ref. 108, and it has found a natural application in the physics of hypernuclei. Several methods have been worked out for the approximate solution of the general equations of the unified theory in conjunction with the shell approach.[86,109,110] The treatment of the channel coupling in the continuum using the shape-resonance approximation makes it possible to justify the regularities of shell calculations of the compound-resonance structure using the BSM and the R-matrix technique of calculating the decay widths.

The wave function of A baryons at energy E in the channel c is written as

$$\Psi^{c(+)}_{E}=\sum_{j=1}^{n} b^{c}_{E}(j)\Phi_{j}+\sum_{i=1}^{m}\int_{\varepsilon_i}^{\infty} dE a^{c}_{E}(E,i)\chi^{i(+)}_{E}, \qquad (37)$$

where the first term contains only bound states and the second contains one particle in the continuum, and ε_i is the threshold energy in the channel i. The details of the formalism for solving multichannel Schrödinger equations and constructing the S matrix can be found in the original studies. To simplify the calculations, the system of channel equations is usually solved with zero-radius spin-dependent ΛN interaction:

$$V_{ij}=-V_0\delta(\mathbf{r}_i-\mathbf{r}_j)(a+bP^{\sigma}_{ij}). \qquad (38)$$

This method has been used to calculate the hypernuclear excitation functions in (K^{-},π^{-}) reactions on the nuclei ${}^{12}\mathrm{C}$, ${}^{14}\mathrm{C}$, ${}^{14}\mathrm{N}$, and ${}^{10}\mathrm{O}$, and in (π^{+},K^{+}) reactions on ${}^{12}\mathrm{C}$, ${}^{16}\mathrm{O}$, ${}^{28}\mathrm{Si}$, and ${}^{56}\mathrm{Fe}$ (Refs. 59, 87, 110, and 111). Here we shall give only some of the results of the calculations of the reac-

tion cross sections for light nuclei taking into account the continuum. The calculated excitation function of $^{12}_{\Lambda}$C in the (K^-,π^-) reaction with simple hole states of the nuclear core ^{11}C, $|p^{-1}(\frac{3}{2})\rangle$ and $|s^{-1}(\frac{1}{2})\rangle$, give a good reproduction of the experimental data[112] at $p_K \simeq 715$ MeV/c and $\theta_\pi \sim 0° - 15°$. The intensities found for the substitution resonances are roughly the same as in the BSM calculations, and the contribution of the quasifree process increases gradually with increasing momentum transfer, from 23% at $\theta_\pi \sim 0°$ to $\approx 70\%$ at $\theta_\pi \sim 15°$.

Let us now consider the 0^+ and 1^+ substitution resonances in the (K^-,π^-) reaction on ^{14}C and ^{14}N, which have been studied using the BSM[50] and the CSM.[87,88] Although thin ^{14}C targets are not suitable for (K^-,π^-) reactions (a ^{14}N target is good), it is interesting to study these examples in order to compare the BSM and CSM results.

For studying the spectra of the daughter hypernuclei it is useful to understand the population of the hypernuclear levels in the nucleon decay of the initial hypernucleus, and also the branching ratio of the Λ-hyperon and nucleon channels. Calculations using translationally invariant BSM 0^+ $p_\Lambda p^{-1}$ states (10 basis functions for isospin $T=\frac{1}{2}$ and 4 for isospin $T=\frac{3}{2}$) showed that the partial widths depend on the ΛN-interaction radius and also on the ratio of Slater integrals $F^{(2)}/F^{(0)}=r$. Although for the standard interaction $r=2.8$ (Ref. 43), the smaller value $r=0.2$ corresponding to a quite large ΛN-interaction radius is possible. The CSM calculation included 12 channels corresponding to the ground and low-lying levels of ^{13}C, $^{13}_{\Lambda}$C, and $^{13}_{\Lambda}$B. The 0^+ resonances of $^{14}_{\Lambda}$C at ~ 11, ~ 14, and ~ 25 MeV dominate in both approaches. The decay scheme and the partial widths calculated in the BSM and the CSM are given in Fig. 13 and Table XVII. We see that as r decreases, the probability for decay via the neutron channel grows, and that the probability of populating the $\frac{3}{2}^+,\frac{5}{2}^+$ doublet in $^{13}_{\Lambda}$C also increases. The CSM model gives a noticeable enhancement of the neutron decay channel compared to the Λ channel for the resonance at 14 MeV and a large probability for populating the $\frac{3}{2}^+$ state for the resonance at 11 MeV. This is obviously due to the effect of the continuum. The very small probability of populating the $\frac{5}{2}^+$ level of $^{13}_{\Lambda}$C given by both the BSM and the CSM can be attributed to the smallness of the corresponding spectroscopic factor. These results show that for sufficiently intense kaon beams, in the (K^-,π^-) reaction on ^{14}C it would be possible to observe characteristic lines in the spectrum of neutrons and γ quanta from the $\frac{3}{2}^+ \to \frac{1}{2}^+$ (ground state) transition in $^{13}_{\Lambda}$C.

If the isospin (T) mixing of channels is neglected, the decay of the highest resonance $|^{14}_{\Lambda}\mathrm{C}(0^+,T=\frac{3}{2})\rangle$ via the Λ channel is strictly forbidden. Decay can occur only to the $T=1$ states of $^{13}_{\Lambda}$C and $^{13}_{\Lambda}$B with the emission of a neutron or a proton. The CSM calculations including the Coulomb isospin mixing of states reveal a small violation of the isospin symmetry: only 0.1% of the decay prob21ability can be attributed to the Λ channel.

The dominant 1^+ resonances of $^{14}_{\Lambda}$N and the probabilities for their decay via the hyperon and proton channels calculated in the CSM are shown in Fig. 14. The most intense resonance, which has the structure $|p_\Lambda(\frac{3}{2})\otimes {}^{13}\mathrm{N}(\frac{5}{2}^-;7.4)\rangle$, decays with Λ emission to the ground state of ^{13}N ($\sim 53\%$) and partially to the excited $\frac{5}{2}^-,\frac{3}{2}^-$ doublet ($\sim 27\%$), which should lead to the subsequent emission of nuclear γ quanta. About 20% of the probability can be attributed to the proton

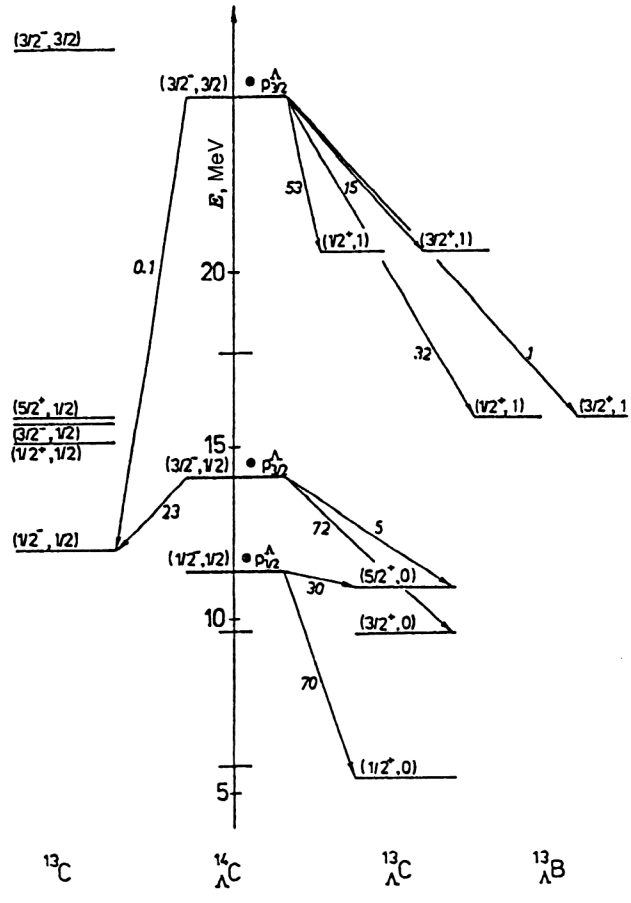

FIG. 13. Excitation spectrum and decay channels of 0^+ resonances in $^{14}_{\Lambda}$C. The arrows off to the side indicate the decay widths (in %) calculated in the CSM (Ref. 111).

TABLE XVII. Comparison of the results of the BSM (B is the standard interaction, $r=2.8$, B' is the modified interaction, $r=0.2$) and CSM (C) calculations of the decay probabilities (in %) of 0^+ resonances of $^{14}_{\Lambda}$C and 1^+ resonances of $^{14}_{\Lambda}$N via nucleon channels with population of $^{13}_{\Lambda}$C levels and via the hyperon channel.

			$^{13}_{\Lambda}$C		^{13}C(^{13}N)		
Hypernucleus	State		$\frac{1}{2}^+$	$\frac{3}{2}^+$	$\frac{5}{2}^+$	$\frac{1}{2}^-$	$\frac{3}{2}^-$
$^{14}_{\Lambda}$C	$p_\Lambda(\frac{1}{2})\otimes\frac{1}{2}^-$	B	100.0	0.0	0.0		
		B'	98.5	0.0	1.5		
		C	70.0	0.0	30.0		
	$p_\Lambda(\frac{3}{2})\otimes\frac{3}{2}^-$	B	7.0	11.4	0.8	80.0	
		B'	12.6	20.5	1.5	65.4	
		C	0.0	72.0	5.0	23.0	
$^{14}_{\Lambda}$N	$p_\Lambda(\frac{1}{2})\otimes\frac{1}{2}^-$	B	68.1	25.3	6.6		
		B'	68.1	25.3	6.6		
		C	59.0	11.0	30.0		
	$p_\Lambda(\frac{3}{2})\otimes\frac{5}{2}^-$	B	0.3	13.2	0.3	70.0	16.2
		B'	0.6	34.6	0.7	51.1	13.0
		C	1.0	14.0	5.0	53.0	25.0

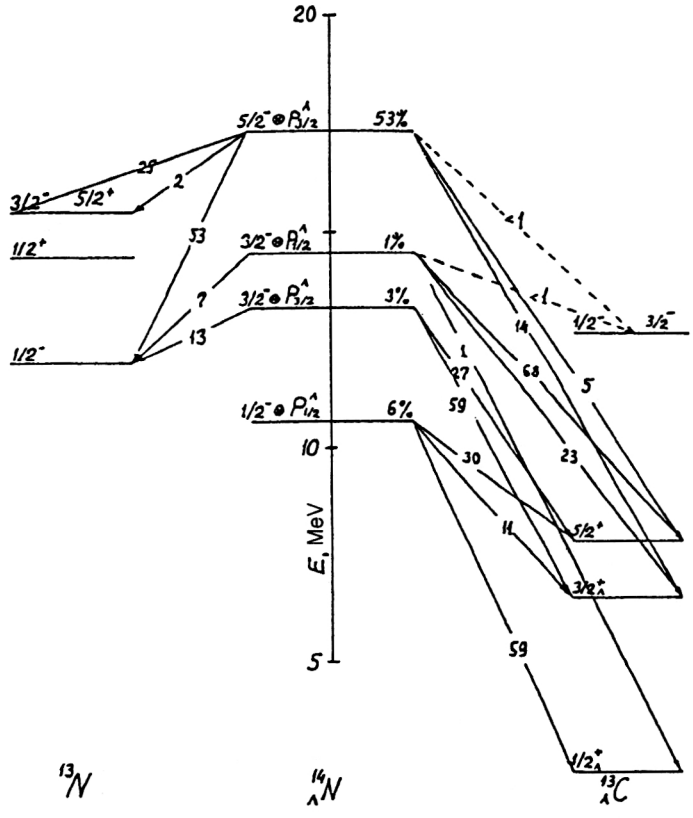

FIG. 14. Excitation spectrum and decay channels of 1^+ resonances in ${}^{14}_{\Lambda}$N. The arrows off to the side indicate the decay widths (in %) calculated in the CSM (Ref. 88).

channel with population of the $\frac{5}{2}^+,\frac{3}{2}^+$ doublet in ${}^{13}_{\Lambda}$C, the deexcitation of which should produce hypernuclear γ quanta. The excitation intensities and partial decay widths of 1^+ resonances calculated in the BSM and the CSM are compared in Table XVII. We see that the two approaches give similar results, which serves as good justification for trusting the BSM calculations.

One of the other methods of including the continuum is that of Kapur and Peierls,[113] which is used in the cluster and shell models of hypernuclei.[114] In this approach, the diagonalization of the Hamiltonian and the subsequent calculations of the effective numbers of neutrons in the (K^-,π^-) and (π^+,K^+) reactions were performed using a special boundary condition on the Λ-hyperon wave function (a diverging spherical wave) for a given channel radius. This makes it possible to describe resonance decay via the Λ channel. Another variant of the CMS including recoil of the nuclear system has been developed by Halderson.[15] It allows the (K^-,π^-) and (π^+,K^+) reactions with large momentum transfer to be described more accurately than in the standard model. The system of coupled excitation channels of ${}^{7}_{\Lambda}$Li and ${}^{16}_{\Lambda}$O in the (K^-,π^-) reaction has recently been solved[89,116] using the oscillator representation of scattering theory.[117] These calculations included decay channels with hyperon and nucleon emission. In the case of ${}^{16}_{\Lambda}$O, along with ordinary particle–hole $(1p-1h)$ $p_\Lambda p^{-1}$ and $s_\Lambda s^{-1}$ configurations, some $2p-2h$ $(s_\Lambda p^{-2}2s)$ configurations—the intruder states mentioned in Sec. 4—were taken into account. It is interesting that the admixture of $2p-2h$ states of this type greatly enhances (compared to the BSM) the neutron decay channel of the resonance $|p_\Lambda(\frac{3}{2})\otimes{}^{15}\mathrm{O}(\frac{3}{2}^-;6.2)\rangle$. Proton decay turns out to be suppressed ($\sim$5%), but it populates the excited state ${}^{15}_{\Lambda}\mathrm{N}(\frac{1}{2}^+_1)$, which agrees with the BSM calculations.

7. WEAK BARYONIC DECAY OF LIGHT HYPERNUCLEI

The evolution of any hypernucleus produced in a nuclear reaction as a result of γ transitions or strong decays terminates in weak mesonic or mesonless decay. These weak processes with changing strangeness are a link between the physics of hypernuclei and important problems in the physics of the weak interactions of elementary particles.

The recent BNL experiments using (K^-,π^-) reactions on ^{6}Li and ^{12}C (Ref. 73) have significantly added to the old results on the weak decays of ${}^{4}_{\Lambda}$H and ${}^{4,5}_{\Lambda}$He and heavier hypernuclei obtained using nuclear photoemulsions and bubble chambers. The rates of mesonless weak decay $\Gamma_{nm}=\Gamma_n+\Gamma_p$ and the ratios $\gamma=\Gamma_n/\Gamma_p$ of the rates of decays induced by Λ interactions with the neutron (Γ_n) and proton (Γ_p) were measured for ${}^{5}_{\Lambda}$He, ${}^{11}_{\Lambda}$B, and ${}^{12}_{\Lambda}$C. The lifetime τ (or $\Gamma_t=\Gamma_{nm}+\Gamma_{\pi^-}+\Gamma_{\pi^0}$, where Γ_π are the rates of mesonic weak decay) of an unidentified light hypernucleus was also measured. According to the shell model, this hypernucleus is ${}^{9}_{\Lambda}$Be, a product of the cluster decay of the $s_\Lambda s^{-1}$ configuration of ${}^{12}_{\Lambda}$C (Ref. 78). All of these results are of great interest for verifying theoretical models of the weak interaction of the Λ hyperon and the nucleon, the hypernuclear weak decay

mechanism, and the empirical $\Delta T=\frac{1}{2}$ rule, which holds in nonleptonic decays of kaons and hyperons.[118]

On the whole, the experimental data on mesonic decays are well described by ordinary nuclear models assuming that a Λ hyperon bound in a nucleus decays into a π meson and a nucleon:[119]

$$\Lambda \rightarrow \pi + N + (\sim 40 \text{ MeV}). \tag{39}$$

As the number of nucleons increases, the probability for weak mesonic decay decreases rapidly owing to Pauli blocking for the nucleon involved in the process (39), while the contribution of weak mesonless decay grows.

It is usually assumed that weak mesonless decay occurs via the intranuclear process

$$\Lambda + N \rightarrow N + N (\sim 176 \text{ MeV}). \tag{40}$$

The theoretical description of weak mesonless decay is based either on a phenomenological approach,[120,121] where the observed Γ_{nm} and γ are expressed in terms of the rate of the reaction (40) for various two-baryon quantum states, or on mesonic theories of these reactions,[122] or on models taking into account the quark degrees of freedom.[123–125] The phenomenological approach is attractive because it allows the extraction of experimental information on the rate of elementary processes $\Lambda N \rightarrow NN$ and allows the validity of the $\Delta T=\frac{1}{2}$ rule to be verified, which is important for checking models. Since at present there is no clear understanding of the data on weak mesonless decays from meson and quark models of the two-baryon reaction, meson models have appeared which allow weak mesonless decay via three-particle reactions:[34,126,127]

$$\Lambda + N + N \rightarrow N + N + N. \tag{41}$$

If weak interactions of this type actually turn out to be important, a more refined experimental method of isolating two-particle weak interactions (40) will be needed. We shall not go into the details of the approximations and models based on the reactions (41), but instead discuss the situation regarding the description of weak mesonless decay based on two-particle interactions (40), assuming that the contribution of (41) is small.

In the phenomenological approach to the weak mesonless decay of the s-shell hypernuclei ${}^{4}_{\Lambda}$H, ${}^{4}_{\Lambda}$He, and ${}^{5}_{\Lambda}$He (Ref. 120), the rates of the reactions (40) are extracted from the experimental data on Γ_{nm} and γ using the relations

$$\Gamma_\lambda = \bar{R}_\lambda({}^{A}_{\Lambda}Z)\rho_A; \quad \rho_A = (A-1)\int \Psi^2_\Lambda(r)\rho(r)dr, \tag{42}$$

where $\bar{R}_\lambda$ is a linear combination of four quantities $R_{\lambda S}$ [the rates of reactions (40) for Λ interaction with a proton ($\lambda=p$) or a neutron ($\lambda=n$) in the singlet ($S=0$) or triplet ($S=1$) state of the ΛN pair], $\rho(r)$ is the nucleon density of the nuclear core, and $\Psi_\Lambda(r)$ is the hyperon wave function. The application of Eq. (42) to different hypernuclei presupposes universality of $R_{\lambda S}$, which can, in general, be violated owing to a difference between the wave functions of the bound ΛN pair in hypernuclei of greatly differing structure.

The six allowed transitions are given in Table XVIII (Refs. 120, 121).

TABLE XVIII. Quantum numbers of baryon states ${}^{2S+1}L_J$ and the corresponding rates of mesonless weak decays.

${}^{2S+1}L_{J_i}$ (ΛN)	${}^1S_0$			${}^3S_1$		
${}^{2S+1}L_{J_f}$ (NN)	${}^1S_0$	${}^3P_0$	${}^3P_1$	${}^3S_1$	${}^1P_1$	${}^3D_1$
T_f	1	1	1	0	0	0
$\Lambda p \rightarrow np$	R_{p0}	R_{p0}	R_{p1}	R_{p1}	R_{p1}	R_{p1}
$\Lambda n \rightarrow nn$	R_{n0}	R_{n0}	R_{n1}	0	0	0

Using the three experimental values for $A=4$:

$$\gamma^{-1}({}^{4}_{\Lambda}\text{He}) = 2.2 \pm 0{,}8; \quad \Gamma_{nm}({}^{4}_{\Lambda}\text{He}) = (0.157 \pm 0.03)\Gamma_\Lambda; \quad \Gamma_{nm}({}^{4}_{\Lambda}\text{H}) = (0.235 \pm 0.06)\Gamma_\Lambda \tag{43}$$

and the condition $R_{n0}=2R_{p0}$ (the $\Delta T=\frac{1}{2}$ rule), the authors of Ref. 120 obtained the following values of $R_{\lambda S}$:[7)] $R_{n0}=(7.4\pm2.4)\Gamma_\Lambda$, $R_{p1}=(9.6\pm3.3)\Gamma_\Lambda$, and $R_{n1}=(19.2\pm6.7)\Gamma_\Lambda$, and also the ratios $R_{n1}/2R_{p1}=1\pm0.7$, $R_{p1}/R_{p0}=2.6\pm1.7$, and $R_{n1}/R_{n0}=2.6\pm1.7$. If the $\Delta T=\frac{1}{2}$ rule is valid, we have the inequality $R_{n1}\leq 2R_{p1}$. For the central quantities, the ratios found in Ref. 120, the triplet channel ($S=1$) dominates over the singlet channel ($S=0$), $R_{n1}\simeq 2R_{p1}$, which distinguishes isospin $T_f=1$ of the NN pair and shows that the ${}^3S_1 \rightarrow {}^3P_1 \times (\Lambda n \rightarrow nn)$ parity-changing transition dominates. Since the measurement errors are still rather large, these conclusions are not solid. Moreover, the question of the applicability of the $\Delta T=\frac{1}{2}$ rule to the reactions (40) remains open.

Next, if we include the BNL data[73] on ${}^{5}_{\Lambda}$He in this analysis, we can abandon the condition $r=R_{n0}/R_{p0}=2$ and obtain the rate ratios directly from the experimental data for hypernuclei with $A=4$ and 5. The contribution of the singlet channel is increased, and the $\Delta T=\frac{1}{2}$ rule is significantly violated.[121,128] For example, from the expressions

$$\gamma_4 \equiv \frac{\Gamma_n}{\Gamma_p}({}^{4}_{\Lambda}\text{He}) = \frac{2R_{n0}}{3R_{p1}+R_{p0}} = 0.40 \pm 0.15, \tag{44}$$

$$\gamma_5 \equiv \frac{\Gamma_n}{\Gamma_p}({}^{5}_{\Lambda}\text{He}) = \frac{3R_{n1}+R_{n0}}{3R_{p1}+R_{p0}} = 0.93 \pm 0.55, \tag{45}$$

$$\bar{\gamma} \equiv \frac{\Gamma_{nm}({}^{4}_{\Lambda}\text{He})}{\Gamma_{nm}({}^{4}_{\Lambda}\text{H})} = \frac{3R_{p1}+R_{p0}+2R_{n0}}{3R_{n1}+R_{n0}+2R_{p0}} = 0.53 \pm 0.22, \tag{46}$$

which do not involve the model-dependent nuclear structure factors ρ_4 and ρ_5, we have $r=R_{n0}/R_{p0}=0.232\pm0.17$ (Ref. 128), which can be interpreted as strong violation of the $\Delta T=\frac{1}{2}$ rule, with the reservation about the universality of $R_{\lambda S}$ for hypernuclei with $A=4$ and 5.

Most models of the reaction (40) are based on interaction potentials $\Sigma_m V_m$ for pole graphs with exchange of π, ρ, and other mesons (m) assuming that the $\Delta T=\frac{1}{2}$ rule is valid. However, the theoretical description of Γ_{nm} and γ has some problems. For example, calculations of Γ_{nm} and γ for ${}^{3}_{\Lambda}$H, ${}^{4}_{\Lambda}$H, ${}^{4}_{\Lambda}$He, and ${}^{5}_{\Lambda}$He using the potentials $V_\pi \pm V_\rho$ give dominant transitions ${}^3S_1 \rightarrow {}^{13}S_1$, ${}^{13}D_1$, but they do not reproduce the entire set of Γ_{nm}, and the values they give for γ_4 and γ_5 are more than an order of magnitude lower than the experimental ones,[129] i.e., the neutron channel is strongly sup-

pressed. The transitions ${}^3S_1 \to {}^{13}D_1$, ${}^{33}P_1$, and ${}^{13}S_1$ dominate in the model with π, ρ, η, ω, K, and K^* exchange,[122] and the acceptable values $\gamma({}^5_\Lambda\mathrm{He}) = 0.77$ (Ref. 130), $\gamma({}^{12}_\Lambda\mathrm{C}) = 0.83$, and $\Gamma_{nm}({}^{12}_\Lambda\mathrm{C}) = 1.2\Gamma_\Lambda$ (Ref. 122) are obtained. However, for ${}^4_\Lambda\mathrm{He}$ and ${}^4_\Lambda\mathrm{H}$ the results $\bar{\gamma} = 1.32$ and $\gamma_4 = 0.06$ are obtained, which do not agree with experiment. An interaction of the form $V_\pi + V_{2\pi}$ (box diagram with two-pion exchange[131]) does not improve the results: $\gamma_5 = 0.07$, $\gamma_4 = 0.03$. Small values of γ for s-shell hypernuclei are also obtained using the interaction $V_\pi + V_{2\pi/\sigma}$, where the second term corresponds to the diagram with exchange of an isoscalar meson σ decaying into two pions in the intermediate state.[132] The simple quark model describing the weak decay of the six-quark bag formed at small distances between baryons[125] or the more complex hybrid quark models taking into account meson exchange in the outer region[123,124] significantly change the individual, purely mesonic amplitudes of the reaction (40) and lead to strong violation of the $\Delta T = \frac{1}{2}$ rule. However, in these approaches, aside from difficult questions about the consistent description of the long-range (mesonic) and short-range (quark bag) parts of the interaction and the structure of the quark bag itself,[133,134] there is the problem of determining the most effective weak-interaction Hamiltonian, which must include hadronic contributions to correctly describe nonleptonic weak decays of strange particles obeying the $\Delta T = \frac{1}{2}$ rule. Many of these aspects of quark models are still in the developmental stage, and so their results regarding the reaction (40) and weak mesonless decay should be viewed as preliminary.

It is clear from this brief description of the status of weak mesonless decays that four quantities, the rates $R_{\lambda S}$ of the elementary reaction (40), play a fundamental role in the physics of weak mesonless decay and directly relate this process to the theory of weak interactions of strange particles at the mesonic and quark levels. Up to now the values of $R_{\lambda S}$ have been determined with very large errors using the characteristics of weak mesonless decays for s-shell hypernuclei. It is therefore of great interest to extend the phenomenological approach[120] to heavier hypernuclei, in particular, hypernuclei of the $1p$ shell, for which some information about weak mesonless decays has already been obtained at BNL. This would provide new, independent data on $R_{\lambda S}$ and clear up the situation regarding the $\Delta T = \frac{1}{2}$ rule, while also giving the limits of applicability of the theory of weak mesonless decay based on the two-particle process $\Lambda N \to NN$.

Equation (42) has been generalized to the weak mesonless decay of an arbitrary hypernucleus taking into account the interaction of the final NN pair with the residual nucleus in Ref. 135 using the approximation that the states of the residual nucleus form a complete set. The corresponding expression for the decay width has the form

$$\Gamma_\lambda = (A-1)\sum_S (2S+1) R_{\lambda S} f_{\lambda S}({}^A_\Lambda Z), \tag{47}$$

where

$$R_{\lambda S} = \pi m^{3/2}\sqrt{\varepsilon}(2S+1)^{-1} \times \sum_{\mu,a} \int d\Omega_k |\langle k,a|V|\Psi_0; S\mu\lambda\rangle|^2 \tag{48}$$

is the rate of decay of a ΛN pair bound in a hypernucleus into two nucleons of energy ε, and $f_{\lambda S}({}^A_\Lambda Z)$ is the hypernuclear structure factor

$$\begin{aligned} f_{\Lambda S}({}^A_\Lambda Z) = \Theta^2 (2J+1)^{-1}(2S+1)^{-1} & \\ \times \sum_{M,\mu,\alpha,\alpha',\zeta} \int \langle i,JM|r & \\ = 0,x,\alpha'\lambda;x_3 \ldots x_{A-1}\rangle & \\ \times \langle \alpha' S\mu\rangle\langle S\mu|\alpha\rangle\langle r & \\ = 0,x,\alpha\lambda;x_3 \ldots x_{A-1}|JM,i\rangle & \\ \times N(\gamma k,b)dx \prod_{j=3}^{A-1} dx_j, & \end{aligned}$$

where

$$\Theta^2 = 1/\Psi_0^2(r=0),$$

$$N(\gamma k,b) = \exp\left\{\frac{\gamma k}{E}\int_{-\infty}^{\infty} V_I(b+\hat{k}t)dt\right\}, \tag{49}$$

$b = x - \hat{k}z$, $\hat{k} = \mathbf{k}/k$, E is the energy of the relative motion of the nucleon in the nucleus, $V_I(r)$ is the imaginary part of the optical potential, and $\langle\{x\}|JM,i\rangle$ is the translationally invariant wave function of the decaying hypernucleus. Equations (48) and (42) coincide for s-shell hypernuclei for $V_I(r) = 0$ if $R_{\lambda S}\Theta^2$ is identified with R_{NS} in Ref. 120. In deriving these expressions we have assumed that, owing to the short-range nature of the weak interaction V and the large momentum transfer k, the main contribution to Γ_λ comes from states of the ΛN pair with orbital angular momentum $L = 0$. The contribution of states with $L \geq 1$ is determined by the long-range part of V, and can in principle be included in models with light-meson exchange. Estimates[136] show that states with $L = 1$ in ${}^{12}_\Lambda\mathrm{C}$ (π, K exchange) give about 5% of the observed decay rate.

Equations (47)–(49) were applied to the decay of ${}^9_\Lambda\mathrm{Be}$, ${}^{11}_\Lambda\mathrm{B}$, ${}^{12,13}_\Lambda\mathrm{C}$ and ${}^{17}_\Lambda\mathrm{O}$. The nuclear core in ${}^{17}_\Lambda\mathrm{O}$ was described by closed shells, and the shell model with intermediate coupling[10] was used for the nuclear cores of the other hypernuclei. The effect of the interaction V_I reduces to an overall factor $\alpha \sim 0.5$:

$$f_{\Lambda S}(V_I \neq 0) \simeq 0.5 f_{\lambda S}(V_I = 0). \tag{50}$$

Equations (47)–(49) can be used to relate the decay characteristics of different hypernuclei. For hypernuclei with nuclear core having zero quantum numbers $J_N = 0$, $T_N = 0$ the structure factors turn out to be equal for Λp and Λn states and independent of the spin S of the ΛN pair ($f_{\lambda S}({}^A_\Lambda Z) = f_A$), which leads directly to the equations

$$\gamma({}^9_\Lambda\mathrm{Be}) = \gamma({}^{13}_\Lambda\mathrm{C}) = \gamma({}^{17}_\Lambda\mathrm{O}) = \frac{\Gamma_n}{\Gamma_p} = \frac{R_{n0}+3R_{n1}}{R_{p0}+3R_{p1}} \tag{51}$$

and the ratios

$$\frac{\Gamma_{nm}({}^{9}_{\Lambda}\mathrm{Be})}{f_9}:\frac{\Gamma_{nm}({}^{13}_{\Lambda}\mathrm{C})}{f_{13}}:\frac{\Gamma_{nm}({}^{17}_{\Lambda}\mathrm{O})}{f_{17}}=8:12:16. \tag{52}$$

If we assume that $R_{\lambda S}\Theta^2$ is the same for ${}^{5}_{\Lambda}$He and $1p$-shell hypernuclei, then $\gamma({}^{5}_{\Lambda}\mathrm{He})$ should be added to Eq. (51). The ratios (52) must obviously be satisfied separately for the proton and neutron decay branches Γ_p and Γ_n. Since the structure factors $f_9=0.098\alpha$, $f_{13}=0.089\alpha$, and $f_{17}=0.084\alpha$ fall off very slowly with increasing A, the quantities Γ_{nm}, Γ_n, and Γ_p are approximately proportional to the number of nucleons in the hypernucleus. The experimental confirmation of these relations would be a clear test of the two-particle decay mechanism $\Lambda N\to NN$.

The phenomenological model of weak mesonless decay can explain the observed ratio $\Gamma_{nm}({}^{9}_{\Lambda}\mathrm{Be})/\Gamma_{nm}({}^{5}_{\Lambda}\mathrm{He})\simeq 2.44$ (Ref. 73), if we define $\Gamma_{nm}({}^{9}_{\Lambda}\mathrm{Be})=\Gamma_{\mathrm{tot}}^{\mathrm{exp}}-\Gamma_{\pi}^{\mathrm{the}}\simeq 1.0\Gamma_{\Lambda}$ ($\Gamma_{\pi}^{\mathrm{the}}\simeq 0.3\Gamma_{\Lambda}$; Ref. 137) and assume that $R_{\lambda S}\Theta^2$ is the same for $A=5$ and 9. The desired ratio is

$$\frac{\Gamma_{nm}({}^{9}_{\Lambda}\mathrm{Be})}{\Gamma_{nm}({}^{5}_{\Lambda}\mathrm{He})}=\frac{64f_9}{(2\pi)^{3/2}r_0^3\rho_5\alpha_5}, \tag{53}$$

where $\rho_5=0.038$ fm^{-3} is the ${}^{5}_{\Lambda}$He structure factor calculated in Ref. 120, and $\alpha_5=\alpha({}^{5}_{\Lambda}\mathrm{He})$ is a coefficient taking into account the interaction of the emitted nucleons with the residual nucleus (for plane waves $\alpha_5=\alpha=1$). For the oscillator parameter $r_0({}^{8}\mathrm{Be})=1.6$ fm and $\alpha_5/\alpha=1$ the ratio (53) coincides with the observed value. Furthermore, if we take into account (52), the ratio

$$\frac{\Gamma_{nm}({}^{13}_{\Lambda}\mathrm{C})}{\Gamma_{nm}({}^{5}_{\Lambda}\mathrm{He})}=\frac{12}{8}\frac{f_{13}}{f_9}\frac{\Gamma_{nm}({}^{9}_{\Lambda}\mathrm{Be})}{\Gamma_{nm}({}^{5}_{\Lambda}\mathrm{He})}\simeq 3.3 \tag{54}$$

is comparable within the experimental error to the observed ratio $\Gamma_{nm}({}^{12}_{\Lambda}\mathrm{C})/\Gamma_{nm}({}^{5}_{\Lambda}\mathrm{He})\simeq 2.8$ (Ref. 73).

We also note that the ratios γ for ${}^{12}_{\Lambda}$C and ${}^{11}_{\Lambda}$B measured at BNL are close: $\gamma({}^{12}_{\Lambda}\mathrm{C})=1.33^{+1.12}_{-0.81}$, $\gamma({}^{11}_{\Lambda}\mathrm{B})=1.04^{+0.59}_{-0.48}$. Application of Eqs. (44)–(49) together with $\gamma_{\mathrm{exp}}({}^{5}_{\Lambda}\mathrm{He})$ to these hypernuclei leads to the expected ranges

$$0.65\leq\gamma({}^{11}_{\Lambda}\mathrm{B})\leq 1.1 \quad 0.55\leq\gamma({}^{12}_{\Lambda}\mathrm{C})\leq 0.95 \tag{55}$$

(for $R_{n0}=2R_{p0}$; the $\Delta T=\frac{1}{2}$ rule) and

$$0.65\leq\gamma({}^{11}_{\Lambda}\mathrm{B})\leq 0.75; \quad \gamma({}^{12}_{\Lambda}\mathrm{C})\simeq 0.65 \tag{56}$$

[for $R_{n0}=0.2R_{p0}$ (Ref. 128); violation of the $\Delta T=\frac{1}{2}$ rule]. These ranges fall within the region allowed by experiment. However, more accurate measurements are needed to check the validity or violation of the $\Delta T=\frac{1}{2}$ rule.

Up to now we have considered the total widths Γ_λ (Γ_n and Γ_p) in the sense that the contributions from all states of the residual nucleus formed in the emission of an NN pair were summed. The authors of Ref. 138 proposed experiments to observe partial transitions in weak mesonless decay assuming the two-particle mechanism $\Lambda p\to np$ and $\Lambda n\to nn$. Here when a proton or neutron is separated from the nuclear core, the residual nucleus can end up in an excited state, which then emits γ quanta. These γ lines are well known for light nuclei, but here they should appear with a delay equal to the hypernucleus lifetime $\tau\sim 10^{-10}$ sec. The nucleus can be identified from the energies of the γ lines, and the emitted particle, proton or neutron, can be determined.

As an example of the delayed γ spectra predicted by the shell model, we studied the case of triplet dominance of the initial S state of the ΛN pair as given by the meson theory.[122] The partial width for decay of the initial hypernuclear state $\Psi_i=|s_\Lambda\otimes s^4p^kE_cJ_cT_c:J_i\rangle$ with formation of the final nucleus in the state $\Psi_f=|s^4p^{k-1}E_fJ_fT_f\rangle$ has the form

$$\Gamma_{f\lambda}=\kappa(k+4)R_{\lambda 1}\left\{\sum_{j,J}G^{E_cJ_cT_c}_{E_fJ_fT_f}(j\lambda)U\left(J_fjJ_i\,\frac{1}{2};J_cJ\right)\right.$$
$$\left.\times U\left(\frac{1}{2}\,\frac{1}{2}\,J1;1j\right)\right\}^2, \tag{57}$$

where κ is a kinematical coefficient related to the integration over the center of mass of the emitted NN pair, j is the total angular momentum of the proton ($\lambda=p$) or neutron ($\lambda=n$) in the hypernucleus, and the coefficient G, which includes the one-particle fractional parentage coefficient, determines the spectroscopic factor: $G^2=C^2S(j\lambda)$. Combining (57) and the known intensities of γ transitions for each nuclear level,[91] we obtain the γ spectra for hypernuclei with $9\leq A\leq 16$ shown in Fig. 15.

As a first step, it would be interesting in general to detect delayed γ quanta and at least determine their energy, which would allow immediate confirmation of the two-particle decay mechanism. As already noted above, owing to the difficulties of the theoretical explanation of the large ratios $\gamma=\Gamma_n/\Gamma_p$, models based on the three-particle interaction $\Lambda NN\to NNN$ have been developed in recent years, where the virtual pion emitted by the Λ hyperon is absorbed by a pair of nucleons in the nucleus. If the contribution of the three-particle mechanism is important (according to the estimates of Ref. 126 it is about 30%), the γ spectra should contain additional γ lines from the residual nuclei formed in the separation of two nucleons.

It was shown in Ref. 139 that the delayed-γ spectrum can be used to determine the ground-state parity of the ${}^{20}_{\Lambda}$Ne hypernucleus. We recall that the ground state of ^{19}Ne is described by the $(2s-d)^3$ shell configuration

$$\left|{}^{19}\mathrm{Ne}\left(\frac{1^+}{2}\,\frac{1}{2};0{,}00\right)\right\rangle=\left|{}^{16}\mathrm{O}(0^+0;0{,}00)\otimes\right.$$
$$\left.\times(2s-d)^3:\ \frac{1^+}{2}\,\frac{1}{2}\right\rangle,$$

and the configuration corresponding to the first excited state of negative parity $\frac{1}{2}^-\frac{1}{2}$, 0.28 MeV, is

$$\left|{}^{19}\mathrm{Ne}\left(\frac{1^-}{2}\,\frac{1}{2};0.28\right)\right\rangle=\left|{}^{15}\mathrm{O}\left(\frac{1^-}{2}\right)\otimes\alpha:\ \frac{1^-}{2}\,\frac{1}{2}\right\rangle.$$

The cluster model predicts[140] that the ground state of ${}^{20}_{\Lambda}$Ne has negative parity, owing to the strong polarization of the nuclear core, whereas according to the shell model,[10] the first state of negative parity is located at 0.7 MeV. If the parity of the ground state of ${}^{20}_{\Lambda}$Ne is positive, transitions of energy

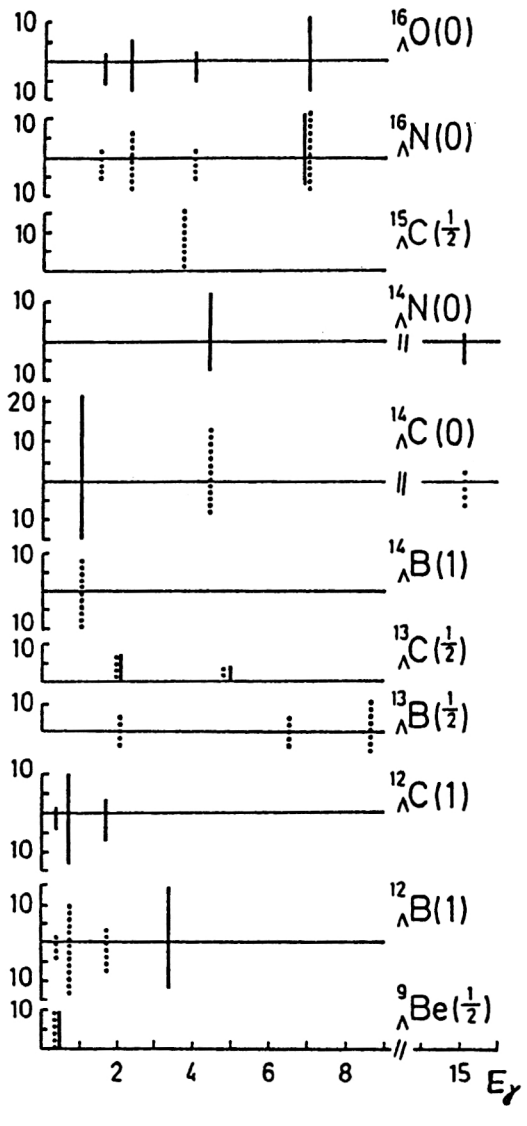

FIG. 15. Intensity of γ lines from the deexcitation of states of daughter nuclei populated in the weak processes $\Lambda p \to np$ (solid lines) and $\Lambda n \to nn$ (dotted lines). The upper lines refer to the ground states, and the lower ones to isomeric states of the hypernuclei.[138]

$E_\gamma = 0.94$ MeV dominate in the delayed-γ spectrum, while in the opposite case the dominant transitions have $E_\gamma = 1.9$ MeV.

CONCLUSIONS

The strong and weak baryonic decays of the levels of $1p$-shell hypernuclei possessing the simple configurations $s_\Lambda p^{-1}$, $p_\Lambda p^{-1}$, and $s_\Lambda s^{-1}$ have been analyzed using the shell model. This area is still not well studied experimentally, and so it holds great promise both for the future development of hypernuclear spectroscopy, and for the deeper understanding of the nature of hyperon–nucleon interactions manifested in the level spectra, the fine structure of the wave functions, and the characteristics of weak mesonless decays. The determination of the exact location of low-lying bound hypernuclear levels which deexcite by γ emission remains a very important problem. The various effective hyperon–nucleon interaction variants, both phenomenological ones and those suggested by the meson theory, are checked using states with configuration $s_\Lambda p^{-1}$. The inadequacy of the experimental information about these states is due to the weak intensity of hypernuclear excitations with $\Delta L = 1$ in the (K^-,π^-) and (π^+,K^+) reactions, especially in transitions requiring baryon spin flip. The experience gained from the studies performed at BNL and KEK shows that further progress in studying low-lying hypernuclear levels which are excited directly in reactions with mesons will be possible only when the intensities of the kaon and pion beams are increased. New results on transitions with spin flip can be expected in hypernucleus photoproduction reactions in the intense photon beam of the CEBAF accelerator.

In this review we have focussed our attention on the possibility of using existing setups to study the low-lying states of daughter hypernuclei populated in nucleon or cluster decays of excited hypernuclear levels in the continuum. In this way it is possible to obtain new information about hypernuclear γ transitions and the spectra of light hypernuclei both in the (K^-,π^-), (π^+,K^+), and $(K^-_{\text{stop}},\pi^-)$ reactions already studied, and in other reactions like (K^-,π^0) which have not yet been used, although plans for using them in hypernuclear spectroscopy already exist.[48]

A nontrivial fact, noted at the beginning of this review, is the characteristic selectivity of excitations of hypernuclear levels depending on the momentum transfer characteristic of each reaction and the spin structure of the one-nucleon amplitude. This means that a wealth of information can be obtained about daughter hypernuclei given the diversity of target nuclei and the enormous range of intense hypernuclear resonances in the continuum for any particular primary hypernucleus.

Among the decays of excited states with the $s_\Lambda p^{-1}$ configuration, the case of the $^{13}_{\Lambda}$C levels built on the known nuclear level ^{12}C($1^+,T=1$;15.11 MeV) should be distinguished. Their decay properties depend on the "purity" of the isospin T, the quantum number of the hypernuclear state. Observation of hypernuclear γ quanta in $^{12}_{\Lambda}$C with energy ~ 15 MeV would provide direct proof of the smallness of the admixture of states of the nuclear core $^{12}_{\Lambda}$C with isospin $T=0$. The absence of this γ line owing to competing decay via the Λ channel would be a strong indication of significant isospin mixing due to the ΛN interaction, which violates charge symmetry.

The theoretical analysis of decays of $p_\Lambda p^{-1}$ states located at energies above ~ 10 MeV shows that the channel with Λ-hyperon emission dominates for hypernuclei of the first half of the $1p$ shell. However, as the number of nucleons increases, the threshold of the Λ channel rises, which at the middle of the $1p$ shell leads to a rapid decrease of the Λ width from a value of the order of several MeV to tenths of a keV. The proton decay channel becomes dominant, which is very important for detecting daughter hypernuclei and the detailed study of the structure of the wave functions of the primary hypernuclear resonance. Here we primarily have in mind the question of the admixtures of intruder states in resonance states of hypernuclei. Such states play practically no role in hypernucleus excitation, but it is essentially they

which realize the nucleon decay process. These admixtures arise both for purely kinematical reasons, when the center-of-mass motion of the hypernucleus is eliminated as in the TIMO, and from the ΛN interaction producing additional mixing of these states. Detection of nucleon decays using the γ quanta from populated levels of daughter hypernuclei can aid in the understanding of the formation mechanisms of wave functions of hypernuclear states in the continuum. A good object for this type of study is the ${}^{16}_{\Lambda}$O hypernucleus, for which the number of intruder states is relatively low.

States with configuration $s_\Lambda s^{-1}$ are located in the uppermost part of the hypernuclear excitation spectrum, as a rule, at energies above 20 MeV. The hypernuclear resonances are strongly fragmented, like the s-hole levels of the nuclear core built on them. In spite of the fact that at such high energies nucleon and many cluster decay channels are open, the cluster channel dominates owing to the sum rules from the Young tableau reflecting the permutation symmetry of the wave function. There is a large probability for the Λ hyperon to combine either with a three-nucleon nucleus (^{3}H or ^{3}He) or with a corresponding light $1p$-shell nucleus, as has been demonstrated for the examples of ${}^{6}_{\Lambda}$Li (Ref. 77), ${}^{12}_{\Lambda}$C (Ref. 78), and ${}^{10}_{\Lambda}$B (Ref. 80) decays.

The application of the shell model to weak mesonless decays of $1p$-shell hypernuclei is quite universal and allows the following:

- Calculation of the structure of the ground and isomer states of hypernuclei undergoing weak decay;
- Determination of the population probabilities of these states in nucleon and cluster decays;
- Calculation of the nuclear structure factors relating the rates of hypernuclear weak decay to the rates of the elementary reactions $\Lambda n \to nn$ and $\Lambda p \to np$;
- Prediction of the population of levels of the daughter nuclei formed in weak decay after the emission of a pair of fast nucleons.

The analysis of the data on the weak mesonless decay of ${}^{5}_{\Lambda}$He, ${}^{9}_{\Lambda}$Be, ${}^{11}_{\Lambda}$B, and ${}^{12}_{\Lambda}$C on the basis of the intranuclear two-particle process $\Lambda N \to NN$ that we have performed here is consistent with the empirical $\Delta T = \frac{1}{2}$ rule and, within the limits of the still-large experimental errors, can explain the characteristics of weak mesonless decays measured at BNL. The statement made earlier[128] about strong violation of the $\Delta T = \frac{1}{2}$ rule on the basis of phenomenological analysis of the weak mesonless decay of only s-shell hypernuclei ${}^{4}_{\Lambda}$H, ${}^{4}_{\Lambda}$He, and ${}^{5}_{\Lambda}$He may have been premature owing to the approximate nature of the expressions used in the phenomenological data analysis.

It will only be possible to make more rigorous conclusions about the validity of the two-particle mechanism and the possible role of the three-particle weak decay process $\Lambda NN \to NNN$ when the errors of measuring the characteristics of weak decay are decreased, and analogous measurements are performed for other $1p$-shell hypernuclei. It is also important to verify the new relations between the characteristics of weak mesonless decay for hypernuclei with zero quantum numbers of the nuclear core derived in the shell model. An equally important task for future experiments is seeking delayed γ quanta from the final nuclear products of weak mesonless decay. All of these experiments can serve as a good test of the two-particle mechanism of weak mesonless decay and, if it is found to be dominant, these experiments will provide a reliable basis for determining the rates of elementary reactions, which are of interest for developing models of the process $\Lambda N \to NN$.

In writing this review during the celebration of the fortieth anniversary of the JINR, we were thinking about the contributions Dubna has made to the development of hypernuclear physics. The unflagging interest of Dubna scientists in the physics of hyperons is understandable, because one of the founding fathers of the Institute was M. A. Markov, who attempted to understand the role played by the new (i.e., strange) particles in the spectrum of elementary particles.[141] Dubna was recognized for the discovery of the $\bar{\Sigma}^-$ hyperon, and searches for the H dibaryon were carried out for many years.[142] The discovery of hypernuclei,[8)] found to be relatively stable systems with a rich spectrum of excited states, raised new questions:

- How does the hyperon affect the properties of the system (its stability and symmetry)?
- How do the properties of the hyperon itself (its lifetime) change in a nucleon medium?

From the link between elementary particle physics and nuclear physics came the brilliant idea of Podgoretskiĭ[37] of using the strangeness-exchange reaction (1) in hypernuclear physics, thus transforming hypernuclear spectroscopy into a fundamental area of intermediate-energy nuclear physics.[85,143] (The group of authors of this review was formed at Dubna to solve the problem of interactions of μ, π, and K mesons with light nuclei.[77]) An example of the effective adoption of nuclear tecniques is the proposal of Polikanov to measure the lifetimes of hypernuclei using the delayed fission of heavy hyperfragments produced in the annihilation of antiprotons on uranium.[144] (More careful study of the hypernuclear fission process showed[145] that the Λ hyperon can play the role of a unique "clock" or "thermostat" in the study of fission dynamics.) Scientists from Dubna working at CERN on the annihilation of slow antiprotons on nuclei discovered not only abundant Λ production,[146] but also cases of the production of light hyperfragments.[35] Unique experiments were performed at the High Energy Laboratory on hypernuclear production in beams of relativistic nuclei,[147] and the lifetimes of the lightest hypernuclei ${}^{3}_{\Lambda}$H and ${}^{4}_{\Lambda}$H were measured. The hypernuclear program planned for the nuclotron contains an original idea: measuring the cross sections for the electromagnetic dissociation of weakly coupled ${}^{3}_{\Lambda}$H and ${}^{6}_{\Lambda}$He hypernuclei in order to accurately determine their binding energies.[148] We believe that, in spite of the heavy losses of last year and the departure of M. I. Podgoretskiĭ, S. M. Polikanov, B. A. Shakhbazyan, É. O. Okonov, and V. I. Ogievetskiĭ, questions of the effect of strange particles on the laws and symmetries of the microscopic world will continue to be a favorite topic of Dubna scientists working at home and abroad, and that the results they obtain will continue to enrich the store of information on hypernuclear physics.

We dedicate this review to the happy memory of M. I.

Podgoretskiĭ, the founder of modern hypernuclear spectroscopy, and to Jan Žofka, with whom we spent ten fruitful, unforgettable years. We also have grateful memories of Mariana Gmitro, who devoted great efforts to the organization of the large-scale international collaboration in intermediate-energy nuclear physics at Dubna.

The authors are sincerely grateful to Academician A. M. Baldin for his long-time support of theoretical studies of hypernuclear spectroscopy.

We would like to thank Yu. Batusov, R. Wünsch, D. Davis, R. Chrien, D. Lanskoĭ, D. Millener, T. Motoba, M. Sotona, H. Tamura, A. Thiessen, S. Frullani, and S. Khorozov for information and discussion of the results, and also V. B. Belyaev, V. G. Neudachin, and V. G. Solov'ev for lively discussions at their seminars.

This work was supported by the Russian Fund For Fundamental Research.

[1)]The hypernuclear γ quanta found and identified with great difficulty correspond to transitions between states of the nuclear core.

[2)]In heavy photoemulsion nuclei (Ag, Br), more than half ($58\pm 15\%$) of the captured slow kaons produce a hyperfragment. The hyperfragment yield in the capture of kaons by light nuclei (C, N, O) is smaller, about 10%.

[3)]A painstaking study combined with laborious analysis of individual events gave the binding energies of 22 light ($A<16$) hyperfragments, which forms the foundation of hypernuclear spectroscopy.[36]

[4)]The study of the decay properties of polarized hypernuclei performed at KEK is one of the interesting new areas in hypernuclear physics.[22,42]

[5)]It was shown in Ref. 59 that the same situation occurs for target nuclei with unfilled proton shells ($J_i\neq 0$) which do not participate in the reaction.

[6)]This is favored by the small density of p^{-1} hole states and the large splitting (10 MeV) of the one-particle hyperon energies.

[7)]Here, following Ref. 121, we give values of $R_{\lambda S}$ slightly differing from those of Ref. 120, which take into account the more accurate value of the Λ-hyperon decay rate, $\Gamma_\Lambda = 3.8\times 10^9$ sec^{-1}.

[8)]M. Danysh, who discovered the hypernucleus in 1953, was later the first vice director of the institute.

[1] A. Gal, Adv. Nucl. Phys. **8**, 1 (1975).
[2] H. Bandō, T. Motoba, and J. Žofka, Int. J. Mod. Phys. A **5**, 4021 (1990).
[3] B. F. Gibson and E. V. Hungerford, Phys. Rep. **257**, 349 (1995).
[4] G. Alexander *et al.*, Phys. Rev. **173**, 1452 (1968); B. Sechi-Zorn *et al.*, Phys. Rev. **175**, 1735 (1968); J. A. Kadyk *et al.*, Nucl. Phys. **175**, 13 (1971).
[5] H. Feshbach, in *Proceedings of the Summer Study Meeting on Nuclear and Hypernuclear Physics With Kaon Beams*, BNL, July 1973, BNL 18335, p. 185; J. Žofka, Czech. J. Phys. B **30**, 95 (1980).
[6] E. V. Hungerford and L. C. Biedenharn, Phys. Lett. **142B**, 232 (1984); T. Yamazaki, Prog. Theor. Phys. Suppl. **85**, 232 (1985).
[7] R. E. Chrien and C. B. Dover, Ann. Rev. Nucl. Part. Sci. **39**, 113 (1989).
[8] *Developments in Hypernuclear Physics—Production, Structure, and Decay—In Memory of the Late Dr. Hiroharu Bandō*, edited by T. Motoba, Y. Akaishi, and K. Ikeda, Prog. Theor. Phys. Suppl. **117**, 1 (1994).
[9] A. Gal, J. M. Soper, and R. H. Dalitz, Ann. Phys. (N.Y.) **63**, 53 (1971); **72**, 445 (1972); **113**, 79 (1978).
[10] D. J. Millener *et al.*, Phys. Rev. C **31**, 499 (1985).
[11] L. Majling, J. Žofka, V. N. Fetisov, and R. A. Eramzhyan, in *Proc. of the 1986 INS Int. Symp. on Hypernuclear Physics*, p. 112.
[12] T. Motoba, H. Bandō, K. Ikeda, and T. Yamada, Prog. Theor. Phys. Suppl. **81**, 42 (1985).
[13] Y. Yamamoto, H. Bandō, and J. Žofka, Prog. Theor. Phys. **80**, 757 (1988); D. E. Lanskoĭ and T. Yu. Tret'yakova, Yad. Fiz. **49**, 1595 (1989) [Sov. J. Nucl. Phys. **49**, 987 (1989)].
[14] J. Mareš and B. K. Jennings, Phys. Rev. C **49**, 2472 (1994).
[15] V. N. Fetisov, L. Majling, J. Žofka, and R. A. Eramzhyan, Z. Phys. A **399**, 399 (1991).
[16] T. Yamada, T. Motoba, K. Ikeda, and H. Bandō, Prog. Theor. Phys. Suppl. **81**, 104 (1985); Y. Yamamoto *et al.*, Czech. J. Phys. **42**, 1249 (1992); J. Hao, T. T. S. Kuo *et al.*, Phys. Rev. Lett. **71**, 1498 (1993).
[17] T. Motoba, Few-Body Systems, Suppl. 9, 495 (1995).
[18] S. Cohen and D. Kurath, Nucl. Phys. **73**, 1 (1965).
[19] D. J. Millener, in *Proc. of the LAMPF Workshop on (π,K) Physics*, Los Alamos, 1990 (AIP Conf. Proc., Vol. 224), p. 128; A. Gal, *ibid.*, p. 173.
[20] B. F. Gibson, Phys. Rev. C **49**, R1768 (1994).
[21] J. Žofka, L. Majling, V. N. Fetisov, and R. A. Éramzhyan, Fiz. Élem. Chastits At. Yadra **22**, 1292 (1991) [Sov. J. Part. Nucl. **22**, (1991)].
[22] S. Ajimura, H. Ejiri *et al.*, Phys. Lett. **282B**, 293 (1992).
[23] H. Outa, M. Aoki *et al.*, Nucl. Phys. **A585**, 109c (1995).
[24] R. S. Hayano, Nucl. Phys. **A547**, 151c (1992); R. S. Hayano *et al.*, Phys. Lett. **231B**, 355 (1989); M. Barakat and E. V. Hungerford, Nucl. Phys. **A547**, 157c (1992).
[25] S. Aoki *et al.*, Prog. Theor. Phys. **89**, 493 (1993).
[26] P. D. Barnes, Nucl. Phys. **A547**, 3c (1992).
[27] R. E. Chrien, C. B. Dover, and A. Gal, Czech. J. Phys. **42**, 1089 (1992).
[28] T. Hasegawa, O. Hashimoto *et al.*, Phys. Rev. Lett. **74**, 224 (1995); Phys. Rev. C **53**, 1210 (1996).
[29] M. May, in *Proc. of the Fifth Conf. on Intersections Between Particle and Nuclear Physics*, Florida, 1994 (AIP Conf. Proc., Vol. 338), p. 607.
[30] R. H. Dalitz and A. Gal, Ann. Phys. (N.Y.) **116**, 167 (1978).
[31] L. Majling, V. N. Fetisov, and R. A. Eramzhyan, Nucl. Phys. **A547**, 73c (1992).
[32] M. M. Block and R. H. Dalitz, Phys. Rev. Lett. **11**, 96 (1963).
[33] J. Cohen, Prog. Part. Nucl. Phys. **25**, 139 (1990).
[34] W. M. Alberico *et al.*, Phys. Lett. **256B**, 134 (1991).
[35] E. Balestra *et al.*, Yad. Fiz. **56**, 6 (1993) [Phys. At. Nucl. **56**, 576 (1993)]; Yu. A. Batusov, Few-Body Syst., Suppl. 9, 161 (1995).
[36] D. H. Davis and J. Pniewski, Contemp. Phys. **27**, 91 (1986); J. Pniewski and D. Zieminska, in *Proc. of the Seminar on the Kaon–Nuclear Interaction and Hypernuclei* [in Russian], Zvenigorod, September, 1977 (Nauka, Moscow, 1979), p. 33.
[37] M. I. Podgoretskiĭ, Zh. Éksp. Teor. Fiz. **44**, 695 (1963) [Sov. Phys. JETP **17**, 470 (1963)].
[38] B. Povh, Ann. Rev. Nucl. Part. Sci. **28**, 1 (1978); in *Proc. of the Intern. Conf. on Nuclear Physics*, Florence, 1983, Vol. 2, p. 455.
[39] H. A. Thiessen, AGS Proposal No. 758, 1980.
[40] C. B. Dover *et al.*, Phys. Rev. C **22**, 2075 (1980).
[41] J. Žofka, Nuovo Cim. A **102**, 327 (1989).
[42] S. Ajimura *et al.*, in *Proc. of the Twenty-Third INS Intern. Symp. on Nuclear and Particle Physics With Meson Beams in the 1 GeV/c Region*, Tokyo, 1995, p. 217.
[43] E. H. Auerbach *et al.*, Ann. Phys. (N.Y.) **148**, 381 (1983).
[44] M. May *et al.*, Phys. Rev. Lett. **47**, 1106 (1981).
[45] R. H. Dalitz, D. H. Davis, and D. N. Tovee, Nucl. Phys. **A450**, 311c (1986).
[46] V. V. Balashov *et al.*, Nucl. Phys. **59**, 417 (1964); Nucl. Phys. **83**, 418 (1966); F. C. Barkev, Nucl. Phys. **83**, 418 (1966).
[47] D. F. Measday, Czech. J. Phys. **42**, 1231 (1992).
[48] R. E. Chrien, in *Proc. of the Twenty-Third INS Intern. Symp. on Nuclear and Particle Physics With Meson Beams in the 1 GeV/c Region*, Tokyo, 1995, p. 161.
[49] V. N. Fetisov, L. Majling, J. Žofka, and R. A. Eramzhyan, Z. Phys. A **314**, 239 (1983).
[50] L. Majling, J. Žofka, V. N. Fetisov, and R. A. Eramzhyan, Phys. Lett. **130B**, 235 (1983).
[51] H. Tamura, R. S. Hayano, H. Outa, and T. Yamazaki, Prog. Theor. Phys. Suppl. **117**, 1 (1994).
[52] H. Tamura, T. Yamazaki *et al.*, Phys. Rev. C **40**, 479 (1989).
[53] T. Bressani, in *Proc. of the Workshop on Physics and Detectors for DAΦNE*, Frascati, April 1991, INFN-LNF, p. 475; M. Agnello *et al.*, *FINUDA, A Detector for Nuclear Physics at DAΦNE*, proposal, LNF 93/021(IR), 1993; M. Agnello *et al.*, in *Proc. of the Fifth Conf. on the Intersections Between Particle and Nuclear Physics*, Florida, 1994 (AIP Conf. Proc., Vol. 338), p. 588; M. Agnello *et al.*, Nucl. Phys. **A585**, 271c (1995); T. Bressani, Nuovo Cim. A **108**, 649 (1995).
[54] L. Majling, Few-Body Syst., Suppl. 5, 348 (1992).
[55] C. B. Dover, Nukleonika **25**, 521 (1980).
[56] V. N. Fetisov, Nuovo Cim. A **102**, 307 (1989).
[57] L. Majling, in *Proc. of the Nat. Conf. on the Physics of Few-Body and Quark Hadronic Systems*, Kharkov, June 1992, KFTI, Kharkov, 1994, p. 345; Nucl. Phys. **A585**, 211c (1995); Few-Body Syst., Suppl. 9, 165 (1995).
[58] M. V. Zhukov *et al.*, Phys. Rep. **231**, 154 (1993); P. G. Hansen, Nucl.

Phys. **A553**, 89c (1993); **A588**, 1c (1995); W. von Oertzen *et al.*, Nucl. Phys. **A588**, 129c (1995); Yu. É. Penionzhkevich, Fiz. Élem. Chastits At. Yadra **25**, 930 (1994) [Sov. J. Part. Nucl. **25**, 394 (1994)].

[59] T. Motoba, H. Bandō, R. Wünsch, and J. Žofka, Phys. Rev. C **38**, 1322 (1988).

[60] E. C. Milner *et al.*, Phys. Rev. Lett. **54**, 1237 (1985).

[61] P. H. Pile *et al.*, Phys. Rev. Lett. **66**, 2585 (1991); R. E. Chrien, in *Some Problems in Contemporary Nuclear Physics, In Honor of the 80th Birthday of Academician I. M. Frank* [in Russian], edited by I. S. Shapiro and L. B. Pikel'ner (Moscow, Nauka, 1989), p. 101.

[62] D. J. Millener, C. B. Dover, and A. Gal, Phys. Rev. C **38**, 2700 (1988); A. Gal, Nuovo Cim. A **102**, 293 (1989).

[63] A. Likar, M. Rosina, and B. Povh, Z. Phys. A **324**, 35 (1986).

[64] H. Ejiri *et al.*, Phys. Rev. C **36**, 1435 (1987); H. Ejiri, T. Kishimoto, and H. Noumi, Phys. Lett. **225B**, 35 (1989).

[65] A. A. Sidorov, Yad. Fiz. **9**, 510 (1969) [Sov. J. Nucl. Phys. **9**, 292 (1969)]; V. N. Fetisov, M. I. Kozlov, and A. I. Lebedev, Phys. Lett. **38B**, 1231 (1972); M. I. Kozlov and V. N. Fetisov, Voprosy Atom. Nauk. Tekh., Ser. Fiz. Vysokikh Énerg. At. Yadra, No. 2(4), Kharkov Physico-Technical Institute, 73-10, 1973, p. 24; S. S. Hsiao and S. Cotanch, Phys. Rev. C **28**, 1668 (1983); C. B. Dover and D. J. Millener, in *Modern Topics in Electron Scattering*, edited by B. Frois and I. Sick (World Scientific, Singapore, 1991), p. 608.

[66] M. I. Kozlov and V. N. Fetisov, Preprint No. 25, FIAN (1974) [in Russian].

[67] R. A. Schumacher, Nucl. Phys. **A585**, 63c (1995); Few-Body Syst., Suppl. 9, 355 (1995); E. Cisbani *et al.*, Few-Body Syst., Suppl. 9, 374 (1995).

[68] M. Sotona, K. Itonaga, and T. Motoba, Nucl. Phys. **A547**, 57c (1992).

[69] S. Shinmura *et al.*, Prog. Theor. Phys. **76**, 157 (1986).

[70] V. N. Fetisov, Prog. Theor. Phys. Suppl. **117**, 391 (1994).

[71] G. Bohm, Nucl. Phys. **B24**, 248 (1970); M. Juric *et al.*, Nucl. Phys. **B47**, 36 (1972).

[72] D. H. Davis, Nucl. Phys. **A547**, 369c (1992).

[73] J. J. Szymanski, P. D. Barnes *et al.*, Phys. Rev. C **43**, 849 (1991).

[74] M. May, S. Bart *et al.*, Phys. Rev. Lett. **51**, 2085 (1983).

[75] L. Majling, J. Žofka, V. N. Fetisov, and R. A. Eramzhyan, Nucl. Phys. **A450**, 189c (1986).

[76] M. Bedjidian *et al.*, Phys. Rev. Lett. B **83**, 252 (1979).

[77] L. Majling, M. Sotona, J. Žofka, V. N. Fetisov, and R. A. Eramzhyan, Phys. Lett. **92B**, 256 (1980).

[78] J. Žofka, L. Majling, and V. N. Fetisov, in *Proc. of the 1986 INS Symp. on Hypernuclear Physics*, Tokyo, p. 23; H. Bandō, T. Yamada, and J. Žofka, Phys. Rev. C **36**, 1640 (1987).

[79] R. E. Chrien *et al.*, Phys. Rev. C **41**, 1062 (1990).

[80] L. Majling, J. Žofka, V. N. Fetisov, and R. A. Eramzhyan, Z. Phys. A **337**, 337 (1990).

[81] H. Tamura, in *Properties and Interactions of Hyperons*, edited by B. F. Gibson, P. D. Barnes, and K. Nakai (World Scientific, Singapore, 1994), p. 67.

[82] H. Tamura *et al.*, in *Proc. of the Twenty-Third INS Intern. Symp. on Nuclear and Particle Physics With Meson Beams in the 1 GeV/c Region*, Tokyo, 1995, p. 199.

[83] V. I. Kukulin, L. Majling, and Yu. F. Smirnov, Nucl. Phys. **A103**, 681 (1967).

[84] K. Itonaga, T. Motoba, and H. Bandō, Prog. Theor. Phys. **84**, 291 (1990).

[85] V. V. Balashov, in *Proc. of the Seminar on the Kaon–Nucleus Interaction and Hypernuclei* [in Russian], Zvenigorod, September 1977 (Nauka, Moscow, 1979), p. 338.

[86] C. Mahaux and H. A. Weidenmüller, *Shell Model Approach to Nuclear Reactions* (North Holland, Amsterdam, 1969); H. W. Barz, I. Rotter, and J. Hohn, Nucl. Phys. **A275**, 111 (1977); I. Rotter, Fiz. Élem. Chastits At. Yadra **15**, 762 (1984) [Sov. J. Part. Nucl. **15**, 341 (1984)].

[87] R. Wünsch, Czech. J. Phys. **42**, 1061 (1992).

[88] R. Wünsch, L. Majling, and J. Žofka, Nucl. Phys. **A450**, 329 (1986).

[89] V. A. Knyr, A. I. Mazur, and Yu. F. Smirnov, Yad. Fiz. **52**, 754 (1990) [Sov. J. Nucl. Phys. **52**, 483 (1990)].

[90] D. E. Lanskoĭ, Yad. Fiz. **49**, 63 (1989) [Sov. J. Nucl. Phys. **49**, 41 (1989)].

[91] F. Ajzenberg-Selove, Nucl. Phys. **A490**, 1 (1988); **A506**, 1 (1990); **A523**, 1 (1991).

[92] C. L. Cocke and P. R. Christensen, Nucl. Phys. **A111**, 623 (1968).

[93] A. Richter, in *Proc. of the Intern. School on Nuclear Structure*, JINR, Dubna, D4-80-385, p. 89.

[94] V. N. Fetisov, L. Majling, J. Žofka, and R. A. Eramzhyan, Czech. J. Phys. B **36**, 451 (1986).

[95] L. Majling and R. A. Eramzhyan, in *Proc. of the Intern. Conf. on Mesons and Nuclei at Intermediate Energies*, Dubna, 1994, p. 759.

[96] A. Gal, Phys. Rev. C **28**, 2186 (1983).

[97] L. Majling, J. Žofka, V. N. Fetisov, and R. A. Eramzhyan, in *Proc. of the Intern. Symp. on Nuclear Spectroscopy and Nuclear Interactions*, Osaka, Japan, 1984, p. 57; R. A. Eramzhyan, L. Majling, J. Žofka, and V. N. Fetisov, in *Proc. of the Tenth Intern. Conf. PANIC*, Heidelberg, 1984, Book of Abstracts, Vol. 2, M21.

[98] V. I. Goldansky, Nucl. Phys. **27**, 648 (1961).

[99] R. Bertini *et al.*, Nucl. Phys. **A368**, 365 (1981); R. Bertini, in *Proc. of the Intern. Conf. on Hypernuclei and Kaon Physics*, Heidelberg, 1982, p. 359.

[100] H. Tyren *et al.*, Nucl. Phys. **79**, 321 (1966).

[101] M. Kirchbach and H. Eger, Yad. Fiz. **29**, 1191 (1979) [Sov. J. Nucl. Phys. **29**, 614 (1979)].

[102] R. A. Eramzhyan, B. S. Ishkhanov, I. M. Kapitonov, and V. G. Neudatchin, Phys. Rep. **136**, 229 (1986).

[103] V. V. Balashov and V. N. Fetisov, Nucl. Phys. **21**, 337 (1961).

[104] Yu. F. Smirnov, in *Clustering Phenomena in Nuclei*, IAEA, Vienna, 1969, p. 153.

[105] Y. Nara, A. Ohnishi, and T. Harada, Phys. Lett. **346B**, 217 (1995).

[106] C. B. Dover *et al.*, Phys. Rev. C **44**, 1905 (1991); C. B. Dover, A. Gal, and D. J. Millener, Nucl. Phys. **A572**, 85 (1994); D. J. Millener, C. B. Dover, and A. Gal, Prog. Theor. Phys. Suppl. **117**, 307 (1994).

[107] T. Yamada and K. Ikeda, Prog. Theor. Phys. Suppl. **117**, 445 (1994).

[108] H. Feshbach, Ann. Phys. (N.Y.) **5**, 537 (1958).

[109] V. V. Balashov, P. Doleshal, and G. Ya. Korenman, Yad. Fiz. **2**, 643 (1965) [Sov. J. Nucl. Phys. **2**, 461 (1966)].

[110] R. Wünsch, Nucl. Phys. **A336**, 446 (1980).

[111] R. Wünsch, L. Majling, and J. Žofka, Czech. J. Phys. B **36**, 441 (1986).

[112] W. Bruckner *et al.*, Phys. Lett. **55B**, 107 (1975); **62B**, 481 (1976); **79B**, 157 (1978).

[113] P. L. Kapur and R. E. Peierls, Proc. R. Soc. London, Ser. A **166**, 277 (1938).

[114] H. Bandō, Nucl. Phys. **A450**, 217c (1986).

[115] D. Halderson, Phys. Rev. C **30**, 941 (1984); D. Halderson and Pingzhi Ning, Nucl. Phys. **A450**, 391c (1986).

[116] V. A. Knyr, A. I. Mazur, and Yu. F. Smirnov, Yad. Fiz. **54**, 1518 (1991) [Sov. J. Nucl. Phys. **54**, (1991)].

[117] Yu. F. Smirnov and Yu. I. Nechaev, Kinam **4**, 445 (1982).

[118] L. B. Okun, *Leptons and Quarks*, 2nd ed. (North-Holland, Amsterdam, 1984) [Russ. original, Nauka, Moscow, 1981].

[119] T. Motoba, Nucl. Phys. **A527**, 485c (1991).

[120] R. H. Dalitz and G. Rajasekhavan, Phys. Lett. **1**, 58 (1962).

[121] J. Cohen, Phys. Rev. C **42**, 2724 (1990).

[122] J. F. Dubach, Nucl. Phys. **A450**, 71c (1986).

[123] D. P. Heddle and L. S. Kisslinger, Phys. Rev. C **33**, 608 (1986).

[124] K. Maltman and M. Shmatikov, Nucl. Phys. **A585**, 343c (1995).

[125] T. Inoue, S. Takeuchi, and M. Oka, in *Proc. of the Intern. Conf. on Hypernuclei and Strange Particle Physics*, TRIUMF, Canada, 1994, p. 39.

[126] A. Ramos, E. Oset, and L. L. Salcedo, Nucl. Phys. **A585**, 129c (1995).

[127] M. Shmatikov, Phys. Lett. **337B**, 48 (1994).

[128] R. A. Schumacher, Nucl. Phys. **A547**, 143c (1992).

[129] K. Takeuchi, H. Takaki, and H. Bandō, Prog. Theor. Phys. **73**, 841 (1985).

[130] C. B. Dover, Few-Body Syst., Suppl. 2, 77 (1987).

[131] M. Shmatikov, Phys. Lett. **322B**, 311 (1994).

[132] K. Itonaga, T. Ueda, and T. Motoba, Nucl. Phys. **A585**, 331c (1995).

[133] V. V. Burov, V. K. Luk'yanov, and A. I. Titov, Fiz. Élem. Chastits At. Yadra **15**, 1249 (1984) [Sov. J. Part. Nucl. **15**, 558 (1984)].

[134] V. G. Neudachin, I. T. Obukhovskiĭ, and Yu. F. Smirnov, Fiz. Élem. Chastits At. Yadra **15**, 1165 (1984) [Sov. J. Part. Nucl. **15**, 519 (1984)].

[135] V. N. Fetisov, Nucl. Phys. **A585**, 197c (1995).

[136] A. Ramos, Benhold C. van Mejgaard, and B. K. Jennings, Phys. Lett. **264B**, 233 (1991).

[137] T. Motoba, K. Itonaga, and H. Bandō, Nucl. Phys. **A489**, 683 (1988).

[138] L. Majling, J. Žofka, V. N. Fetisov, and R. A. Eramzhyan, Phys. Lett. **202B**, 489 (1988).

[139] L. Majling, J. Žofka, T. Sakuda, and H. Bandō, Prog. Theor. Phys. **79**, 561 (1988).

[140] T. Sakuda and H. Bandō, Prog. Theor. Phys. **78**, 1317 (1987).

[141] M. A. Markov, *Hyperons and K mesons* [in Russian] (Fizmatgiz, Moscow, 1958).
[142] B. A. Shahbazian *et al.*, Z. Phys. C **39**, 151 (1988); Phys. Lett. **235B**, 208 (1990); **316B**, 593 (1993).
[143] *Proc. of the Intern. Conf. on Mesons and Nuclei at Intermediate Energies*, Dubna, May 1994, edited by M. Khankhasayev and Zh. Kurmanov (World Scientific, Singapore, 1995).
[144] J. P. Bocquet *et al.*, Phys. Lett. **182B**, 146 (1986); S. Polikanov, Nucl. Phys. **A478**, 805c (1988); M. Rey-Campagnolle, Nuovo Cim. A **102**, 683 (1989); T. A. Armstrong *et al.*, Phys. Rev. C **47**, 1957 (1993).
[145] H. J. Krappe and V. V. Pashkevich, Phys. Rev. C **47**, 1970 (1993).
[146] PS179 Collaboration, Yad. Fiz. **50**, 1524 (1989) [Sov. J. Nucl. Phys. **50**, 945 (1989)]; F. Balestra, Yu. A. Batusov *et al.*, Nucl. Phys. **A526**, 415 (1991).
[147] S. Avramenko *et al.*, Nucl. Phys. **A547**, 95c (1992).
[148] S. A. Avramenko *et al.*, Nucl. Phys. **A585**, 91c (1995).

Translated by Patricia A. Millard